1986

Vibration identification of nuclear reactor components by statistical analysis of neutron noise

John Thomas Sankoorikal
Iowa State University

Sankoorikal, John Thomas

VIBRATION IDENTIFICATION OF NUCLEAR REACTOR COMPONENTS BY STATISTICAL ANALYSIS OF NEUTRON NOISE

Iowa State University PH.D. 1986

PLEASE NOTE:

In all cases this material has been filmed in the best possible way from the available copy. Problems encountered with this document have been identified here with a check mark __✓__.

1. Glossy photographs or pages _____
2. Colored illustrations, paper or print _____
3. Photographs with dark background ✓
4. Illustrations are poor copy _____
5. Pages with black marks, not original copy _____
6. Print shows through as there is text on both sides of page _____
7. Indistinct, broken or small print on several pages ✓
8. Print exceeds margin requirements _____
9. Tightly bound copy with print lost in spine _____
10. Computer printout pages with indistinct print _____
11. Page(s) _____ lacking when material received, and not available from school or author.
12. Page(s) _____ seem to be missing in numbering only as text follows.
13. Two pages numbered _____. Text follows.
14. Curling and wrinkled pages _____
15. Dissertation contains pages with print at a slant, filmed as received _____
16. Other _____

_____

_____

University
Microfilms
International

Vibration identification of nuclear reactor components by statistical analysis of neutron noise

by

John Thomas Sankoorikal

A Dissertation Submitted to the
Graduate Faculty in Partial Fulfillment of the
Requirements for the Degree of
DOCTOR OF PHILOSOPHY

Major: Nuclear Engineering

Approved:

Signature was redacted for privacy.
In Charge of Major Work

Signature was redacted for privacy.
For the Major Department

Signature was redacted for privacy.
For the Graduate College

Iowa State University
Ames, Iowa

1986

TABLE OF CONTENTS

LIST OF TABLES

LIST OF FIGURES

LIST OF ACRONYMS

UTR-10 University Teaching and Research Reactor - 10 KW

EW East-West

NS North-South

APSD auto-power spectral density

CPSD cross-power spectral density

LVDT Linear Variable Differential Transformer

FFT Fast Fourier Transform

REG ROD Regulating rod

UNFLO Unflooded

FLO Flooded

THEOR Theoretical

EXPTL Experimental

PWR Pressurized Water Reactor

BWR Boiling Water Reactor

I. INTRODUCTION

Signals associated with process variables in a nuclear reactor show fluctuations around a mean value. These fluctuations, which are commonly referred to as noise, carry information regarding the behavior of components inside the reactor. Proper analysis of this noise can be used to determine information about the source. In a nuclear reactor there are a large number of components, for example fuel rods and control rods, which can undergo flow induced vibrations during normal operation. The movement of an absorber in a reactor induces neutron density fluctuations (1) which appear as noise in the signals of the neutron detectors.

The importance of localizing vibrating components and their vibration amplitudes is illustrated by the observation (2) that excessive motion of fuel assemblies has led to fuel rod cladding failure in a number of PWRs. The loose parts resulting from such failures increase the possibility of local flow blockages and coolant boiling. Control rod vibrations (3) have also been observed in reactors. This may lead to poor performance or unavailability of the rods in an emergency, or to damage to core structure. Hence, component vibrations are potential safety issues. Breakdown or malfunctions of reactor components may be prevented if they are monitored continuously.

Some of the advantages of using neutron noise analysis are:

- it can be performed without disturbing normal plant operations,
- existing instrumentation can be used,
- there is no need to come into contact with the hostile environment in the reactor,
- it provides a means for continuous surveillance.

The use of neutron noise analysis for the identification of vibrations has been investigated for several years (3-33). However, the use of statistical techniques has not been found in the literature. Statistical errors, associated with measurements, must be taken into account in order to obtain reliable information, and the techniques developed for the identification of vibrations must be statistically sound. The purpose of this research may be summarized as follows:

1. Develop techniques with firm statistical basis to locate and estimate vibration amplitudes of moving reactor core components. Study the possibility of using the information matrix to identify optimal detector patterns and numbers.
2. Investigate the applicability of these techniques by performing computer based experiments. Also, investigate the effects of measurement error,

external noise, model bias, and detector patterns on the techniques developed.

3. Perform an experiment on the UTR-10 reactor to verify the validity of the techniques.

Vibrations are characterized, in a two-dimensional system, by two location and three vibration amplitude parameters. These vibration parameters, compatible with observed detector readings, were estimated using the maximum likelihood and confidence region techniques (34, 35). Both techniques rely on the knowledge of the statistical distribution of the measured signals. The maximum likelihood method yields a point estimate for the parameters, and a confidence region technique gives a set estimate with an associated confidence factor. It may be noted that the maximum likelihood estimate always lies in the confidence region and the confidence that the actual value is within the confidence set is given by the confidence factor. Both of these methods are sensitive to the presence of other unrelated (external) noise sources, data variance, model bias, and the detector pattern used. The effects of these factors on the techniques developed were studied.

The problems of the optimal positioning and selection of the number of detectors may be treated as one in optimal experimental design (36). The minimum variance attainable

for the parameters was determined from the Fisher information matrix. An optimal detector pattern was chosen by evaluating the variances and looking for a pattern that gives the minimum variance.

The applicability of the techniques developed were then investigated by using a one-group, square, bare, homogenous reactor model to generate simulated detector signals. Simulated signals were generated for an assumed vibrator location and amplitude parameters. Statistical measurement error was modeled using a multiplicative type error which yields a log-normal distribution for the detector signals.

In order to experimentally verify the techniques developed, a vibrating (29) thermal neutron absorber was operated in the fuel region of the UTR-10 reactor at Iowa State University. The vibrator moved in one-dimension at a single frequency of 2.5 Hz. This case of a single vibrating rod undergoing periodic motion was considered, since, among many rods, only one may be vibrating above a threshold and the rods usually vibrate at their natural frequency. Signals from four detectors were analyzed using a Frequency Spectrum Analyzer to obtain the auto-power spectral densities. In order to estimate the vibration parameters, one requires a computer code that will adequately calculate the detector response. The static code, Exterminator-2 (37), was modified and used for this purpose. The vibration

parameters were estimated for different conditions of the experiment using the statistical techniques described previously.

In this dissertation, the theoretical background for the problem is developed in Chapter III, using the adjoint and forward formulations for the response of a neutron detector. The statistical techniques are also developed in this chapter. Chapter IV deals with the numerical testing of the techniques developed. Chapter V describes the experimental verification of the problem. Conclusions and suggestions for future work are also included in chapters VI and VII, respectively.

II. LITERATURE REVIEW

Weinberg and Schweinler (1) were the first investigators to show that oscillations of a neutron absorber will lead to fluctuations of the neutron field in a nuclear reactor. They concluded that the motion produced a space dependent 'local' or short range component as well as a space independent 'global' or long range component in the response.

The observation of a peak in the auto-power spectral density of neutron detector signals at the Oak Ridge research reactor, by Stephenson et al. (3), was the first experimental evidence for noise induced by vibrations. This noise was due to the motion of a faulty control rod. Lucia et al. (4) were able to correlate the neutron noise spectra of fuel element vibrations with signals recorded by accelerometers attached to the elements. The detection of internal vibrations in power reactors has also been reported by a number of authors (5, 6).

Thie (7) reviewed a variety of techniques, both indirect and direct, available to detect movements of in-vessel components. In the indirect method, sensors not intended for motion sensing are used and the characteristics of normal signals from these sensors are related to the motion. Indirect methods, like the ones using signals from neutron detectors, ex-vessel ion chambers, or thermocouples,

require theoretical modeling. The direct methods make use of motion sensors or strain gauges, which give an absolute amplitude of motion. Kosály (8) reported on the status of the theoretical (physics) aspects of different noise phenomena. He discussed the general features of noise detected by in-core (power monitors inside the reactor core) and ex-core (outside the reactor core) detectors. He pointed out that while the point-reactor and adiabatic models are adequate in small research reactors, sophisticated space dependent models are necessary, for neutron noise analysis, in power reactors. Examples of direct practical applications and the development of neutron noise analysis techniques for malfunction diagnostics may be found in the proceedings of the international specialists meetings of reactor noise analysis (9, 10, 11) which are held periodically. Thie (12) provides an excellent summary, and a bibliography of the applications of neutron noise analysis for the diagnosis of anomalies of PWRs. A recent application (13) involved the use of neutron noise, measured with in-core neutron detectors, to diagnose abnormal vibrations of fuel assemblies caused by water jetting through clearances in the baffle plates.

Fry et al. (14) reported on the experiences with and assessments of neutron noise analysis in commercial light water reactors. They concluded that ex-core neutron

detector noise can be used to monitor in-vessel structural component vibrations in PWRs, provided that the contribution of individual structures can be separated from the total noise spectrum. In this paper, they point out that the neutron noise, from both PWRs and BWRs, is essentially Gaussian in nature and that the PWR noise contains periodic components presumably related to the vibrations of internal core structures.

Sweeney and Renier (15) presented a sophisticated method, using transport theory, to calculate the response of ex-core neutron detectors to in-core perturbations. It was pointed out that the noise level, due to fuel vibrations, is altered by fuel burnup, boron concentration, and xenon poisoning. The noise level increases over a fuel cycle. This must be taken into account before conclusions are drawn regarding fuel assembly vibrations. Their work demonstrated the feasibility of calculating the detector responses (both the real and imaginary components) in power reactors. They also interpreted experimental noise data based on calculated detector responses.

A theoretical model of vibration-induced noise, that was of practical interest, was presented, first, by Williams (16). Some of the earlier analyses (16, 17) used one-energy group, point-reactor models. The point-reactor model assumes a space-independent transfer function, which for a

large reactor would not be a good assumption. Pázsit (18) used a one-group model to show the space dependence of the neutron-noise field around a vibrating absorber. In reflected reactors, with a two-group analysis, Pázsit (19) showed that the local component has a different importance in the reflector than in the core. This analysis was based on the adjoint formulation suggested by Van Dam (20) which reduces the calculational efforts involved, especially if multiple sources are present.

In an actual situation, vibrating components can move in two-dimensions and therefore, the detector signals depend on the actual trajectory of motion. Pázsit and Analytis (21) developed a theoretical model for the analysis of such situations. The analysis is complicated since the diagnostic problem involves an infinite number of possible trajectories. A trajectory needs to be assumed in this case, and normally one assumes either a vibration which is equally likely in all directions or a periodic motion. Lee and Albrecht (22) derived the frequency dependent, two-group diffusion equations and used the adjoint technique to solve the problem of two-dimensional control rod vibrations. They discussed a 'contour' (points with equal response for a random vibration at a certain location) method to localize a vibrating control rod.

Pázsit and Glöckler (23) pointed out that an infinite number of vibration trajectories can be described by two spatial components of motion, which can be eliminated using measured detector signals. They derived an equation, which is independent of the trajectory of motion, for the localization problem involving periodic vibrations. The unknown location parameter is obtained by searching for the root of this equation. Their second paper (24) deals with the case of stochastic vibrations. In such cases, expressions for the auto-power spectral densities of the vibration amplitudes have been derived (18), but an expression for the cross-power spectral density between the two components was not available in the literature. They derived an expression for the cross-spectra from first principles and the stochastic vibrations were characterized by two parameters. The same procedure described in the case of periodic vibrations was also applied to this problem. They carried out numerical investigations using simplified reactor models.

It was observed that none of the previous approaches dealt with the measurement error associated with detector signals. The techniques developed in this work take this into account. The well-developed statistical estimation methods (34, 35), involving the application of maximum-likelihood and confidence region, are used here. The

questions of the estimation of a location and also the estimation of vibration amplitudes were addressed. The statistical uncertainty of the estimates can also be determined in the process. The question of the number of detectors and pattern required for an optimal estimation of the vibration parameters was also investigated.

A report of the work done at Iowa State University, in vibration detection, may be found in reference (25). Several theoretical models (26, 30) were developed for the UTR-10 reactor to obtain detector responses to a vibrating absorber. Al-Ammar (26) developed a one-dimensional diffusion code to calculate the frequency-and space-dependent detector response functions for the UTR-10 reactor. Hennessy (30) developed an analytical model to calculate the detector response using two-group diffusion equations, which were solved using Green's function methods. Experimental measurements were carried out in the reflector region (26, 28, 30) of the UTR-10 reactor. Al-Ammar designed and constructed a vibrating neutron absorber apparatus which was operated in the central vertical stringer of the UTR-10 reactor. The experimental investigations showed the validity of the local-global concept. He suggested the monitoring of the behavior of the normalized cross-power spectral density to detect vibrating components. Borland (28) improved Al-Ammar's apparatus and

his measurements verified Al-Ammar's results. He demonstrated that the local component of the detector response could be isolated when the plane of the absorber motion is adjacent to the detector. Experimental work conducted by Hennessy (30) showed that the ratio of the responses of two detectors to a vibrating absorber compared very well with that obtained from calculations using the model he developed. A vibrating absorber was also operated in the fuel region (29, 32). Sankoorikal (29) designed and constructed a vibrator assembly to be operated in the fuel region of the UTR-10 reactor. The detector response was found to depend on the detector-vibrator orientation which can be explained in terms of the local and global response of the detector. It was observed that the noise generated had different characteristics if the vibrator was immersed in water compared to air. Kalbasi (32) designed a vibrating apparatus that could be operated in various planes of motion relative to a detector array. His results showed that the detector response depended on the plane of motion of the vibrator, which can be explained on the basis of the different gradients involved. A report on a preliminary study conducted for the work discussed in this dissertation may be found in reference (33).

III. THEORETICAL BACKGROUND

In this section, the theory of the detector response to a vibrating absorber will be developed. Two methods of analysis, the forward solution and the detector adjoint function techniques, will be described. Statistical concepts like maximum likelihood, confidence region and information matrix are discussed and used to develop statistical techniques for the identification of reactor component vibration.

A. Development of the Detector Response to a Vibrating Absorber

The time-dependent, homogeneous (source free) equation governing the population of neutrons in a reactor system is given, in operator notation, by (38)

$$v^{-1}\frac{\partial \phi}{\partial t} = L_1 \phi, \tag{3.1}$$

where

$$L_1 = L_p + \sum_j \lambda_j C_j \chi_j. \tag{3.2}$$

The jth delayed neutron precursor concentration, C_j, is given by

$$\frac{\partial}{\partial t} C_j + \lambda_j C_j = \iint \beta_j \nu \Sigma_f \phi' \, d\Omega' \, dE'. \tag{3.3}$$

All the constants in equations (3.1) to (3.3) have standard

meaning (38) and the functional dependence is dropped for convenience.

In transport theory, L_1 represents the transport operator (38) and in multigroup diffusion theory, L_1 represents the multigroup diffusion operator (39). L_p is the prompt neutron operator.

The vibration of a component in the reactor is assumed to result in small fluctuations in group cross sections such as

$$\Sigma(r,t) = \Sigma(r) + \Delta\Sigma(r,t) \ . \tag{3.4}$$

The perturbation is assumed to be first order in nature implying an unaltered static flux even in the presence of vibrations. The fluctuations in cross sections are represented as small perturbations in the diffusion (transport) operator

$$L_1(r,t) = L_1(r) + \Delta L_1(r,t), \tag{3.5}$$

resulting in small stochastic fluctuations of the neutron and delayed neutron precursor populations as

$$\phi(r,t) = \phi(r) + \Delta\phi(r,t), \tag{3.6}$$

$$C(r,t) = C(r) + \Delta C(r,t). \tag{3.7}$$

Equations (3.5) and (3.6) are substituted into equation (3.1), the second order terms are neglected (linearizing)

and the steady state terms are removed (since they sum to zero) to obtain

$$L_2(r,t)\Delta\phi(r,t) = \Delta L_1(r,t)\phi(r), \qquad (3.8)$$

where L_2 includes the time derivative term. The Fourier transform of equation (3.8) yields

$$L(r,\omega)\Delta\phi(r,\omega) = \Delta S(r,\omega), \qquad (3.9)$$

where

$$\Delta S(r,\omega) = \Delta L(r,\omega)\phi(r). \qquad (3.10)$$

Equation (3.10) describes the Langevin source (40), which is the product of the Fourier transform of the fluctuations in the operator (or group cross sections) and the steady state flux. Equation (3.9) represents the Langevin equation for $\Delta\phi$, the Fourier transform of the fluctuations in the neutron population for a source ΔS. The delayed neutron terms are eliminated by substituting the Fourier transform of the fluctuations in precursor concentration, $\Delta C(r,\omega)$, into the operator $L(r,\omega)$. A simplified development of equation (3.9) based on the two-group diffusion theory approximation can be found in Appendix A.

Equation (3.9) may be solved for the forward solution, which is the flux response, or the adjoint function technique (20) may be used to derive an expression for the

detector response. The operator L in equation (3.9) is not always self adjoint and the equation adjoint to (3.9) is given, in operator notation (38), as

$$L^{+}(r,\omega)\psi(r,r_{p},\omega) = -\Sigma_{d}(r,\omega). \qquad (3.11)$$

The operator L^{+} is the adjoint operator. In multigroup diffusion theory L^{+} is the transpose of L. The two-group diffusion adjoint operator can be found in Appendix A. The adjoint system in the case of the transport equation is given by Sweeney and Renier (15). The adjoint function, ψ, may be interpreted as the response of a detector of cross section Σ_{d}, located at r, to a unit strength point (delta function) source at r_{p}.

The following development provides a better understanding of the physical meaning of the adjoint system. The inner product of ψ with equation (3.9) and $\Delta\phi$ with equation (3.11) is taken and upon using the definition of the adjoint operator (38), given by

$$<L\Delta\phi,\psi> = <\Delta\phi,L^{+}\psi>, \qquad (3.12)$$

one obtains

$$<\Delta\phi,\Sigma_{d}> = -<\Delta S,\psi>, \qquad (3.13)$$

where '< >' represents integrations over the respective variables. The left hand side of equation (3.13) gives the

Fourier transform of the response, $\Delta R(r,r_p,\omega)$, of a detector of cross section Σ_d, and volume V_d, at location r due to sources at r_p in the reactor volume. Therefore, in terms of the adjoint function, the detector response is

$$\Delta R(r,r_p,\omega) = \langle\langle \Delta S(r_p,\omega), \psi(r,r_p,\omega)\rangle_{V_{rp}}\rangle_{V_d}, \quad (3.14)$$

where the integrations over the various sources, $\langle\ \rangle_{V_{rp}}$, and the detector volume, $\langle\ \rangle_{V_d}$, are explicitly written.

In general, in frequency domain calculations the forward (equation 3.9) and adjoint (equation 3.11) systems are complex. As an example, consider the adjoint system. The L^+ and ψ are complex and from a practical standpoint, the detector cross section is assumed to be real and independent of frequency. Therefore,

$$(L_R^+ + jL_I^+)(\psi_R + j\Psi_I) = -\Sigma_d \quad , \quad (3.15)$$

where the subscripts R and I represent the real and imaginary parts of L^+ and ψ. Equating real and imaginary parts, equation (3.15) can be written as

$$L_R^+\psi_R - L_I^+\psi_I = -\Sigma_d \ , \quad (3.16a)$$

$$L_R^+\psi_I + L_I^+\psi_R = 0, \quad (3.16b)$$

which behave as a coupled set of equations with $L_I^+\psi_I$

representing an upscatter term and $L_I^+\psi_R$ a down scatter term. A static code which can handle up and down scattering and a source may be used to solve these types of equations. Note that in two-group calculations, four coupled equations need to be solved.

The frequency range of interest, (20) in the study of reactor component vibrations, coincides with the plateau region ($\lambda << \omega << \beta/\ell$) of the reactor transfer function (41). It can be shown (20) that in this region, $L_I^+ \sim 0$ which makes equations (3.16a) and (3.16b) weakly coupled. Also, ψ_I is negligible (20) compared to ψ_R and equations (3.16) reduce to

$$L_R^+(r)\psi_R(r,r_p) = -\Sigma_d(r). \qquad (3.17)$$

A similar result can be obtained for the forward system.

$$L_R^+(r)\Delta\phi_R(r,r_p) = \Delta S(r). \qquad (3.18)$$

Equations (3.17) and (3.18) are real and both the forward and adjoint functions are real and are independent of frequency. Equations (3.17) and (3.18) may be evaluated using a static code capable of solving a source problem (the non-homogenous equations).

A source ΔS is specified at the location of the vibrator and equation (3.18) is solved to yield the forward solution. To solve equation (3.17) the detector is

considered as an adjoint source, that is, a source Σ_d is specified at the detector location.

To solve equation (3.17) or (3.18) analytically, the Green's function technique (42) may be used. The two-dimensional problem can be solved using series expansions (43). As an example, consider the forward problem. The Green's function solution, $G(r,r_p)$, is the solution to equation (3.18), when the source is replaced by a unit strength point source (delta function). Therefore, G satisfies the equation

$$L_R G = \delta(r-r_p). \tag{3.19}$$

The Green's function can be interpreted as the transfer function between the source location and the detector location. Once G is obtained, the total flux response, $\Delta\phi(r,\omega)$, at r due to sources at locations r_p, of strength ΔS, may be obtained by

$$\Delta\phi(r,\omega) = \langle G(r,r_p), \Delta S(r_p) \rangle_{V_{rp}}. \tag{3.20}$$

The detector response in terms of the forward Green's function solution is obtained by substituting equation (3.20) into the left hand side of equation (3.13) and is given by,

$$\Delta R(r,r_p,\omega) = \langle\langle G(r,r_p), \Delta S(r_p,\omega)\rangle_{V_{rp}}, \Sigma_d \rangle_{V_d}. \tag{3.21}$$

In order to see the relationship between G and ψ, consider a point detector at r_d with unit cross section and a single point source with unit strength. From equations (3.14) and (3.21) one obtains

$$\psi(r_d,r)|_{r=r_p} = G(r,r_p)|_{r=r_d} \quad , \qquad (3.22)$$

where it is assumed that ψ is independent of frequency. Therefore, it can be seen that the detector adjoint function evaluated at r_p for a detector at r_d is equal to the forward Green's function evaluated at r_d due to a source at r_p. If ψ is determined using a detector cross section Σ_d, G must be multiplied by it and if the point source strength is ΔS both sides of equation (3.22) are multiplied by ΔS. The detector adjoint function gives the detector view over the entire reactor, while the forward Green's function represents the effect of the source over the entire reactor. If there are many sources and few detectors involved it may be advantageous (considering the computational effort involved) to perform an adjoint calculation. The forward Green's function technique is better in the case of many detectors and few sources.

1. The vibrating absorber

In the case of the two-dimensional motion of a thin, infinitely long absorber, the noise equivalent source, in the time domain, is given (16) for a thermal absorber, by

$$\Delta S(r,t) = \gamma\phi_2(r)(\delta(r-r_p-\delta r(t))-\delta(r-r_p)), \quad (3.23)$$

where r_p represents the static position of the rod and $\delta r(t)$ describes its mechanical trajectory. The thermal-neutron flux is ϕ_2 and the thermal-absorber strength is γ. To obtain the detector response, the Fourier transform of equation (3.23) is substituted into equation (3.14) which yields

$$\Delta R(r,r_p,\omega) = \langle\langle\gamma\phi_2(r')\int_{-\infty}^{\infty} e^{-j\omega t}dt(\delta(r'-r_p-\delta r(t)) - \delta(r'-r_p)),\psi(r,r')\rangle_{V_{rp}}\rangle_{V_d}. \quad (3.24)$$

With the assumption of a point detector and formally interchanging the order of time and space integration, the space integration (over the perturbations) is carried out, and using the property of delta functions one obtains

$$\Delta R(r,r_p,\omega) = \gamma\int_{-\infty}^{\infty} e^{-j\omega t}dt \{\phi_2(r_p+\delta r(t))\psi(r,r_p+\delta r(t))-\phi_2(r_p)\psi(r,r_p)). \quad (3.25)$$

The two-dimensional Taylor's series expansion of $\phi(r_p+\delta r(t)\psi(r+r_p+\delta r(t))$ about r_p, after neglecting terms of order two and higher in $\delta r(t)$, may be written as

$$\phi\psi + \nabla_{rp}(\phi\psi)\ \delta r(t). \tag{3.26}$$

where in rectangular coordinates

$$\nabla_{rp} = \bar{i}\partial/\partial x + \bar{j}\partial/\partial y\ , \tag{3.27}$$

and

$$\delta r(t) = \bar{i}\delta x(t) + \bar{j}\delta y(t), \tag{3.28}$$

where $\bar{i}$ and $\bar{j}$ are unit vectors and $\delta x(t)$ and $\delta y(t)$ represent the x and y components of the two-dimensional trajectory of the motion of the rod.

Substitution of equation (3.26) into equation (3.25) yields, upon completing the Fourier transform,

$$\Delta R(r,r_p,\omega) = \gamma\nabla_{rp}(\phi\psi)\ \Delta r(\omega). \tag{3.29}$$

In this equation, ψ may be replaced with G, under the assumptions, stated earlier, for the equivalence of G and ψ. Equation (3.29) may be written in rectangular coordinates, by substituting equations (3.27) and (3.28) into equations (3.29) as

$$\Delta R(r,r_p,\omega) = W_x(r,r_p)\delta x(\omega) + W_y(r,r_p)\delta y(\omega). \tag{3.30}$$

The quantities W_x and W_y may be interpreted as the detector response for unit amplitudes of vibration in the x and y direction, respectively. These unit responses are given by

$$W_x = \gamma \partial(\phi\psi)/\partial x, \tag{3.31a}$$

and

$$W_y = \gamma \partial(\phi\psi)/\partial y. \tag{3.31b}$$

The general case of the response of a detector to N vibrators may be derived from equation (3.24). A change in notation will be convenient at this stage. Let subscript i represent the ith detector located at r_i, and k the kth vibrator located at r_k. Then, the total response, ΔRT_i, of detector i due to vibrators located at various r_k, is given by the sum of the responses at r_i due to individual vibrators,

$$\Delta RT_i = \sum_{k=1}^{N} (W_{x_{i,k}} \delta x_k + W_{y_{i,k}} \delta y_k). \tag{3.32}$$

Often, the auto-power spectral density (APSD), R_i, of a detector signal and the cross-power spectral density (CPSD), R_{ij}, between detectors are measured. These are given (44) by,

$$R_i(\omega) = \Delta RT_i \Delta RT_i^* \tag{3.33a}$$

and

$$R_{ij}(w) = \Delta RT_i^* \Delta RT_j \tag{3.33b}$$

where '*' represents the conjugate operation. In this study, only the APSDs of the detector responses are considered. For the special case of only one vibrator (set N=1 and drop subscript k in equation 3.32) the APSD of the ith detector is given by

$$R_i = W_{x_i} W_{x_i}^* APSD_{\delta x} + W_{y_i} W_{y_i}^* APSD_{\delta y} + 2Re(W_{x_i} W_{y_i}^* CPSD_{\delta y \delta x}), \tag{3.34}$$

where the APSDs of the two components of motion are

$$APSD_{\delta x} = \delta x \delta x^*, \tag{3.35a}$$

and

$$APSD_{\delta y} = \delta y \delta y^*, \tag{3.35b}$$

and the CPSD between the components of motion is

$$CPSD_{\delta x \delta y} = \delta y^* \delta x. \tag{3.35c}$$

The calculation of the quantities in equations (3.35) will be shown, next, for the case of two-dimensional periodic motion.

2. Detector response for two-dimensional periodic motion

In the case of periodic motion, the x and y components may be written

$$\delta x(t) = a_x \cos(\omega_o t), \tag{3.36a}$$

and

$$\delta y(t) = a_y \cos(\omega_o t+\alpha), \tag{3.36b}$$

where a_x and a_y are amplitudes of motion in the x and y directions, α is the phase angle between the two components, and ω_o is the vibration frequency. Different values of a_x, a_y and α generate different vibration patterns. To evaluate (3.35c), first the cross correlation function, $\Delta XY(\tau)$, is calculated using (44)

$$\Delta XY(\tau) = \lim_{T\to\infty} \frac{1}{T} \int_o^T \delta x(t)\delta y(t+\tau)dt. \tag{3.37}$$

Equations (3.36a) and (3.36b) are substituted into (3.37), the terms are expanded and the integrations are carried out (over one period, $2\pi/\omega_o$, of the waveform) to obtain

$$\Delta XY(\tau) = 2^{-1} a_x a_y (\cos\alpha \cos(\omega_o\tau) - \sin\alpha \sin(\omega_o\tau)). \tag{3.38}$$

The $CPSD_{\delta x\delta y}$ is given by the Fourier transform of equation (3.38) as

$$CPSD_{\delta x\delta y} = 2^{-1} a_x a_y (\cos\alpha+i\sin\alpha)\delta(f-f_o), \tag{3.39}$$

where $\delta(f-f_o)$ represents a delta function at the frequency f_o corresponding to ω_o. Similarly,

$$APSD_{\delta x} = 2^{-1}a_x^2\delta(f-f_0), \tag{3.40}$$

and

$$APSD_{\delta y} = 2^{-1}a_y^2\delta(f-f_0). \tag{3.41}$$

It should be noted that if G or ψ are assumed to be real, the functions W_x and W_y are real. Equations (3.39), (3.40), and (3.41) are substituted into equation (3.34) to obtain the APSD of the detector response at location i as

$$R_i(r_p,\omega) = (2^{-1}W_{x_i}^2 X1 + 2^{-1}W_{y_i}^2 X2 + W_{x_i}W_{y_i} X3)\delta(f-f_0), \tag{3.42}$$

where X1, X2, and X3 are used to represent a_x^2, a_y^2 and $a_x a_y \cos\alpha$, respectively. This analysis, assuming two-dimensional periodic motion, is realistic, since rods tend to vibrate at their natural frequency and therefore will have approximate periodic motion.

In the case of stochastic vibrations, the determination of the APSDs and CPSD of the displacement spectra, in equation (3.34), is not straightforward but is possible (24). Usually, the APSDs are determined easily (17), but

the CPSD is not. A simplified approach (45) may be attempted. The third term in equation (3.34), involving the CPSD may be replaced with an approximation involving only APSDs. This approximation will be either an upper bound or a lower bound for the third term and will result in an upper bound (UB), R_{iUB}, or a lower bound (LB), R_{iLB}, for the response of the detector, such that

$$R_{iLB} < R_i < R_{iUB}. \tag{3.43}$$

An upper bound (UB), for the third term in equation (3.34) is given by

$$2|\mathrm{Re}(W_{x_i} W_{y_i}^{*} \mathrm{CPSD}_{\delta y \delta x})|_{UB} = 2|W_{x_i}||W_{y_i}^{*}| \cdot (\mathrm{APSD}_{\delta x} \mathrm{APSD}_{\delta y})^{1/2}. \tag{3.44}$$

In arriving at equation (3.44) we have used the following three relationships:

- The magnitude of a complex number is greater than or equal to the magnitude of its real part.
- The magnitude of the product of complex numbers is equal to the product of the magnitude of the individual complex numbers (46).
- The magnitude of the CPSD is always less than or equal to the square root of the product of the APSDs (44).

The lower bound of the third term (less than zero) is obtained by taking the negative of the upper bound term (3.44). Substitution of equation (3.43) or its negative counterpart into equation (3.34) results in expressions for the upper and lower bounds for the detector responses, involving only APSDs of the amplitudes of motion. When trying to interpret measured detector signals with these two expressions one gets a range of possible values for the unknowns (location and amplitudes of motion). True values of the parameters will be bounded by these ranges of values and conservative values for the unknowns may be used in making decisions. Note that, in the case of periodic motion, the lower and upper bounds are obtained when $\cos\alpha$ in equation (3.42) takes the values of minus one and plus one, respectively. Thus,

$$R_{iLB} = 2^{-1}W_{x_i}^2 X1 + 2^{-1}W_{y_i}^2 X2 - |W_{x_i} W_{y_i}|(X1X2)^{1/2}, \tag{3.45}$$

and

$$R_{iUB} = 2^{-1}W_{x_i}^2 X1 + 2^{-1}W_{y_i}^2 X2 + |W_{x_i} W_{y_i}|(X1X2)^{1/2}, \tag{3.46}$$

The actual value for R_i is bounded by R_{iLB} and R_{iUB}.

B. Development of Statistical Techniques

It can be seen from equation (3.42) that the APSD of the detector response is a function of the vibrator location r_p (XP, YP) through the W_x and W_y functions, and the vibration trajectory characteristics given by X1, X2 and X3. The problem of vibration identification for two-dimensional space involves the estimation of the five parameters XP, YP, X1, X2, X3, represented by the vector 0, that characterize the vibration, from measured detector signals. Note that when multiple sources are involved, a set of five parameters are associated with each one of them. Even though there may be many sources, it was assumed that one (in this study) or only a few may malfunction and vibrate above a certain amplitude threshold. Experimental measurements, like the detector response, are always subject to measurement error. An appropriate statistical probability model describing the error structure must be specified to be able to make statements about the reliability of the parameter estimates.

The measurement error can be modeled statistically by assuming an additive or a multiplicative type of error. The APSD of the detector response given by equation (3.42) is considered as a median value, R'_i, of the distribution. The APSD of the measured detector signal, R_i, is then given, for an additive type of error, as

$$R_i = R'_i(1 + \sigma_f z), \tag{3.47}$$

where σ_f is the fractional standard deviation of the normally distributed observed responses, and z is a normally distributed random deviate with zero mean and unit variance, that is, $z \sim N(0,1)$. With this model, R_i may become negative for large values of σ_f. A more appropriate statistical model may be one with a multiplicative type of measurement error, especially when large values of σ_f are involved. In this case (47),

$$R_i = R'_i \exp(\sigma_f z), \tag{3.48}$$

where σ_f is the coefficient of variation of the lognormally distributed responses R_i with mean value $\ln R'_i$. With this model, R_i is always assumed to be positive and the error is a constant proportion of the detector signals. Note that these two models may be appropriate under the assumption of large sample space as assured by the central limit theorem. But, it must be noted that the inference may depend heavily upon the model selected when small sample sizes are used. In this study, a log-normal model was used.

The detector signal may also be contaminated with signals from sources other than the vibrations (external noise). In this study, external noise was assumed to be a constant proportion (EN) of the measured detector signal. The detector signal, R_{ENi}, with external noise is given by

$$R_{ENi} = R_i(1 + EN), \tag{3.49}$$

where R_i is defined by equation (3.48).

Another factor that needs to be considered is an error in modeling the detector response by equation (3.42). It is not possible to model the detector responses exactly since all theoretical formulations involve some approximations. This type of error may also be modeled as a bias, B, similar to the external noise. But in this case, the bias can add or subtract. The effect of the measurement error, σ_f, external noise, EN, and the model bias, B, on the estimation procedures developed, must be studied.

The estimation process may be described as follows: Given the sample $\{x : x_1,\ldots,x_n\}$ from a parent population distribution, $f(x;\theta)$, which is known if the parameter set θ is known, one selects the value of the parameter set θ' or a function of $g(\theta')$ that will closely identify the sample to the parent population. A statistic or a function that defines the value of the estimate is an estimator. If the estimator provides a single value it is a point estimate, but if a set of plausible values are determined it is a set estimate. Optimum estimators must satisfy certain properties like unbiasedness and minimum variance. These properties assure the closeness of the estimate to the true value. The mean square error of the estimator is defined as

the sum of the squares of the bias and variance of the estimate and a minimum value of this is usually desired. Estimators that become unbiased and attains minimum variance as the number of observations become larger are known as consistent estimators.

1. Method of maximum likelihood

There are several methods (34, 35, 48) for finding point estimators, for example, the method of maximum likelihood and the method of least squares. The method of least squares may be used when the sample distribution is not known. If an asymptotically minimum variance unbiased estimator exists, the method of maximum likelihood will yield this. It should be noted that if the sample distribution is normal, the least squares and maximum likelihood techniques are identical.

The method of maximum likelihood, used to estimate vibration parameters, is explained as follows. Let $X_1,\ldots,X_n$ be random samples from a distribution function $f(x;0)$, where 0 is the set of population parameters, then the likelihood function, $L(x_1,\ldots,x_n;0)$ (34), is given by the joint density of the n random variables

$$L(x_1,\ldots,x_n;0) = \prod_{i=1}^{n} f(x_i;0). \qquad (3.50)$$

If we assume a multiplicative type of measurement error, each detector signal has a log-normal distribution as given

by equation (3.48). The likelihood function in this case associated with the measurements of m detector signals, $R_1,\ldots,R_m$ is given by

$$L(R_1,\ldots.R_m;0) = (2\pi)^{-m/2}\sigma_f^{-m} \exp(-2^{-1}\sum_{i=1}^{m}\sigma_f^{-2}(\ln R_i-\ln R'_i)^2). \tag{3.51}$$

The maximum likelihood estimate (0') of the parameters 0, is obtained as a solution to the equations

$$\frac{\partial L}{\partial 0} = 0. \tag{3.52}$$

Note that 0 is a vector and so the same number of equations as the number of parameters will be obtained. In the case of non-linear equations, as shown in (3.51), the easiest way to obtain maximum likelihood estimates would be to use direct search procedures. In such cases, estimates, 0', of 0 that will maximize equation (3.51) will be found by direct search in the five-dimensional parameter space. Note that the maximum of (3.51) is given by the minimum of the exponent of equation (3.51). A modification to this exponent when repeated measurements are taken, will be explained in the next section.

2. Confidence set method

The point estimate of a parameter does not provide an indication of the possible error of the estimate. It is desirable to obtain a range of plausible values (called a confidence region or set), together with a statement regarding the confidence that the true value of the parameter lies in this range. A measure of confidence, T, is called a confidence coefficient. One of the methods, for finding the confidence set is the pivotal quantity method (34). Consider a random sample $X_1 \ldots, X_n$ from a distribution $f(x;\theta)$ and $Q = q(x_1 \ldots, x_n;\theta)$, a function of the observations and the parameter set θ. If Q has a distribution that does not depend on θ, then Q is defined to be a pivotal quantity. Let q_1 and q_2 be independent of θ and $q_1 < q_2$; then the confidence, T, that Q lies within the range $[q_1, q_2]$, is given by the probability statement

$$P(q_1 < Q < q_2) = T. \qquad (3.53)$$

There may be many intervals $[q_1, q_2]$ that satisfy equation (3.53). An optimum interval is one which makes the average of the range, $[q_1, q_2]$ the smallest. The inequality stated in the probability statement, in equation (3.53), may now be inverted or pivoted to obtain

$$t_1(x_1, \ldots, x_n) < t(\theta) < t_2(x_1, \ldots, x_n), \qquad (3.54)$$

a plausible range of values for the parameter set 0 or a function, t(0), of 0.

In order to obtain confidence regions for the parameters, a pivotal quantity is first obtained. Consider a set of observations $R_1,\ldots,R_m$ from m detectors. This is a sample from a log-normal distribution when the measurement error is multiplicative. Then the quantity

$$Z_i = (\ln R_i - \ln R'_i)/\sigma_f \qquad (3.55)$$

is normally distributed with zero mean and unit variance. The square of Z_i is chi-squared distributed with one degree of freedom (35) and the sum of m such squared quantities is chi-squared distributed with m degrees of freedom. The pivotal quantity, Q, in this case, is given by

$$Q = \sum_{i=1}^{m} (Z_i)^2 \sim \chi^2_m \ . \qquad (3.56)$$

Usually, one takes repeated (n) measurements of $\ln R_i$ and in this case it can be shown that (49)

$$Q = n \sum_{i=1}^{m} \sigma_f^{-2} (\overline{\ln R}_i - \ln R'_i)^2 + K, \qquad (3.57)$$

where K is a quantity independent of 0, with a distribution $\chi^2_{m(n-1)}$. This latter term is neglected since it is a random constant noise that will bring in instability to the calculations. The first term of equation (3.57) involves the mean value, $\overline{\ln R}_i$, and variance, σ_f^2/n, of the n

measurements. It also has a chi-squared distribution with m degrees of freedom.

Once, the pivotal quantity is obtained, a range of possible values of the parameter set, 0, may be obtained as follows. Select a confidence coefficient T, and from tabulated values of χ^2 find the value $q_1 = \chi^2_m(1-T)$ and $q_2 = \chi^2_m(T)$. As an example with T =.9 and m = 3, $\chi^2_m(.9)$ is 6.25. Then find the values of the parameter set such that Q (given by equation (3.57) without the K) is bounded by q_1 and q_2. In actual practice only the upper limit q_2 was used assuming that q_1 was close to zero, which may not always be true. It must be pointed out that the exponent in equation (3.51) is given by Q in equation (3.56) divided by minus two. When repeated measurements are involved Q given by equation (3.57) may be minimized. Thus it can be seen that the maximum likelihood estimate corresponds to the minimum of the chi-squared distributed quantity, Q, (given by equation (3.57)) in the five-dimensional space. The confidence region represents those values of the parameter set that bounds Q by q_1 and q_2. In the case of only two parameters, q_1 and q_2 represent planes through a three dimensional plot of Q. The intersection of these planes with this plot of Q is projected onto the respective axes to get a confidence region for the parameters.

When a model bias or an external noise is included in the detector signal, a noncentrality will be introduced into the χ^2_m distribution. For example if the external noise, (EN), is added as shown in equation (3.49) with a multiplicative type model, the distribution of Q in equation (3.57) is $\chi^2_{m,\lambda}$ where λ, the noncentrality factor, can be shown to be equal to (35)

$$\lambda = n \sum_{i=1}^{m} \sigma_f^{-2} (\ln(1+EN))^2. \qquad (3.58)$$

In the development of both the maximum likelihood and confidence region methods, it was assumed that σ_f is known. This is usually not true and σ_f must be obtained from measurements. In such cases the distribution is no longer chi-squared as shown below. Let R_{ij} be the jth measurement using the detector i. If n measurements are taken using m detectors then the constant unbiased sample variance, S^2, is given by

$$S^2 = m^{-1}(n-1)^{-1} \sum_i \sum_j (\ln R_{ij} - \overline{\ln R_i})^2. \qquad (3.59)$$

It can be shown that

$$Q_1 = n/m \sum_{i=1}^{m} S^{-2}(\overline{\ln R_i} - \ln R'_i) \sim F^m_{m(n-1)}. \qquad (3.60)$$

The quantity Q_1 with an estimate S^2 of the variance, σ^2_f, has an F distribution. In order to arrive at this

conclusion the following results (35) were used:

1. the first term of equation (3.57) is χ^2_m distributed,
2. $m(n-1)S^2/\sigma^2$ is $\chi^2_{m(n-1)}$ distributed,
3. (1) and (2) (above) are independent,
4. and the ratio of (1)/m to (2)/(m(n-1)) has an F distribution.

3. Information matrix

The parameter set, 0, characterizing the vibrations of a component, can be estimated efficiently, if an optimal number and pattern of detectors are used. The variance of a parameter is a measure of how well the data estimate the parameter. The information matrix (50) provides lower bounds for these variances. Different detector patterns may be compared based on these variance estimates. The detector pattern that gives the lowest variance for the estimates may be chosen as the optimum detector pattern. A disadvantage of this technique is that one needs to have some knowledge about the values of the unknown parameters.

Silvey (36) presents the information matrix as a method for optimizing the design of an experiment. The logarithm of the likelihood, lnL, associated with the measurements of m detectors, each with n repeated measurements, is given, for a multiplicative type error model, by

$$\ln L(.;0) = Z_1 - 2^{-1} n \sum_{i=1}^{m} \sigma_f^{-2} (\overline{\ln R_i} - \ln R'_i)^2 - K/2, \tag{3.61}$$

where equation (3.57) divided by minus two instead of the exponent in equation (3.51) was used. The logarithm of the constants in equation (3.51) is represented by Z_1 which is independent of 0. The constant K is also independent of 0. The (ℓ,k)th component of the Fisher information matrix, $I_{\ell,k}$, is given in terms of the expectation operator, E_0, by (50)

$$I_{\ell,k} = -E_0(\partial^2 \ln L(.;0)/\partial 0_\ell \partial 0_k), \tag{3.62}$$

where 0_ℓ and 0_k are the components of the parameter set 0. It is shown in Silvey (50) that the inverse, $[I_{\ell,k}]^{-1}$ of the information matrix is the lower bound covariance matrix for the estimator. The diagonal elements, $[I_{\ell,\ell}]^{-1}$, represent the lower bound variances of the parameter estimates $0_{\ell\ell}$.

The information matrix is singular if the number of detectors is less than the number of parameters. To reduce the number of detectors to a practical level a conditional information matrix may be obtained using only a subset of the parameter set 0. The rest of the parameters in the set are assumed to be known. The conditional variances of the parameters may be compared for various patterns to obtain optimum patterns.

IV. NUMERICAL INVESTIGATION

The techniques developed in the previous section were verified by means of simulated computer experiments based on a bare homogenous reactor (21). The procedures developed to investigate the statistical techniques and a discussion of the results are presented in this chapter.

A. Generation of the Simulated Detector Signals

Equation (3.18) may be written for a bare, homogenous reactor with only one energy group, in the plateau region of the reactor frequency response, as

$$\nabla^2\Delta\phi + B^2(\omega)\ \Delta\phi = \Delta\Sigma_a\phi_0/D, \qquad (4.1)$$

where

$$B(\omega)^2 = K_\infty(1-\beta)M^{-2} - M^{-2} - B_z^2. \qquad (4.2)$$

and B_z^2 is the transverse buckling. The infinite multiplication factor, K_∞, and the migration area M^2, are given by $\nu\Sigma_f/\Sigma_a$ and D/Σ_a, respectively. The Green's function, G, for (4.1) is obtained when the right hand side is replaced by $\delta(r-r_p)$. To solve the two-dimensional problem, G is expanded in an infinite series (43) of the form

$$G(x,XP,y,YP) = \sum_{n=1}^{\infty} X_n Y_n \quad , \tag{4.3}$$

where

$$X_n = -2a^{-1} \sin(B_n x)\sin(B_n XP). \tag{4.4}$$

and B_n is given by $n\pi/a$, where a is the side dimension of the square reactor. Equation (4.3) is substituted into the two-dimensional equation satisfied by G and using the orthogonality relations of the sine functions, one gets the following equation which is satisfied by Y_n

$$d^2Y_n/dy^2 - K_n^2 Y_n = \delta(y-y_o), \tag{4.5}$$

where K_n^2 is given by

$$K_n^2 = B_n^2 - B(\omega)^2. \tag{4.6}$$

The solution of (4.5) depends on the sign of K_n^2. If K_n^2 is negative the solution involves sine terms and if it is positive the solution involves hyperbolic or exponential terms. The solutions are obtained by solving the homogenous equations for the cases when y, the detector location, is less than YP, the vibrator location and also for y greater than YP. The source (δ function) is taken into account using continuity and jump conditions at the interface (y = YP). Boundary conditions are used to evaluate the rest of the constants. The Green's function solutions, G(x, y, XP, YP), for the forward system may be written as,

if $K_n^2 < 0$

$$G = \sum_{n=1}^{\infty} X_n K_n^{-1} \sin(K_n y)[\cos(K_n YP) - \sin(K_n YP)/\tan(K_n a)]$$

$$\text{if } y < YP \qquad (4.7a)$$

$$G = \sum_{n=1}^{\infty} X_n K_n^{-1} \sin(K_n YP)[\cos(K_n y) - \sin(K_n y)/\tan(K_n a)]$$

$$\text{if } y > YP \qquad (4.7b)$$

and if $K_n^2 > 0$

$$G = \sum_{n=1}^{\infty} X_n 2^{-1}(\exp(-K_n(YP-y)) + \exp(-K_n(2a+y-YP)) -$$

$$\exp(-K_n(2a-y-YP)) - \exp(-K_n(y+YP)))$$

$$\text{if } y < YP \qquad (4.8a)$$

$$G = \sum_{n=1}^{\infty} X_n 2^{-1}(\exp(-K_n(y-YP)) + \exp(-K_n(2a+YP-y)) -$$

$$\exp(-K_n(2a-YP-y)) - \exp(-K_n(y+YP)))$$

$$\text{if } y > YP \qquad (4.8b)$$

The critical flux in the reactor is given by

$$\phi = \phi_o \sin(B_1 x)\sin(B_1 y). \qquad (4.9)$$

The APSD of the detector response (with the assumption of a point detector of unit cross section and a single point source of unit strength) may now be evaluated for two-dimensional periodic motion using equation (3.42) (see Appendix C program RESPON). The following values, $K_\infty = 1.0152$, $M^2 = 56\ cm^2$, $\beta = .007$, $B_z^2 = 0.0$ and $a = 270$ cm, were used for the reactor constants. In the following analysis the vibrator was assumed to be located at (125 cm, 125 cm) in the square reactor. Figure 4.1 shows the locations of the detectors and the vibrator used in this chapter. The origin of the coordinate system is at one corner of the reactor. The detector response, calculated using equation (3.42) is taken as the median value of a log-normal distribution. Simulated measured detector signal may now be generated using equation (3.48) (see Appendix C program SIMDET). The normally distributed random numbers, z, are available from a subroutine on the computer, and a value is assumed for σ_f. Note that noisy signals are generated by using larger values of σ_f. These detector signals were used in obtaining maximum-likelihood estimates or confidence regions for the various vibration parameters.

It was pointed out in the last section that the information matrix could be used to obtain optimum patterns of detectors required in the estimation process. Since the vibrator location is already known, the procedure for

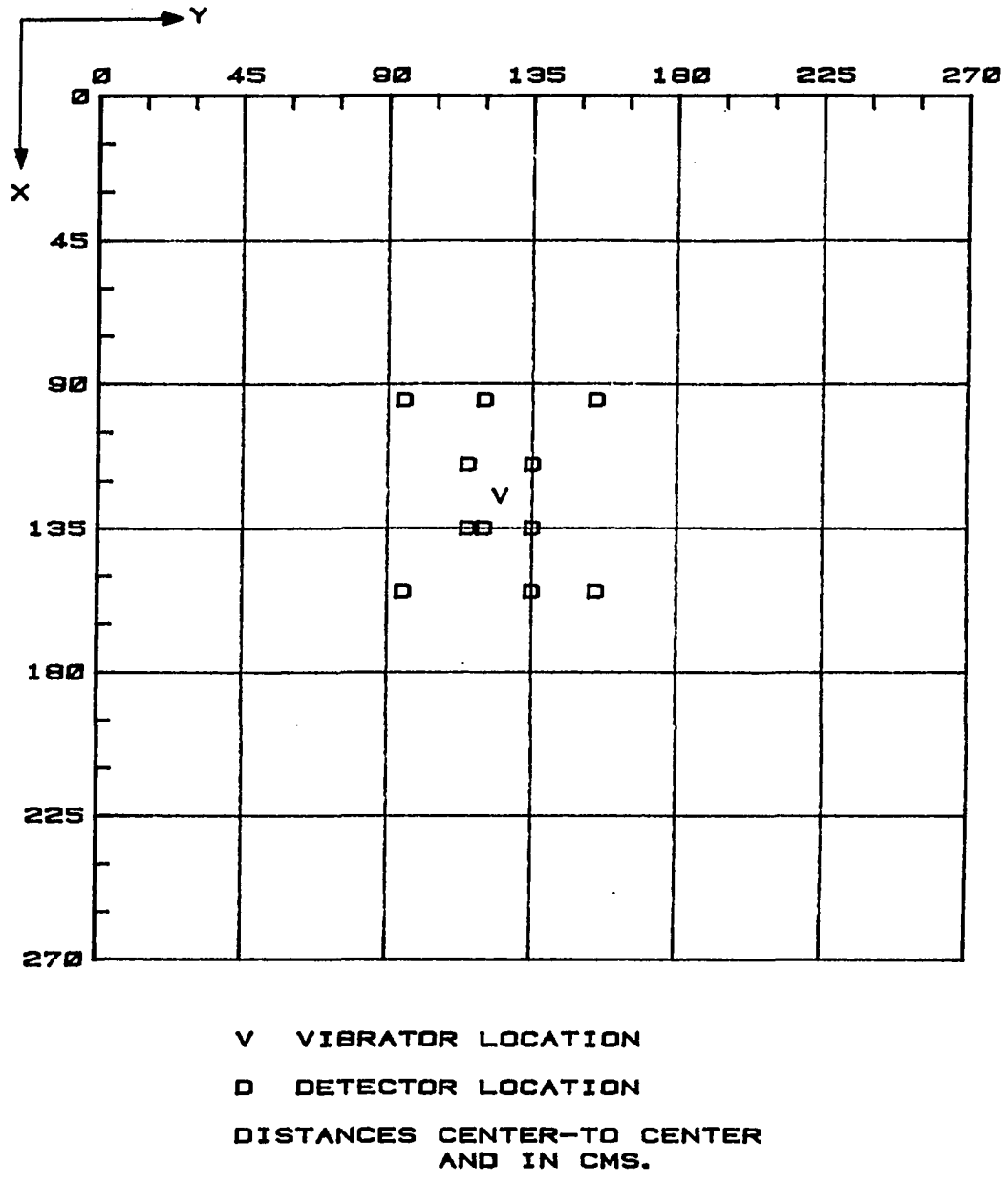

FIGURE 4.1. Locations of the vibrator and detectors used in Chapter IV

selecting an optimum detector pattern will be demonstrated first. Note that the calculation of the information matrix does not involve the use of measured data.

B. Analysis Using Information Matrix

The conditional information matrix, assuming the parameter X3 to be known, may be calculated using equation (3.62), for the vibrator location (125, 125) cm. The inverse of the resulting 4 x 4 matrix is the covariance matrix. The results are summarized for various cases in Table 4.1. The minimum number of detectors required is four since there are four unknown parameters.

The first case is one with four detectors located symmetrically about 14 cm from the vibrator. The minimum standard error (square root of the variance) of the four parameters, two location (XP and YP) and two amplitude parameters (X1 and X2) is given in Table 4.1. These standard errors are very large indicating that at least two of the detectors have approximately the same response. If the responses of two detectors were exactly the same, the rank of the information matrix would be one less than its order, and the matrix would be singular. In such cases there is no way to differentiate between the two detectors. Since the variances are large it may be concluded that this pattern is not 'good'. It should be noted that a spatially

TABLE 4.1. Standard errors of the parameter estimates for the various cases considered in Chapter IV

	Actual values[a]			125.	125.	0.01	0.01
CASE	DETECTOR PATTERN[b]		i/j/k[c]	XP (cm)	YP (cm)	X1 (cm^2)	X2 (cm^2)
1	(115,115) (135,135) (115,135) (135,115)		.1/0./30	3.65E6	3.65E6	6.52E3	6.52E3
2	(115,115) (135,135) (115,135) (135,120)		.1/0./30	5.83	5.81	0.12E-1	0.11E-1
3	(115,115) (135,135) (115,135) (135,120)		.5/0./30	29.17	29.05	0.57E-1	0.55E-1
6	(95,95) (155,155) (95,155) (155,95)		.1/0./30	very large			
7	(95,95) (155,155) (95,155) (95,120)		.1/0./30	0.61	3.76	0.24E-2	0.19E-2
8	(95,95) (155,155) (95,155)	(155,135) (155,95)	.1/0./30	0.37	0.75	0.23E-3	0.19E-3
9	(95,95) (155,155) (95,120) (155,135) (95,155) (155,95)		.1/0./30	0.31	0.22	0.12E-3	0.17E-3

[a] $X3=0.0071\ cm^2$.

[b] (x,y) location in cm.

[c] i/j/k; fractional standard deviation/EN/number of averages.

symmetric pattern is not necessarily symmetric as far as the detector response is concerned. In case 2 (Table 4.1), one of the detectors is replaced with another at the location shown. This reduces the standard errors to reasonable numbers. Case 3 shows the effect on the standard errors of the parameters of increasing the σ_f to 0.5. It can be seen that the increase is proportional to the change in σ_f. In case (6), the detectors are moved out to about 41 cm from the vibrator. This again is a symmetric pattern resulting in large variances. In case 7, one detector from the previous pattern is moved to another location. In this case the minimum standard error of the location parameter XP is less than 0.7 cm and that of YP is about 3.8 cm. The standard errors of the amplitude parameters are of the same order as the parameters themselves. In case 8, one more detector is added to the detector pattern in case 6 and as expected all the standard errors are smaller. The location parameter YP may be estimated within 0.6 cm. The addition of one more detector (total 6 detectors) reduced the standard errors of the amplitude parameters by a factor of ten from that in case 7. The standard error of the location parameters was less than 0.31 cm.

The above study shows the effect of the detector pattern and number of detectors on the standard errors of the parameter estimates. An optimum detector pattern may be

selected from a set of available detectors, using the standard error as a criterion, provided an approximate range of values of the parameters (like the approximate location) is known. Even though the detector pattern in case 7 yields better standard error values it may not be that much of an improvement from the detector pattern in case 6.

Often, it may be of interest to find a region where a vibration can be localized using a given detector pattern. In this case the conditional variances of the location parameters in the region of interest may be determined. Variances for the location parameters were calculated using the detector pattern in case 7. Figure 4.2 shows the standard errors of the location parameter, XP, at different locations along the y direction for three fixed values of x. Figure 4.3 shows standard errors for the estimate of the YP parameter for the same situation as above. If, for a particular location, the standard error is small, a vibrator at this point may be located easily. A converged solution was not obtained along lines passing through the detector locations. Therefore, the standard errors along lines passing through a detector location were not calculated. In Figures 4.2 and 4.3 the points where the plots go to zero are on lines passing through the detector locations. Also, at some locations very large values of standard errors were obtained, and for convenience in plotting, points with a

standard error larger than 8 cm were set to 8 cm. For practical reasons, a standard error larger than 8 cm may be considered to be too large. Figures 4.2 and 4.3 show that the standard errors are large for locations far away from the detectors (170 cm). These plots show that the standard errors for the two location parameters are less than 2 cm along a line passing through 70 cm and 120 cm for x locations and for y locations close to the detector pattern. Similar analysis may be done for the entire region and the locations with standard errors less than some reasonable value may be determined. Thus, the analysis of the problem with the information matrix will help to resolve the question of optimal positioning or number of detectors required to identify vibrating components.

The numerical testing of the maximum likelihood and confidence region methods is described next.

C. Analysis Based on the Maximum Likelihood Method

In order to obtain the maximum likelihood estimates of the parameters XP, YP, X1, X2 and X3, equation (3.57) is minimized with respect to these parameters. If some of the parameters are known they may be used to obtain conditional estimates of the rest of the parameters. To take into account n repeated measurements of a detector signal, the detector responses were generated using n random numbers for

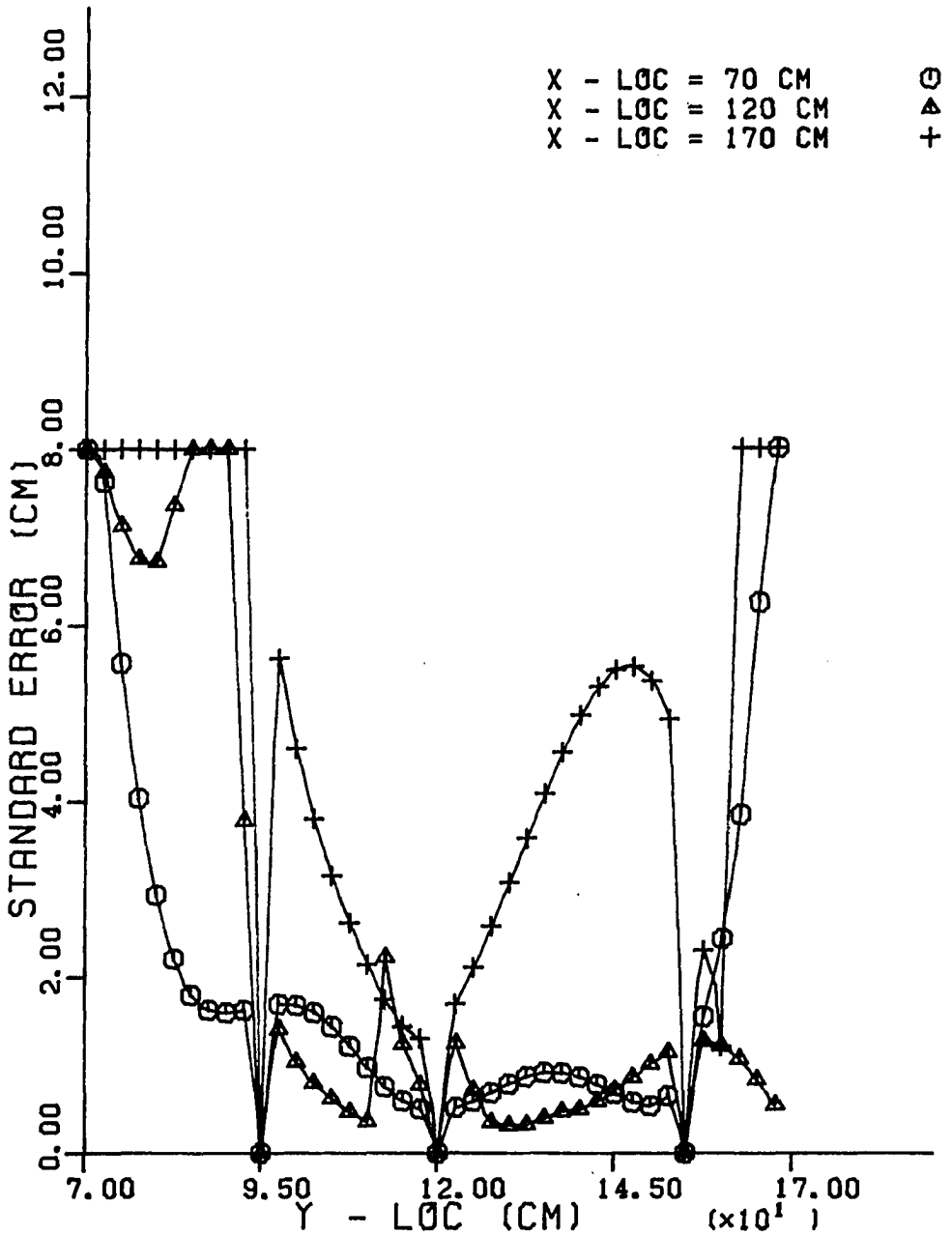

FIGURE 4.2. Standard error for the XP parameter for different locations for the detector pattern in case 7

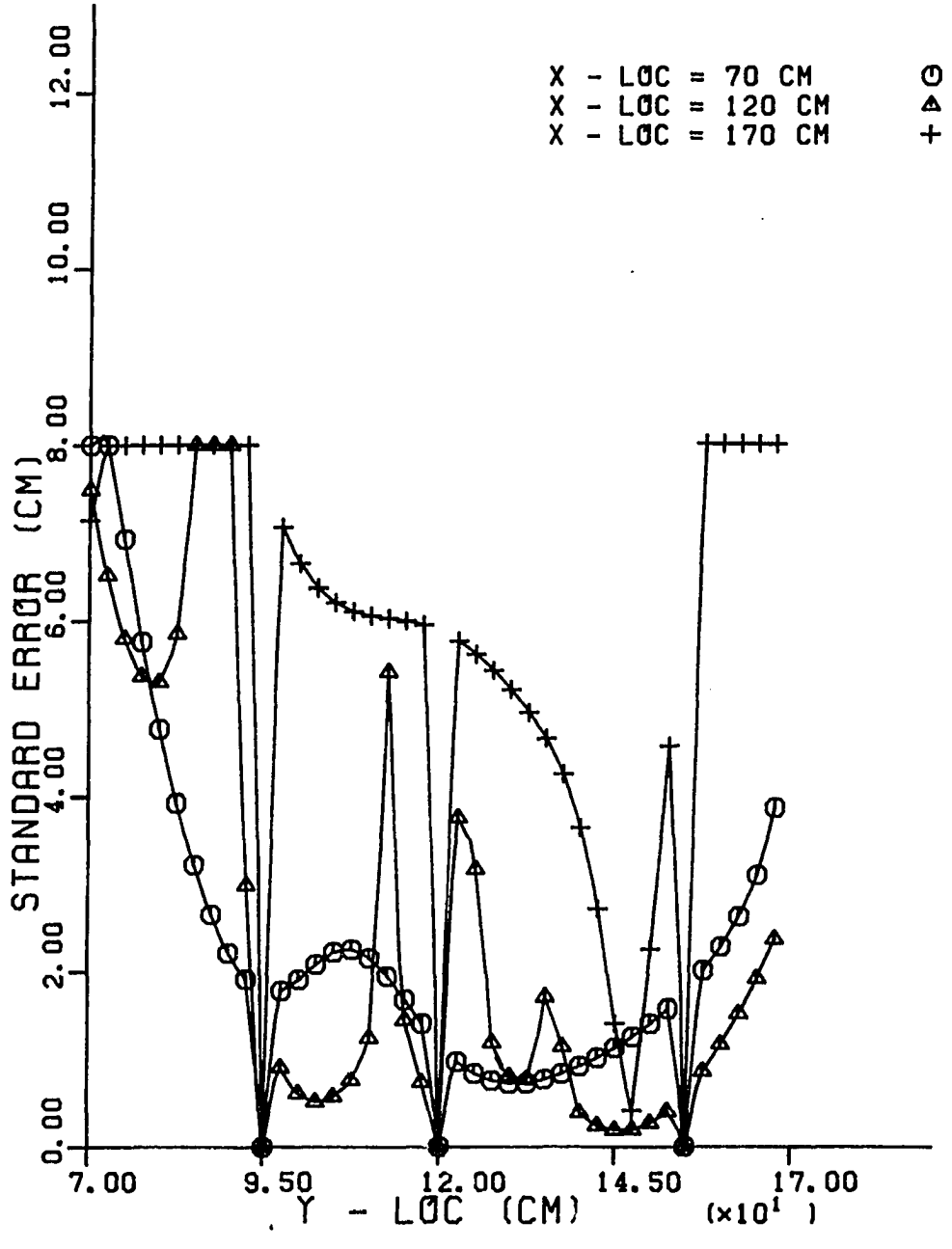

FIGURE 4.3. Standard error for the YP parameter for different locations for the detector pattern in case 7

each detector and then averaged to obtain $\overline{\ln R_i}$ for use in equation (3.57).

The minimization was carried out by searching through the parameter space (see Appendix C program MINXAM). The value of the function, Q, given by equation (3.57) is calculated at a starting value of the parameter set and also on either side of the starting point at values determined by a given step size. The parameter set for which the function Q is a minimum is used as the next starting value. When the parameter set value does not change within a specified limit the step size is decreased. This process is continued until the absolute minimum is found within a user defined accuracy. Other efficient techniques of minimization are available but were not used since the problem was simple enough to be handled by the above approach.

Since there are five parameters to be determined, one would expect to use at least five detectors for the estimation process. If all the parameters are allowed to vary continuously the number of detectors must be equal to the number of parameters. But, it was observed that in such cases the problem converged very slowly. The convergence rate was increased by the addition of one more detector. In the following analysis six detectors were located at x and y distances (in cms) (81, 81), (81, 135), (108, 81), (108, 135), (162, 81) and (162, 135), in the reactor. The

vibrator was located at XP = 135 cm and YP = 108 cm, with vibration parameters X1 = X2 = .01 cm^2 and X3 = .0071 cm^2. A fractional standard error of 50% was used to generate simulated detector signals. A search through the parameter space was performed to obtain the minimum of equation (3.57). The location parameters were estimated to within 0.25 cm and the intensity parameters within 3% of the actual values. This analysis demonstrated the feasibility of estimating all the five parameters simultaneously. To reduce the complexity of the problem, one of the parameters, namely X3, was assumed to be known. In the following analysis X3 was taken as 0.0071. Note that since one of the parameters was assumed to be known the other parameter estimates are conditional estimates. To generate the simulated detector signals, the vibrator was assumed to be located at (125 cm, 125 cm), (see Figure 4.1) and the two amplitude parameters were assumed to be 0.01 cm^2. The maximum likelihood estimates were obtained for the various detector patterns considered in Table 4.1 and the results are summarized in Table 4.2.

The detector patterns which yielded high values for the variances, cases 1 and 5, were also studied. As can be seen they also yielded reasonably good results but this discrepancy was not completely understood. It may be because the detector signal obtained after the randomization

TABLE 4.2. Maximum-likelihood estimates of the parameters for the different cases considered in Chapter IV

Actual values[a]				125.	125.	0.01	0.01
CASE	DETECTOR PATTERN[b]		i/j/k[c]	XP (cm)	YP (cm)	X1 (cm^2)	X2 (cm^2)
1	(115,115) (135,135) (115,135) (135,115)		.1/0./30	125.18	125.23	1.03E-2	1.02E-2
2	(115,115) (135,135) (115,135) (135,120)		.1/0./30	125.01	125.2	1.03E-2	9.88E-3
3	(115,115) (135,135) (115,135) (135,120)		.5/0./30	124.84	125.20	1.03E-2	1.02E-2
4	(115,115) (135,135) (115,135) (135,120)		.1/.2/30	125.21	124.94	1.10E-2	1.10E-2
5	(115,115) (135,135) (115,135) (135,120)		.5/0./8	125.93	125.53	1.10E-2	9.63E-3
6	(95,95) (155,155) (95,155) (155,95)		.1/0./30	120.84	134.50	1.10E-2	1.10E-2
7	(95,95) (155,155) (95,155) (95,120)		.1/0./30	126.75	124.93	1.05E-2	1.05E-2
8	(95,95) (155,155) (95,155) (155,95)	(155,135)	.1/0./30	125.21	127.43	1.07E-2	1.06E-2
9	(95,95) (155,155) (95,120) (155,95)	(155,135)	.1/0./30	125.63	125.43	1.01E-2	1.04E-2

[a] X3=0.0071 cm^2.

[b] (x,y) location in cm.

[c] i/j/k; fractional standard deviation/EN/number of averages.

corresponded to that of a good pattern. Case 1 uses four detectors and a σ_f of 10%, EN of 0.0% and 30 averages of the detector signals. The estimates of the parameters and their actual values are given in Table 4.2. In case 2, one of the detectors is moved to a new location. The estimates are only slightly better, even though the information matrix analysis showed a remarkable difference in the two patterns. An increase in σ_f from 10% to 50% had very little effect on the estimates as shown by case 3. In case 4, the effect of external noise, EN, of 20%, is shown and the next case (5) shows the effect of reducing the number of averages from thirty to eight. The estimates, especially for the location parameters, are different from the actual value by as much as 9.5 cm in case 6 where a symmetric detector pattern was used. This may be explained on the basis of the high variance observed for this pattern. When one of the detectors in case 6 was moved, to form the detector pattern in case 7, the estimates were within 2 cm of the actual location parameters and within 5% of the actual amplitude variables. In cases 8 and 9, the effect of adding one and two more detectors, respectively, is shown. In all cases, except case 6, the location parameters were obtained within 2 cm and the amplitude parameters within 10% of the true values even in the presence of large (50%) values of σ_f and external noise (20%). Model bias, as pointed out earlier,

is treated the same way as external noise and this was therefore not investigated. The effect of the external noise is to increase the value of the minimum of Q. This indicates that it may not be possible to estimate external noise, with such minimization techniques, at least when the noise is additive as in equation (3.49). But, the insensitivity of the parameter estimates to external noise shows that its presence may be neglected without losing much accuracy in the estimation.

In reality, it may not be necessary to treat the parameters as continuous variables. The discretization of the space variables limits the number of potential vibrator sites. This limits the search space and the resulting advantages are discussed in the following paragraph.

In a reactor, the detector and vibrator locations are fixed and are known. The search over the location parameters may be limited to these discrete and finite number of locations. The unit response functions, for example, W_x and W_y, may be precalculated for a particular core configuration and stored. These numbers may be used in the estimation process as long as there is no significant change in core configuration. The minimization may be done as follows. A grid of potential vibrator sites are assumed to be present in the reactor. For each grid location, a minimum of the function Q is determined with respect to the

amplitude parameters X1, X2, and X3. The grid point at which the grand minimum (smallest Q) is obtained is the actual vibrator site. A global search, over the whole reactor, may be done first with a coarse mesh to identify a potential region that contains the vibrator. A finer mesh may be used in this region to isolate a particular vibrating component.

With three unknown amplitude parameters at each grid point one needs to use more than three detectors. If only three detectors are used, the minimization will result in values of the parameters such that Q is equal to zero at each grid point. In this case it is not possible to differentiate between the various potential vibrator sites and therefore, at least one more detector (in this case 4) than the number of parameters is required. This is still one less than the total number of parameters and this apparent reduction in the number of detectors required, may be due to the discretization of the space variables. In practice, it may be necessary to use more detectors, since some detectors may not be optimally located.

A study with the square reactor and a 5 x 5 potential vibrator grid separated by one cm was also carried out for different cases. In all the cases the location estimate, corresponding to the grand minimum of the twenty five vibrator locations, was within 2 cm of the actual value and

the vibration amplitudes, X1, X2 and X3, were obtained within 10%. The results showed the insensitivity of the estimates to the various factors like measurement error, external noise or bias, and detector pattern.

D. Analysis Based on Confidence Region

Confidence regions are determined using equation (3.57). A x^2_m value is determined for the number of detectors (equal to the degrees of freedom) and a required confidence coefficient. For example, if a 90% confidence is required and there are 3 detectors (3 degrees of freedom), one obtains, from tabulated values of chi-squared, $x^2_m(.9) = q_2 = 6.25$. In the following analysis only this upper limit is considered. The values of the parameters for which Q (in equation 3.57) is less than q_2 is determined, by searching through the entire parameter space (see Appendix C program CONFID). This represents the 90% confidence set or equivalently, there is a 90% confidence that the true value is within this set. A conditional confidence set is obtained when some of the parameters assume specified values, for example the true value or the maximum likelihood estimate of that parameter. The 90% confidence regions (conditional, since true values were assumed for the rest of the parameters) were determined for the two location parameters, XP and YP and the two amplitude parameters X1

and X2, for the different cases studied in the previous section (Table 4.2). The actual values of the parameters were the same as in the previous section. The detector pattern in case 2 (Table 4.2) is used for the following analysis. Figures 4.4 and 4.5 represent the 90% confidence regions for X1 and X2 and XP and YP, respectively, for two different fractional sigma. The size of the region increases as the error in the measurement increases and there is less certainty in the estimation of the parameters. For the same detector pattern, Figures 4.6 and 4.7 show the effect of external noise for X1 and X2 and XP and YP respectively. A larger region is obtained when an external noise is added. In this case the noncentral chi-squared distribution was used. The noncentrality factor, λ, was calculated using equation (3.58) for the parameters of case 4 as 399.0. For this case the noncentral chi-squared value is 455. The size of the confidence regions decreased when a larger number of measurements were used as shown in Figures 4.8 and 4.9 for X1 and X2 and XP and YP, respectively.

Figures 4.10 and 4.11 show the effect of various detector patterns on the confidence region for X1 and X2. A pattern closer to the vibrator evidently gives a smaller confidence region. The patterns which showed high variances (Table 4.1) yielded confidence regions which were in some cases smaller than others. This apparent anomaly could be

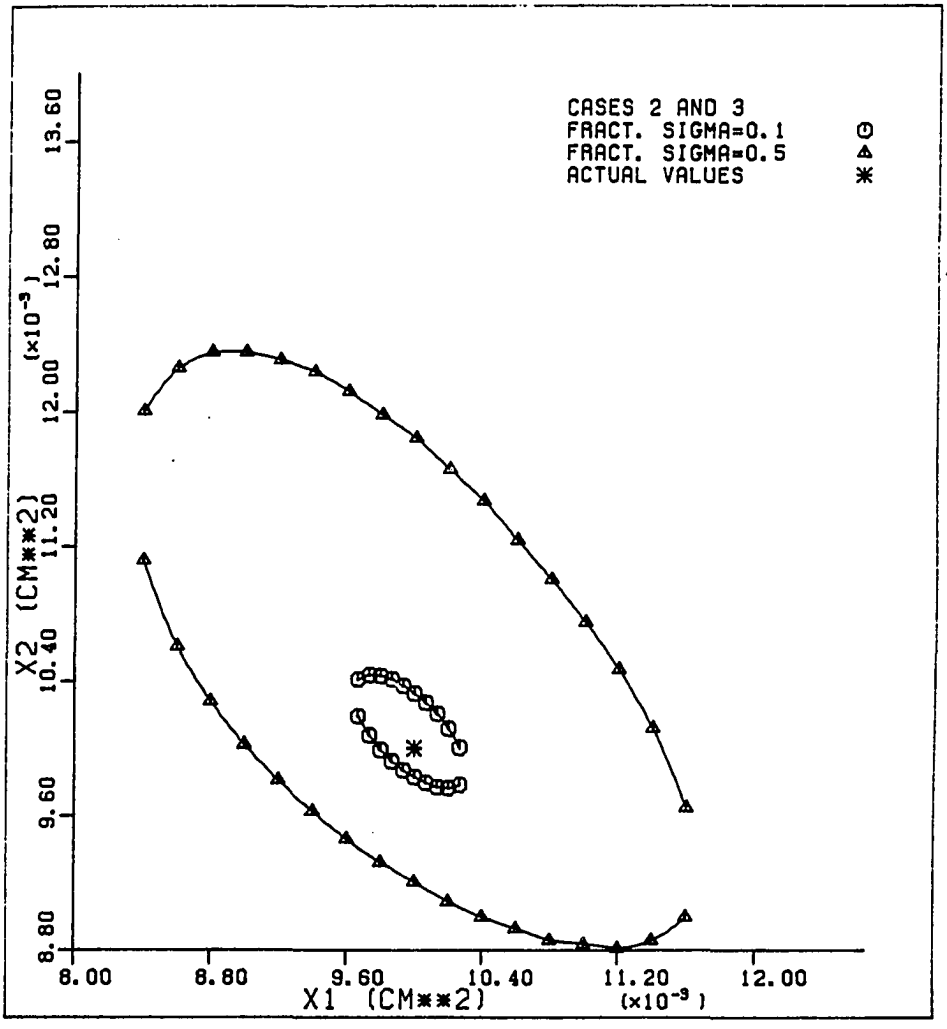

FIGURE 4.4. The 90% confidence region for X1 and X2 for two different values of σ_f

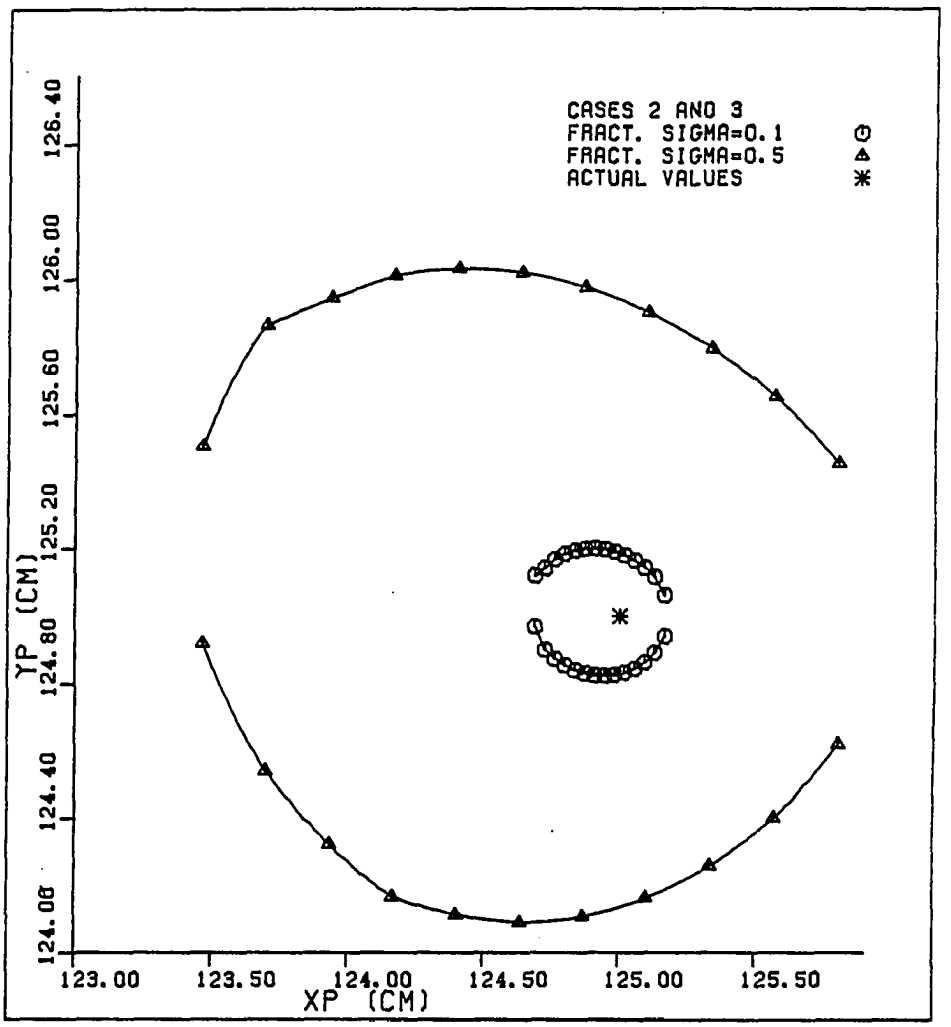

FIGURE 4.5. The 90% confidence region for XP and YP for two different values of σ_f

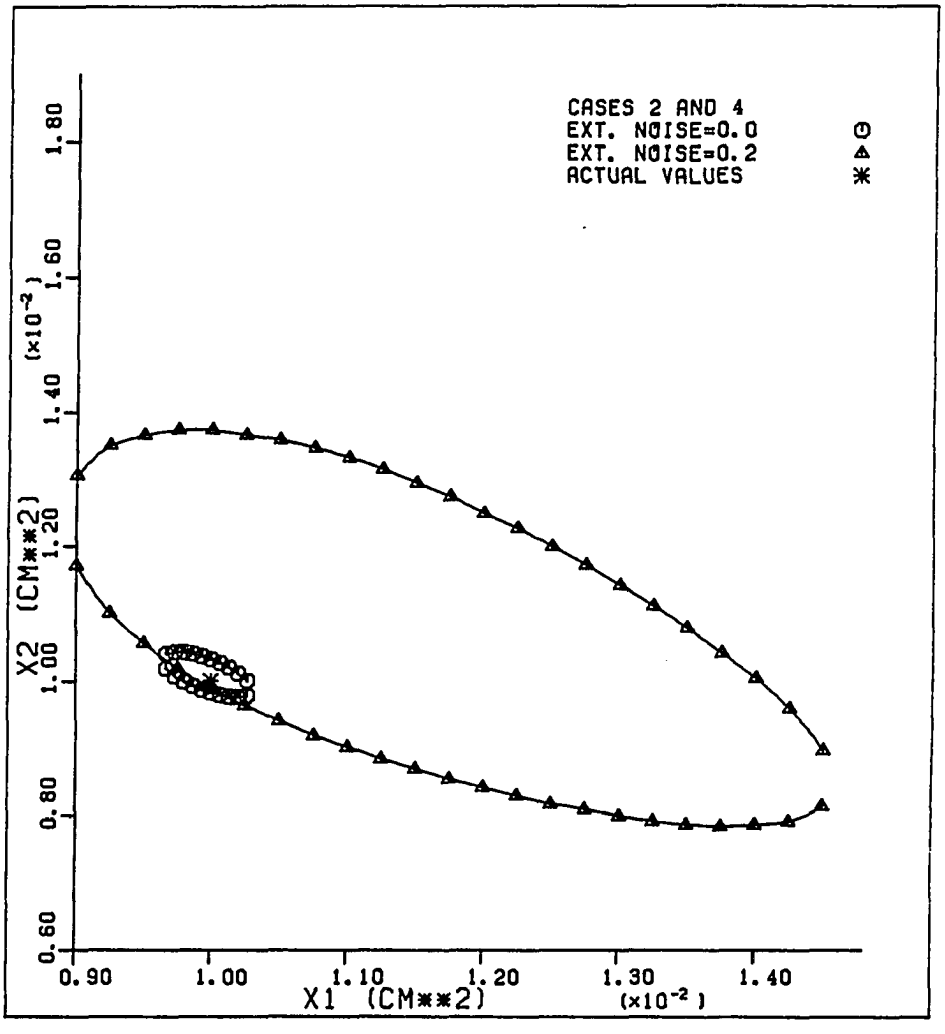

FIGURE 4.6. The 90% confidence region for X1 and X2 for two different values of external noise

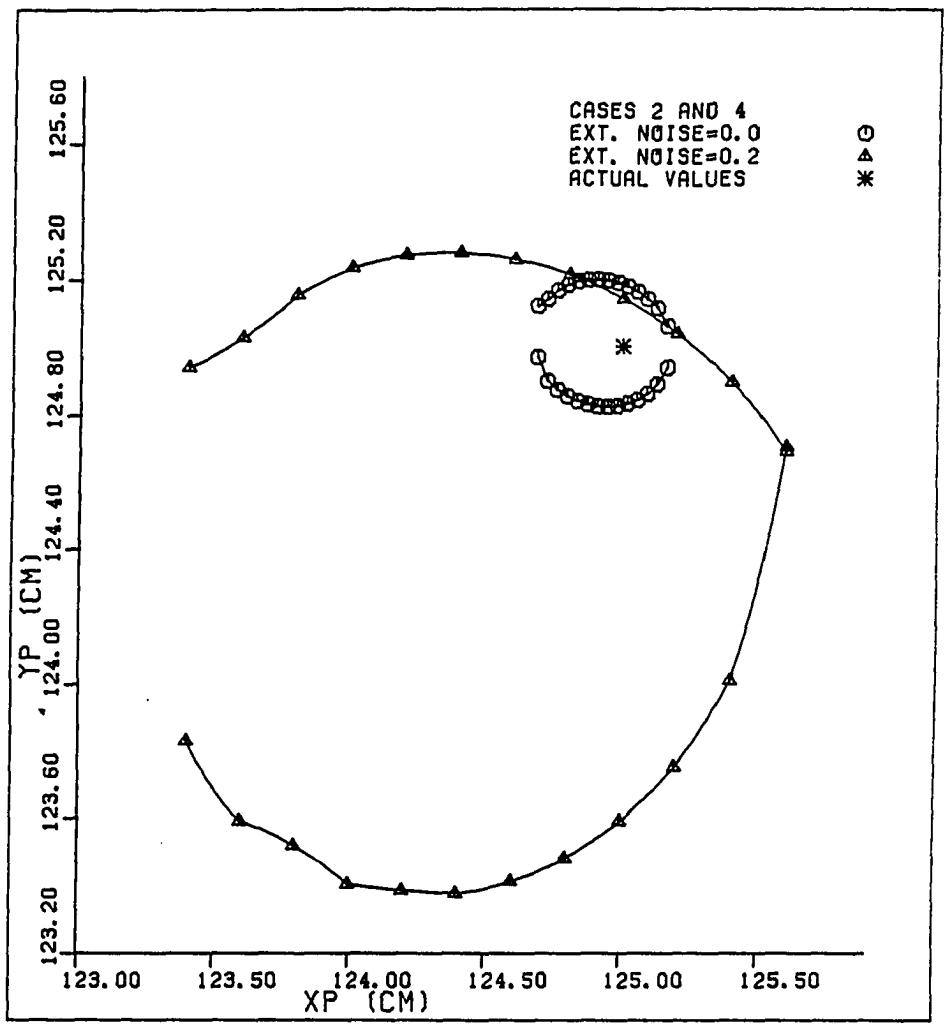

FIGURE 4.7. The 90% confidence region for XP and YP for two different values of external noise

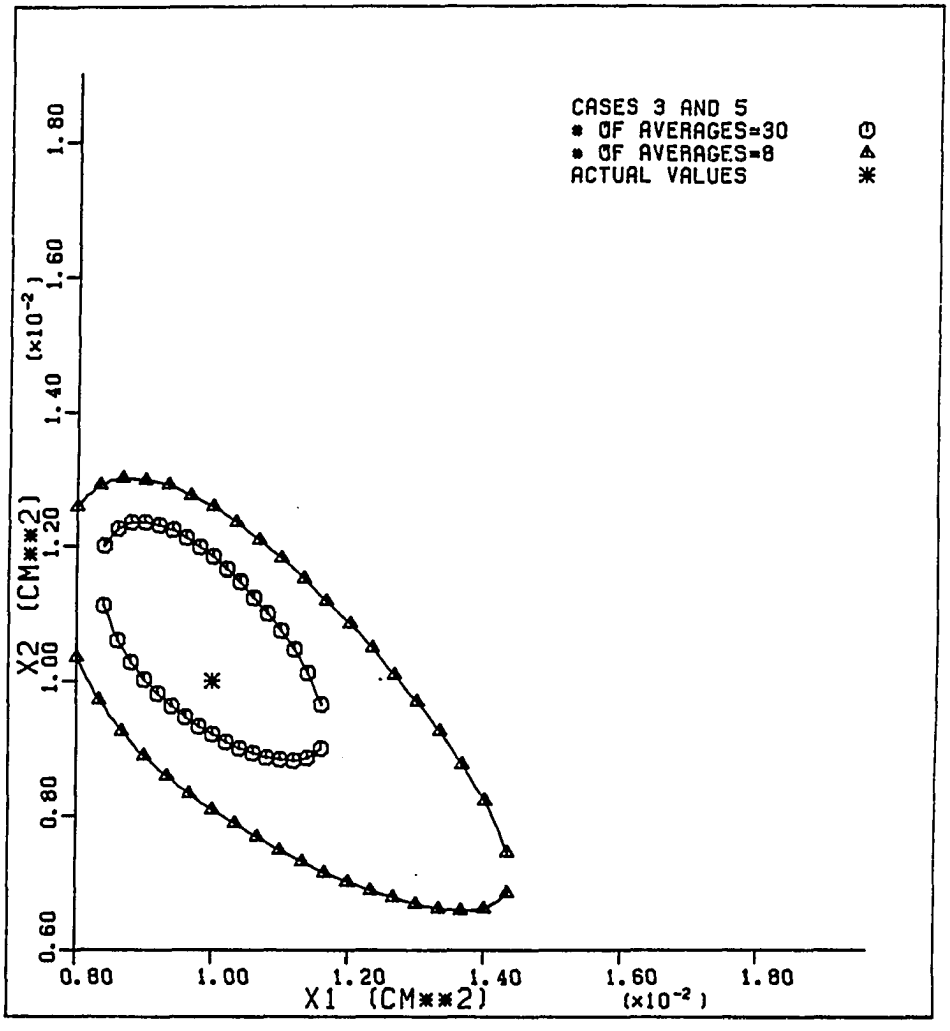

FIGURE 4.8. The 90% confidence region for X1 and X2 for two different number of averages

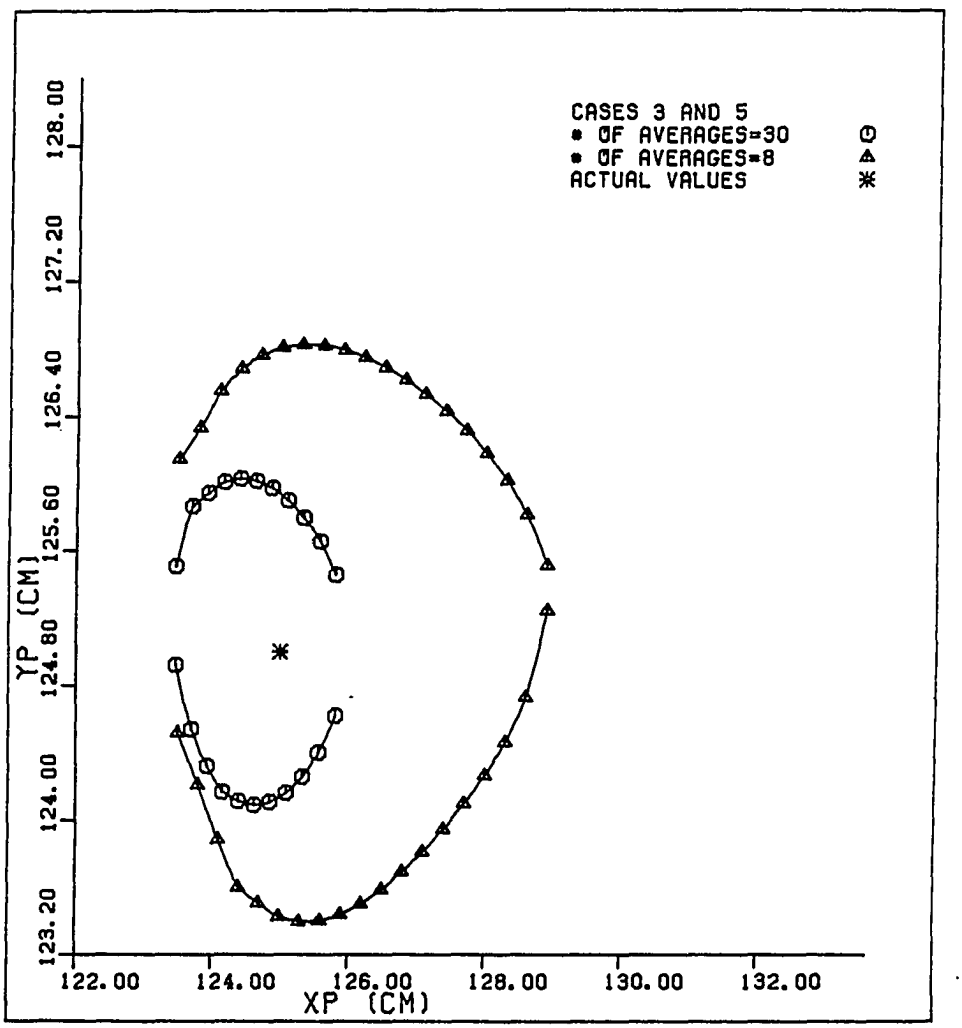

FIGURE 4.9. The 90% confidence region for XP and YP for two different number of averages

due to the effect of randomizing the detector responses. Other patterns that yielded reasonably high variances produced larger confidence regions. The results from the information matrix may be more reliable since it does not involve any randomization. Figure 4.11 shows that the addition of two more detectors did not make any significant change in the confidence region for X1 and X2.

The 90% confidence regions for the location parameters and the effect of detector patterns on this are shown in Figures 4.12 and 4.13. Figure 4.12 shows that the size of the confidence region increased as the detectors were moved out from about 14 cm to about 41 cm. The symmetric pattern (case 6) resulted in an elongated pattern as shown in figure 4.13. Note that the maximum likelihood estimates obtained for the same pattern were also significantly different from the true value. The addition of one more detector changed the shape of the region. A much tighter region resulted with six detectors. The location parameters seem to be more sensitive to the detector pattern than the vibration amplitude parameters.

As in the previous section the location parameters were discretized and the amplitude parameters were considered to be continuous. The values of Q (equation 3.57) were calculated for different grid positions by minimizing equation 3.57 with respect to the amplitude parameters at

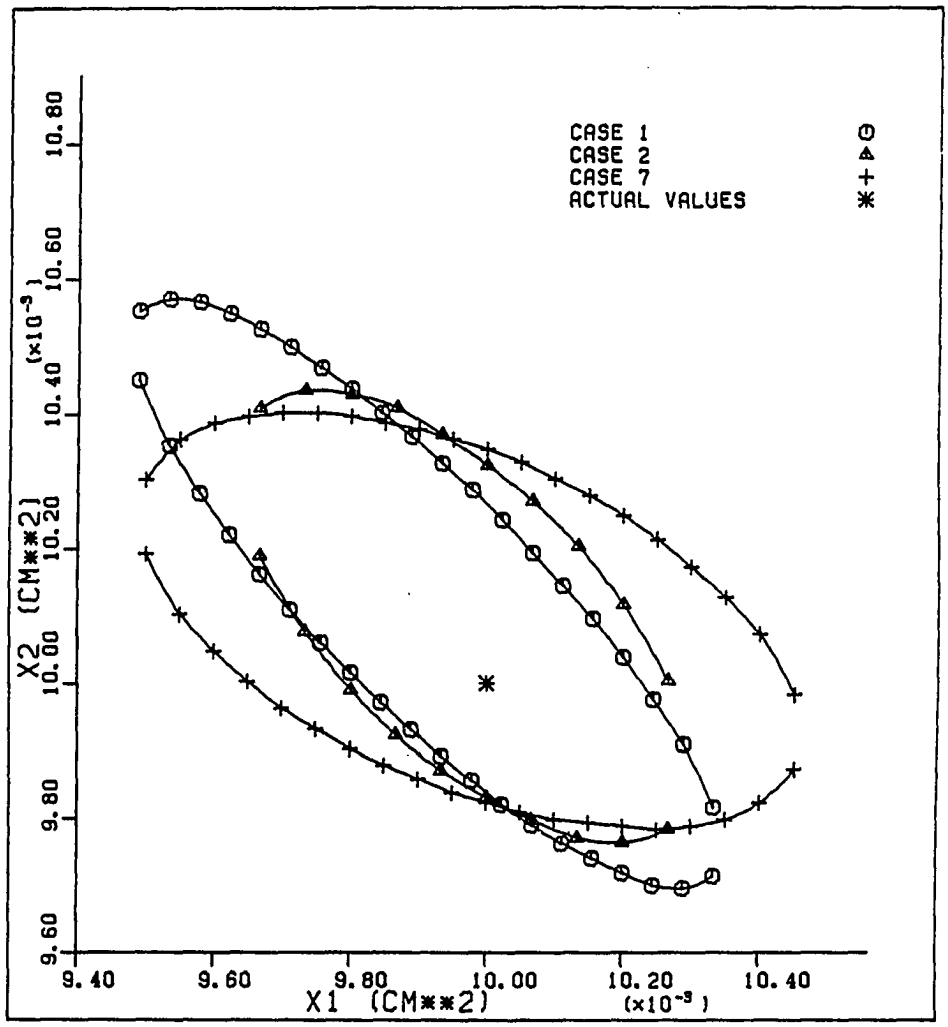

FIGURE 4.10. Effect of detector patterns on the 90% confidence region for X1 and X2

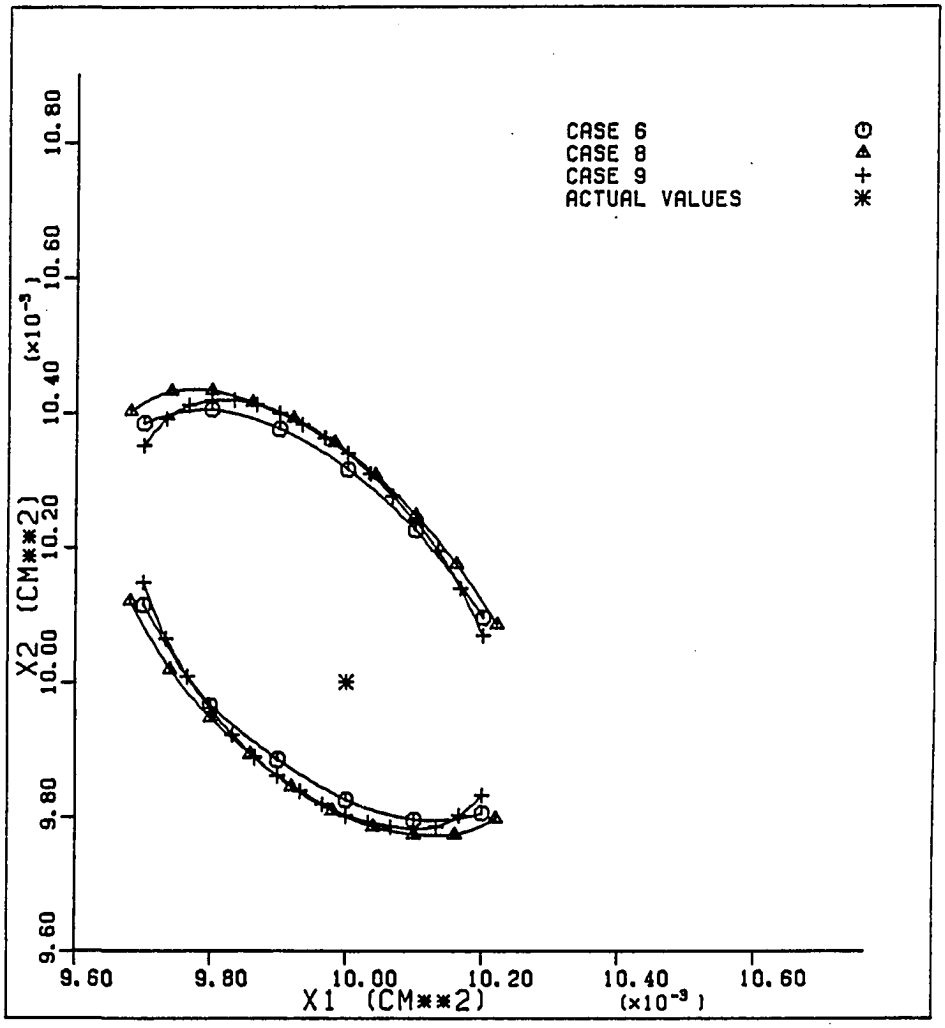

FIGURE 4.11. The 90% confidence region for X1 and X2 for different detector patterns

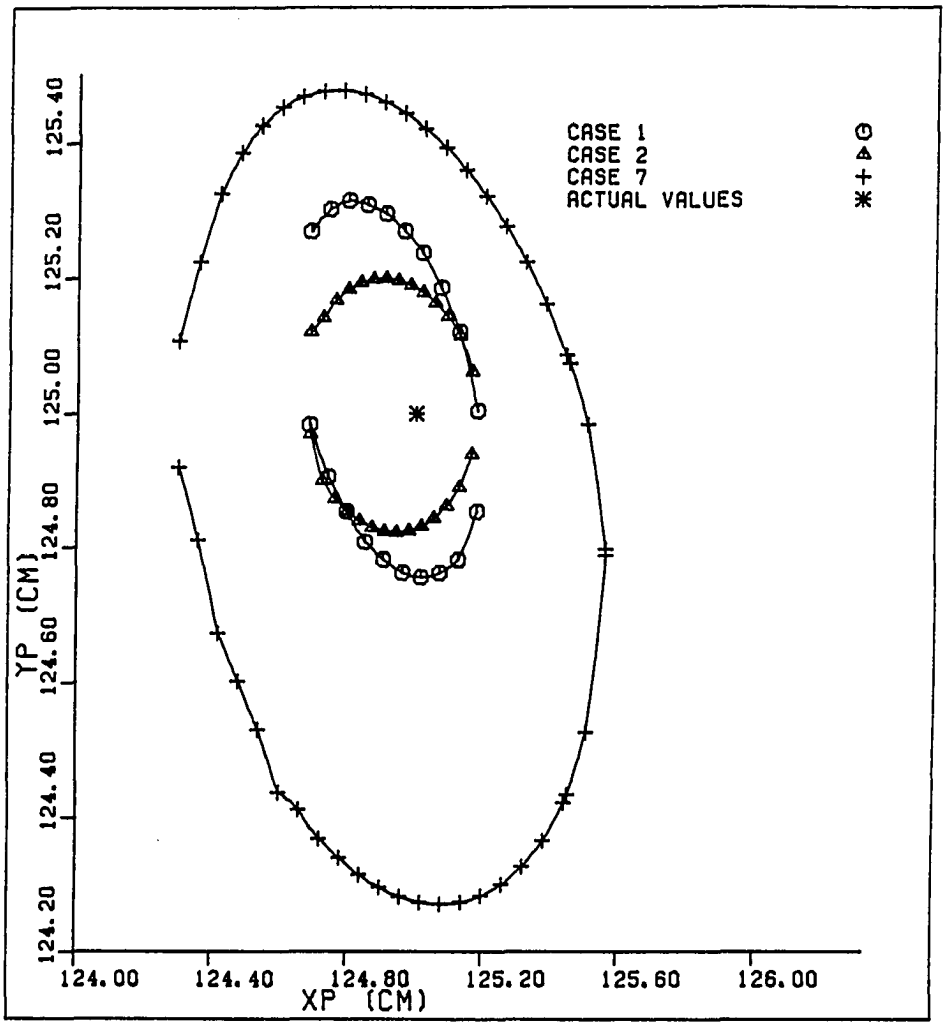

FIGURE 4.12. Effect of detector patterns on the 90% confidence region for XP and YP

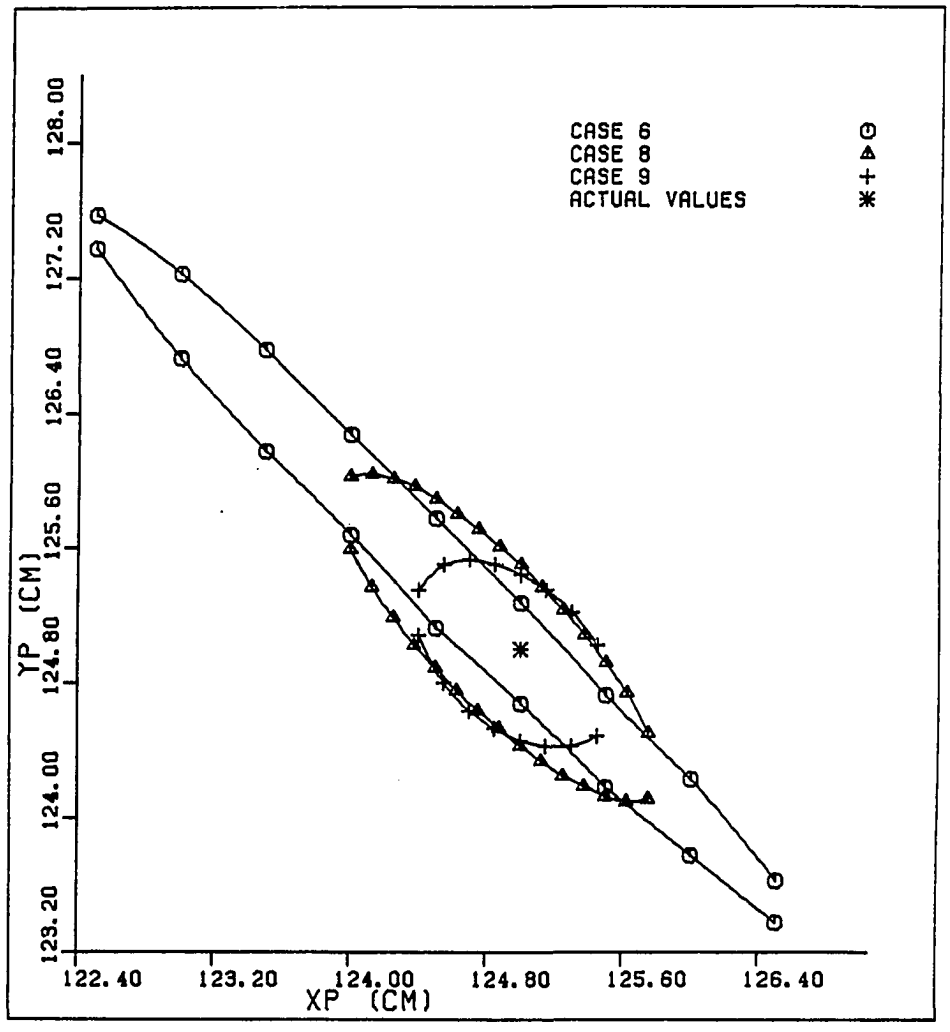

FIGURE 4.13. The 90% confidence region for XP and YP for different detector patterns

each grid point. This was compared to the tabulated value of the 90% chi-squared for the number of detectors. Out of twenty-five potential sites, the locations with a value of Q less than the $\chi^2_m(.9)$ were taken as potential locations. This result would be more conservative than the maximum likelihood estimate. The effect of σ_f and external noise was as expected. More locations were predicted as possible vibration sites as σ_f and external noise increased. The size and shape of the confidence region showed sensitivity to the various factors like σ_f, EN, or model bias, detector pattern, etc. Hence, it may be more informative to obtain confidence regions than the maximum likelihood estimates. Note that the confidence region method provides a measure of confidence, that may be associated with the estimates. It may be possible to obtain more conservative (smaller region) estimate of the confidence region for a subset of the parameter by substituting known or estimated values for other parameters.

The numerical investigation described in this section proved the soundness of the statistical techniques developed. The results were encouraging enough to consider application of the techniques to the identification of a vibrator, in the UTR-10 reactor. This is dealt with in the next section.

V. EXPERIMENTAL VERIFICATION

The experimental verification of the theory and techniques developed in Chapter III are presented in this section. A vibrating absorber was operated in the Iowa State University UTR-10 reactor and measurements were taken with detectors placed at four different locations. The experimental set up, including the UTR-10 reactor, the vibrating absorber and the data acquisition system will be described. The calculation of the detector responses, for the UTR-10 reactor, will be discussed. The use of the information matrix and simulated detector signals to identify optimal detector patterns will be demonstrated. Measurement procedure and the analysis of the data will be described and the results will be discussed.

A. Experimental Arrangement

Additional details related to this section may be found in reference (29).

1. The UTR-10 reactor

The UTR-10 reactor (51), a plan view of which is shown in Figure 5.1, is a heterogeneous, light water moderated and cooled, graphite reflected coupled core system. The maximum licensed power of the reactor is 10 KW. The core tanks (51 cm x 16 cm x 145 cm deep), separated by a distance of 46 cm,

are embedded in a graphite stack 142 cm long, 112 cm wide and 122 cm deep. A core tank holds six fuel assemblies each with twelve fuel plates. Fuel loading pattern B-1 (29) was used during the experiment. For this pattern, fuel element S2 has only eleven fuel plates. The third fuel plate from the south side was removed, resulting in a gap of about 2.2 cm. The vibrating absorber and a detector were located in this gap in two aluminum thimbles. Figure 5.2 shows a three-dimensional view of the vibrator and detector thimbles located in S2. Five removable graphite stringers are provided in the reflector region between the core tanks. The central graphite stringer is 9.525 cm x 9.525 cm x 122 cm long and the other four stringers are 3.0175 cm x 8.097 cm x 122 cm long. These stringers may be replaced with experimental apparatus. The graphite thermal column also contains removable stringers. The central stringer, which consists of two parts (9.8 cm x 9.8 cm x 48. cm and 9.8 cm x 9.8 cm x 127 cm), can be removed and replaced with modified stringers holding neutron detectors.

2. The vibrating absorber

The vibrating neutron absorber, the front and side views of which are shown in Figure 5.3, consists of a 9.0 cm x 0.85 cm x 0.05 cm cadmium strip attached to an aluminum rod which is pivoted near the top. A coil switching unit (29) driven by a signal generator (Wavetek model 111)

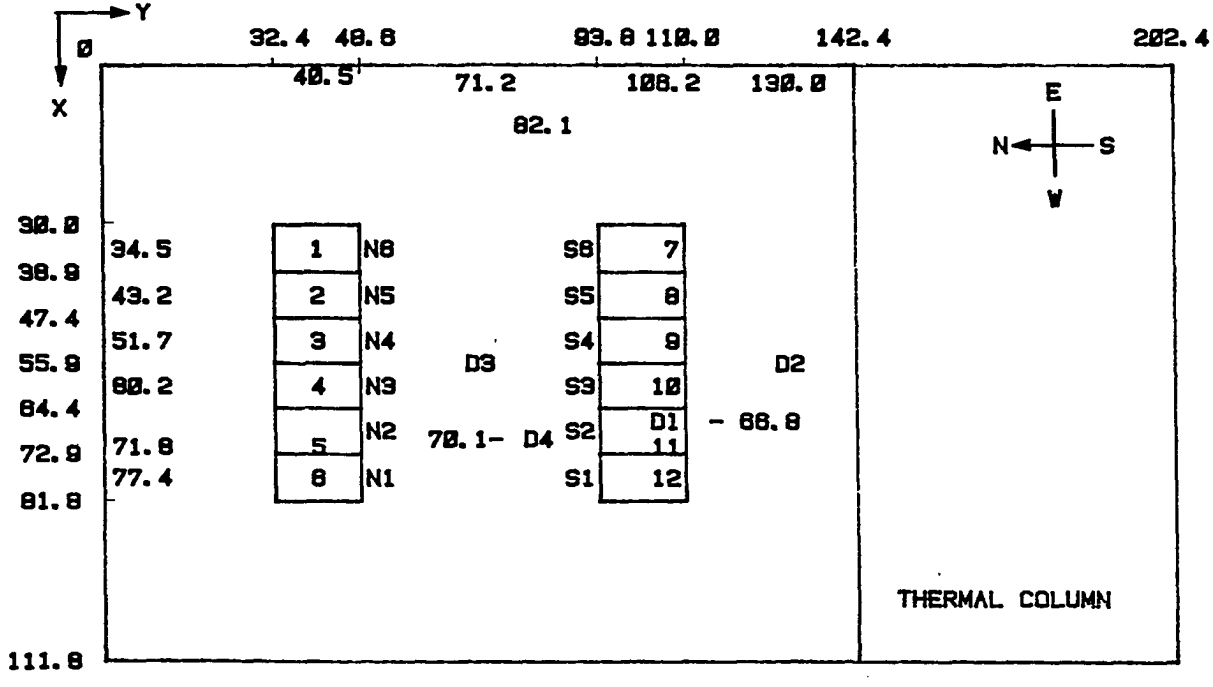

D1, D2, D3, D4 - DETECTOR LOCATIONS
1, 2.., 12 - POTENTIAL VIBRATOR LOCATIONS
11 - ACTUAL VIBRATOR LOCATION
ALL DISTANCES CENTER-TO-CENTER AND IN CMS.

FIGURE 5.1. Plan view of the UTR-10 reactor

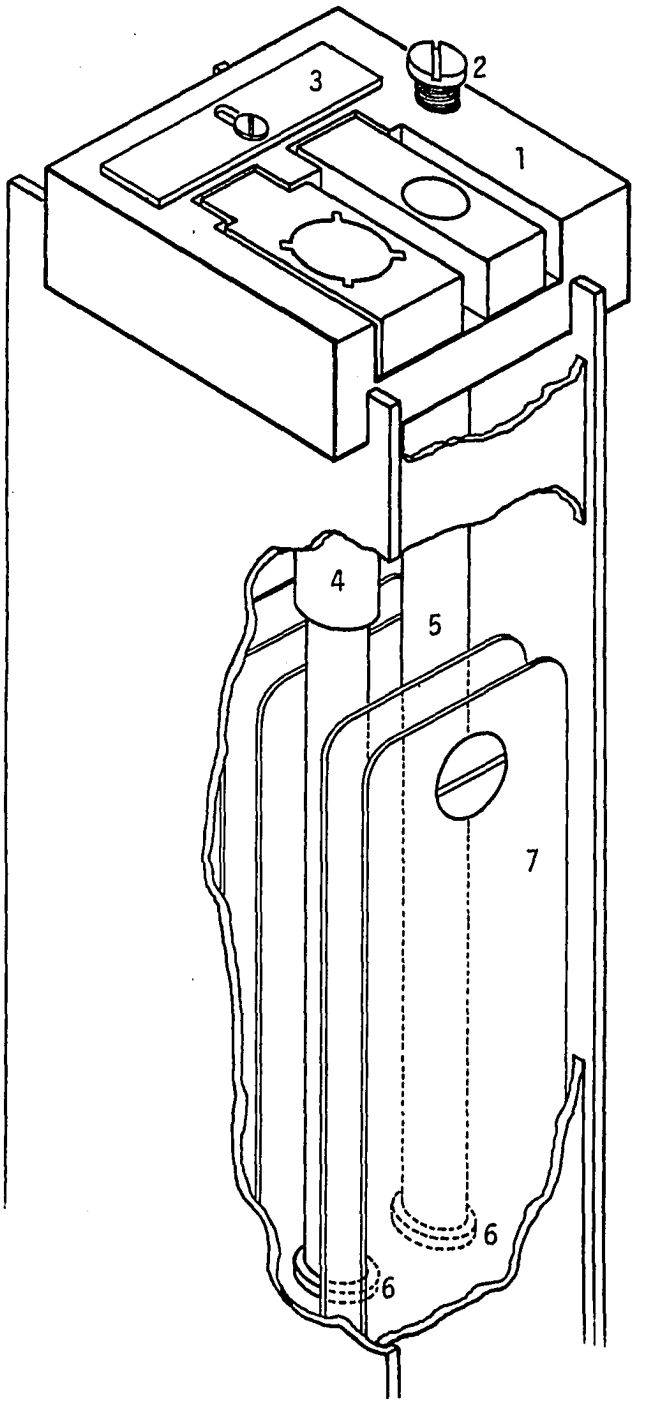

1. Mounting plate
2. Teflon screw
3. Tightening plate
4. Vibrator thimble
5. Detector thimble
6. Plastic screw
7. Fuel element

FIGURE 5.2. Vibrator assembly-core tank configuration

energizes two 12 V DC push type coils alternately, to move the absorber back and forth in one-dimension, like the motion of a pendulum. Even though the major component of motion was in one direction, there was a small two-dimensional motion due to the long rod being pivoted at one end. The maximum vibration amplitude of the absorber which is approximately 1.25 cm, may be varied by adjusting the voltage applied to the coils. A Linear Variable Differential Transformer (LVDT) (Schaevitz model 100MHR) attached to the aluminum rod measures the position of the absorber. The aluminum thimble, which holds the vibrator assembly, may be flooded with water or kept dry during the experiment. The vibrator assembly could be rotated ninety degrees resulting in two planes of vibration, one east-west (EW) and the other north-south (NS).

3. The data acquisition system

A block diagram of the data acquisition system is shown in Figure 5.4. The LVDT signal passed through a signal conditioner (Schaevitz model LPM 210), which removed the high frequency carrier signal, and a band-pass filter (Krohn-Hite model 330-A) with a low-pass cut off of 0.2 Hz and a high pass cut off of 50 Hz.

Four detectors (D1, D2, D3, and D4 in Figure 5.1) were used to monitor the neutron fluctuations produced by the absorber motion. All the detectors were N.Wood, 1.59 cm

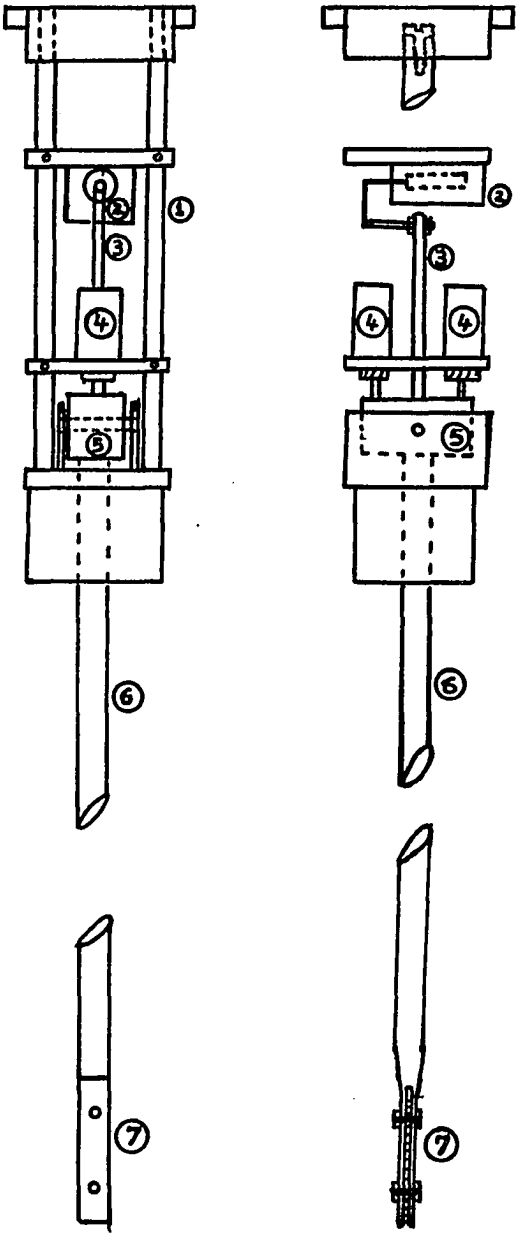

1. Aluminum structure
2. LVDT
3. LVDT connecting rod
4. Coils
5. Aluminum block
6. Aluminum rod
7. Cadmium (absorber)

FIGURE 5.3. Front and side views of the vibrator assembly

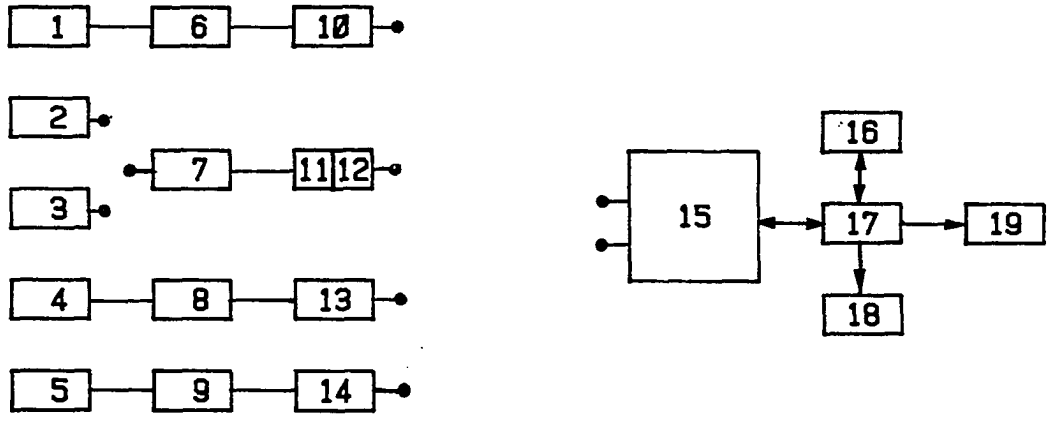

1 BF3 DETECTOR (N. WOOD G-5-3)
2, 3, 4, BF3 DETECTOR (N. WOOD G-5-8)
5 LVDT (SCHAEVITZ 100MHR)
6, 7, 8 PREAMPLIFIER (ALE 1818)
9 SIGNAL CONDITIONER (SCHAEVITZ LPM-210)
10, 14 BAND PASS FILTER KROHN-HITE 330-A)
11, 12 LOW AND HIGH PASS FILTER (KROHN-HITE 3321)
13 BANDPASS FILTER (TEXTRON N170)
15 FRQUENCY SPECTRUM ANALYZER (HP-3582A)
16 DISK DRIVE (HP-82902M)
17 MICROCOMPUTER (HP-85)
18 PRINTER (HP-2671G)
19 PLOTTER (HP-7225A)

FIGURE 5.4. Data acquisition and analysis system

(5/8"), 60 cm of gas pressure, BF_3 detectors operated as ion chambers. A high voltage of -90 V was applied to the central electrode. The detector current output was converted to an output voltage using locally constructed DC preamplifiers (Ames laboratory 1616). Detector D1 was a 7.62 cm (3") detector (G-5-3) located approximately 4.8 cm from the vibrator in the fuel assembly S2 (Figure 5.1). The signal from this detector was filtered using a bandpass filter (Krohn-Hite model 330-A) with a passband of 0.2 Hz to 50. Hz. Detector D2 (22.9 cm, G-5-9) was located in the thermal column inside a modified 48 cm graphite stringer. This detector was located horizontally at the midelevation with respect to the reactor core. Two filters (both Krohn-Hite model 3321) were used, one as a low-pass filter and the other as a high-pass filter, to bandpass filter the detector signal in the 0.2 Hz to 50. Hz range. Detector D3 (22.9 cm, G-5-9) was located in a 71.1 cm (28") modified stringer in the central vertical stringer above another 50.8 cm stringer. The detector signal was filtered using a bandpass filter similar to the one used in detector channel D1. Detector D4 (22.9 cm, G-5-9) was located in a modified stringer in the south west internal reflector location. Detector D4 was placed in a slot on the south side of this stringer. The midplane of all detectors corresponded to the midplane of the reactor. A Textron model N170 bandpass

filter, with a passband of 0.2 Hz to 50.0 Hz, was used in this channel.

A two-channel frequency spectrum analyzer (Hewlett Packard 3582A) was used to analyze the detector or LVDT signals. The analyzer calculates the auto-power spectral densities of the two input signals, the transfer function magnitude and phase and the coherence between the two signals. The data are stored on disk using an HP-85 microcomputer for later analysis.

B. Detector Response Calculation for the UTR-10 Reactor

The usefulness of the statistical techniques, developed in Chapter III, relies on the availability of an accurate neutronic noise model for the system. The computer code Exterminator-2 (37), which can solve a source problem as well as the eigenvalue problem, in rectangular geometry, was used in this study. The adjoint functions for the four detector locations used in the experiment as well as the regular flux for the critical system were calculated.

The reactor was modeled in two dimensions using two neutron energy groups. Calculations were restricted to the plateau region of the frequency response and hence, the adjoint functions were real. As shown in Appendix A, for this approximation, the fission source term is reduced by the factor $(1-\beta)$.

In order to obtain sufficient detail in the calculation, the reactor (Figure 5.1) was assumed to be made up of eight different region types. Region type 1 is the graphite region, type 2 the fuel assemblies N2, N3, N4, N5 (grouping based on approximate fuel loading) and S3, S4 AND S5, type 3 the fuel assemblies N1 and S6. The types 4, 5 and 6 are fuel assemblies N6, S1 and S2, respectively. Type 7 is the water gap in S2 and type 8 is the detector region.

The two-group macroscopic cross sections, required by Exterminator-2, were calculated using the computer code LEOPARD (52). It requires volume fractions of aluminum and water and atom densities of U-235 and U-238. A buckling of 0.002892 cm^{-2} (based on fuel meat height of 58.42 cm) and a temperature of 26.7C (normal operation temperature) were used. A non lattice fraction (30) may also be specified. The Table B.1 in Appendix B shows the volume fractions, atom densities and the non lattice fractions for each type of region (see references 26, 27, 30 for details of the calculations). The two-group cross sections obtained are shown in Table B.2 of Appendix B.

The computer code Exterminator-2 solves the five-point finite difference form of the multigroup neutron diffusion equations using the equipoise method (53). A 53 x 88 mesh was used for the calculation. Table B.3 in Appendix B shows the x-y mesh pattern used for the calculation. The

selection of the number of mesh points was based on three requirements:

- The mesh spacing must be of the order of, or smaller than, the diffusion length.
- Since the solution in a source region is sharply peaked, a large number of closer mesh points are required around this region.
- To calculate the derivative of the fluxes and the adjoint functions, differences between values at two adjacent mesh points were used. From the definition of the derivative two closer points are desired. But from a numerical point of view the mesh points should be separated by a distance so that the differences in the function values are larger than numerical round-off errors. To reduce the effect of the round-off errors, calculations were done with a high level of accuracy. To achieve this, the Exterminator-2 code was modified to do calculations in double precision. A detailed study, which will be explained in a later section, was carried out to compare the Exterminator solutions with analytical solutions.

The first step in setting up a problem is to obtain a critical reactor. Based on eigenvalue calculations, using the Exterminator-2, the transverse buckling was adjusted to

0.00190 cm^{-2} to obtain an effective multiplication factor, Keff, of 0.9995. The critical flux obtained was used in the calculation of the detector response. Figure 5.5 shows the three dimensional plot of the thermal group flux in the UTR-10 reactor. Note the flux peaking in the region (water gap) where the fuel plate was removed in S2. A close mesh pattern was required in this region to see this effect. See reference (37) for the normalization used to obtain the numbers in Figure 5.5. Note that if the absolute value of the flux is not known, only relative values of the vibration parameters can be determined. In this study, a quantity involving this normalization and other constants was estimated using one of the detector signals. This is explained in the data analysis section.

It can be shown that the use of adjoint solutions involved fewer calculations, especially for evaluating gradients. In order to determine the gradient of the adjoint function the slope of the adjoint function is determined at the vibrator site. A single computation of the adjoint function for a detector location gave all the numbers required for a gradient calculation. The gradient of the forward solution is the change in the value of the forward solution at the detector site for unit change in the source location in the x or y direction. To find the gradient the source is displaced in the x or y direction and

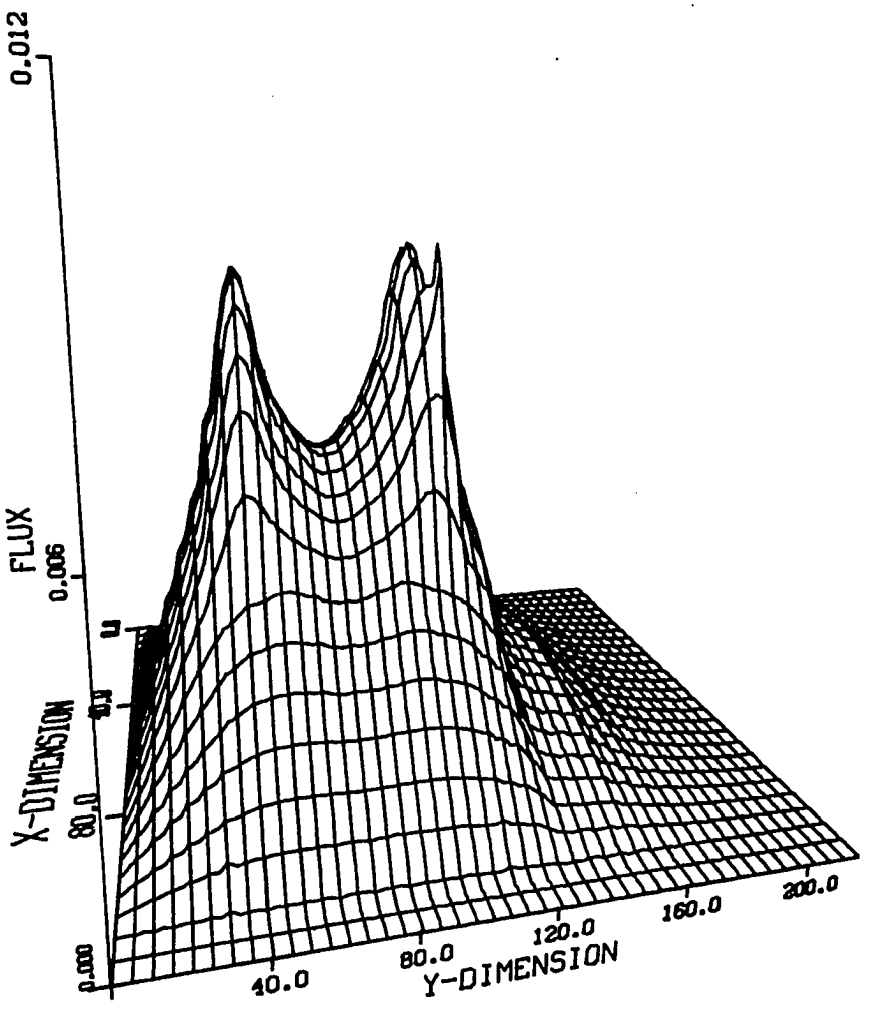

FIGURE 5.5. Thermal flux in the UTR-10 reactor

the computations are repeated. Note that these are two different derivatives, but they yield the same value under the conditions required for the equality of the adjoint function and the forward solution (see equation 3.22)

In order to obtain the adjoint functions a square unit source region of dimensions 1 cm x 1 cm was specified at the detector location. As shown in Appendix A, an equivalent problem given by equations (A.14) and (A.15) is solved using Exterminator-2. The constants (see equations A.16 through A.20 in Appendix A) used for the adjoint computation are shown in Table B.4 in Appendix B. Note that a solution exists for the source problem only if the system without a source has a multiplication factor less than the required value (which is usually one). The multiplication of $\nu\Sigma_f$ by $(1-\beta)$ will guarantee this. Figures 5.6, 5.7, 5.8 and 5.9 show the thermal group adjoint functions for the four detector locations in the UTR-10 reactor. The adjoint functions are normalized to the constant source.

The Exterminator-2 code solutions for the adjoint system were tested against an analytical model. The square, bare, homogeneous, one-group reactor model used in chapter IV was used here. The analytical solutions for the adjoint functions are given by equations similar to (4.7) and (4.8). The strength of the point source to be used in the Exterminator code is given by the right hand side of the

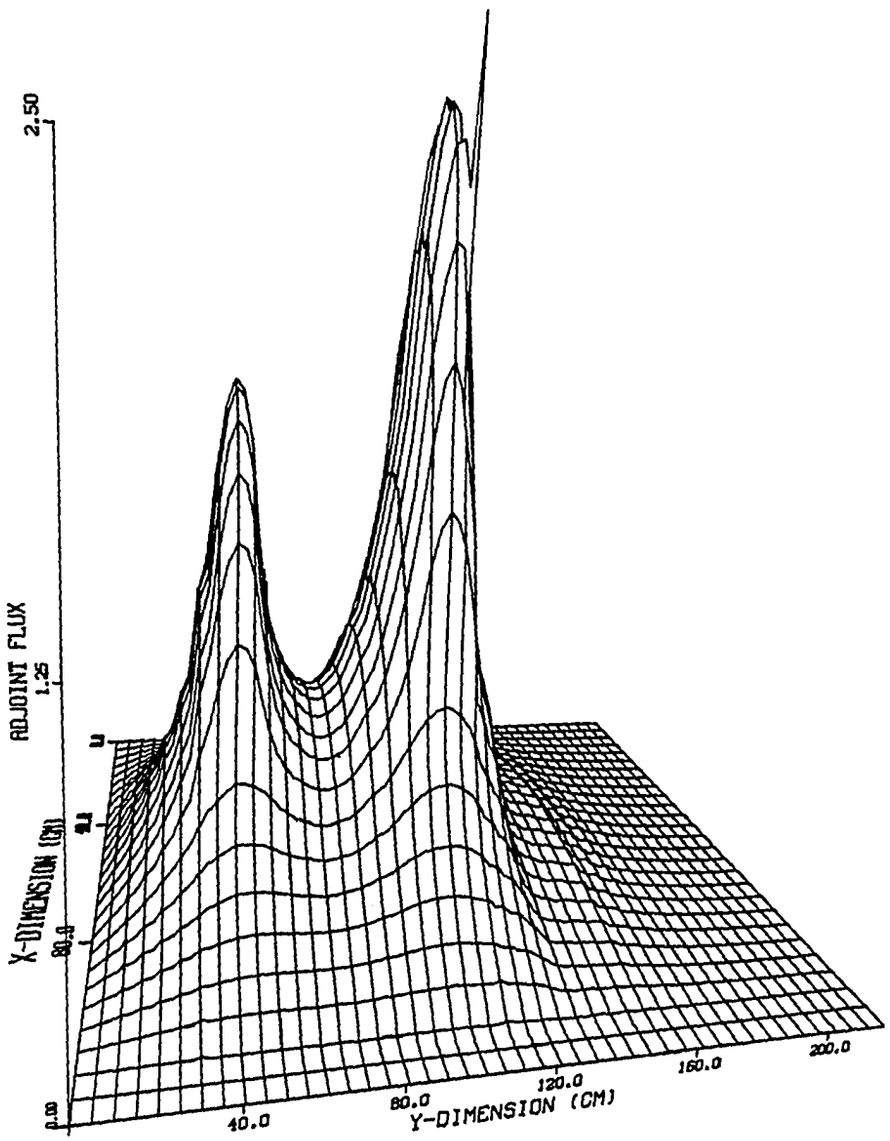

FIGURE 5.6. Thermal adjoint flux for the detector D1

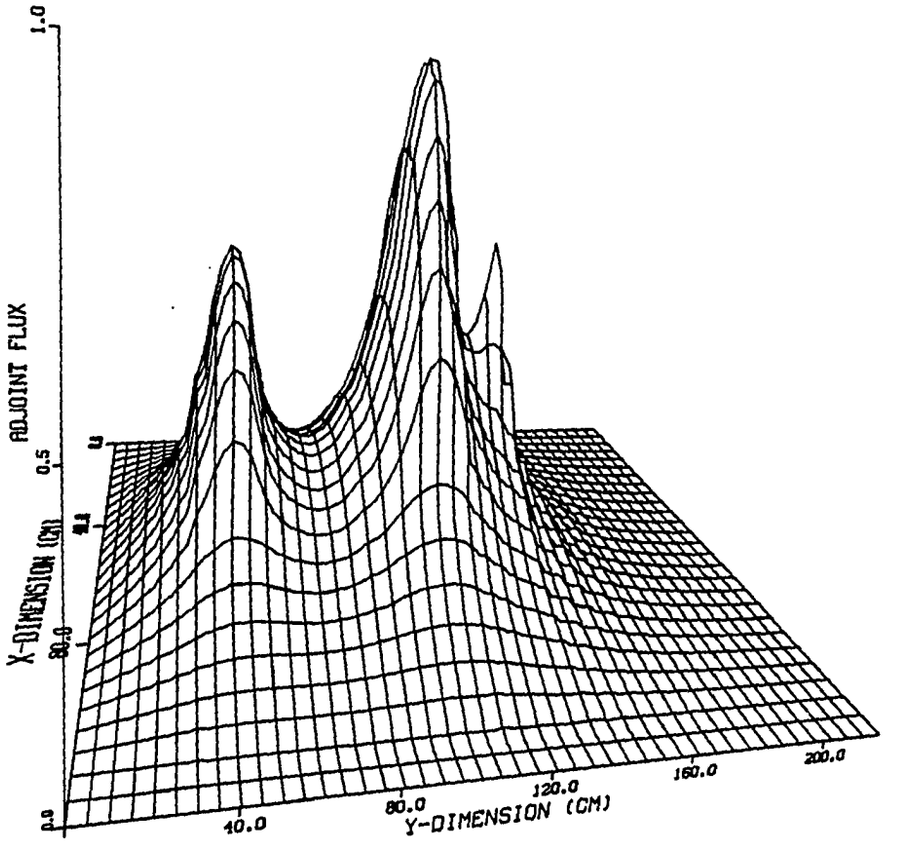

FIGURE 5.7. Thermal adjoint flux for the detector D2

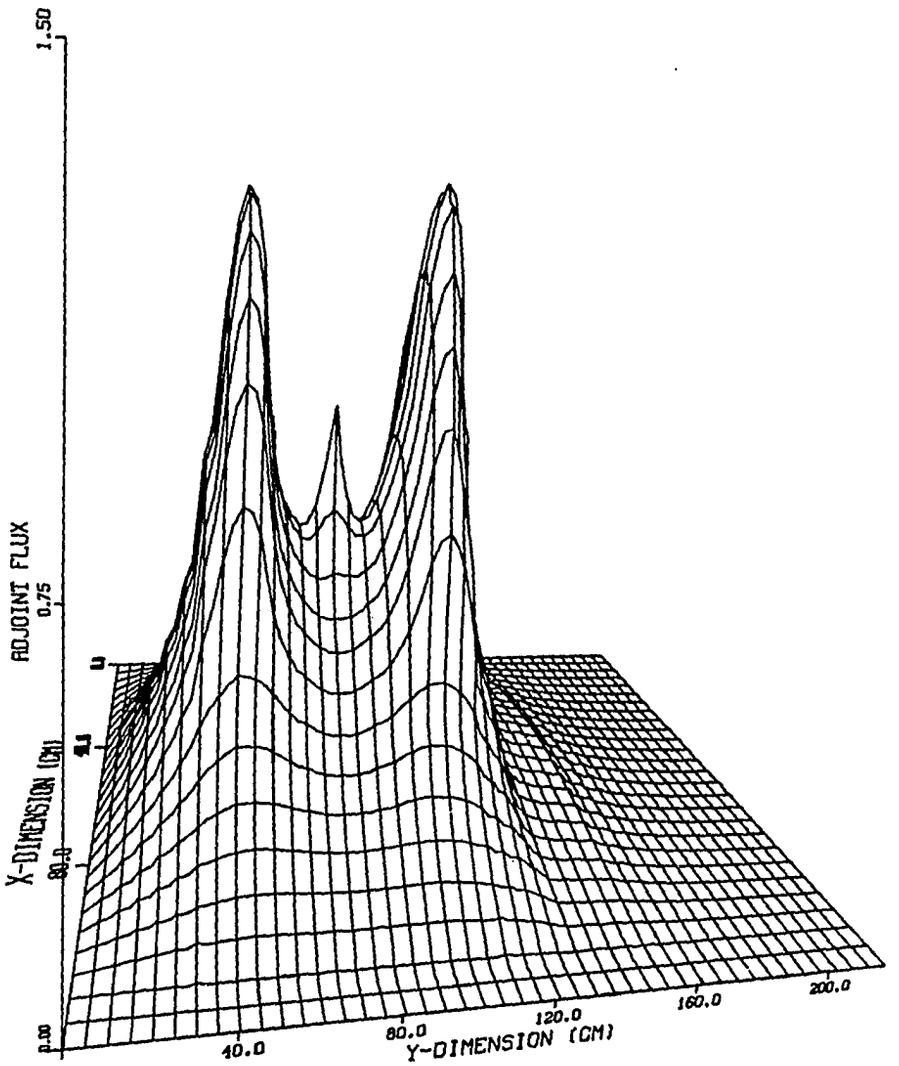

FIGURE 5.8. Thermal adjoint flux for the detector D3

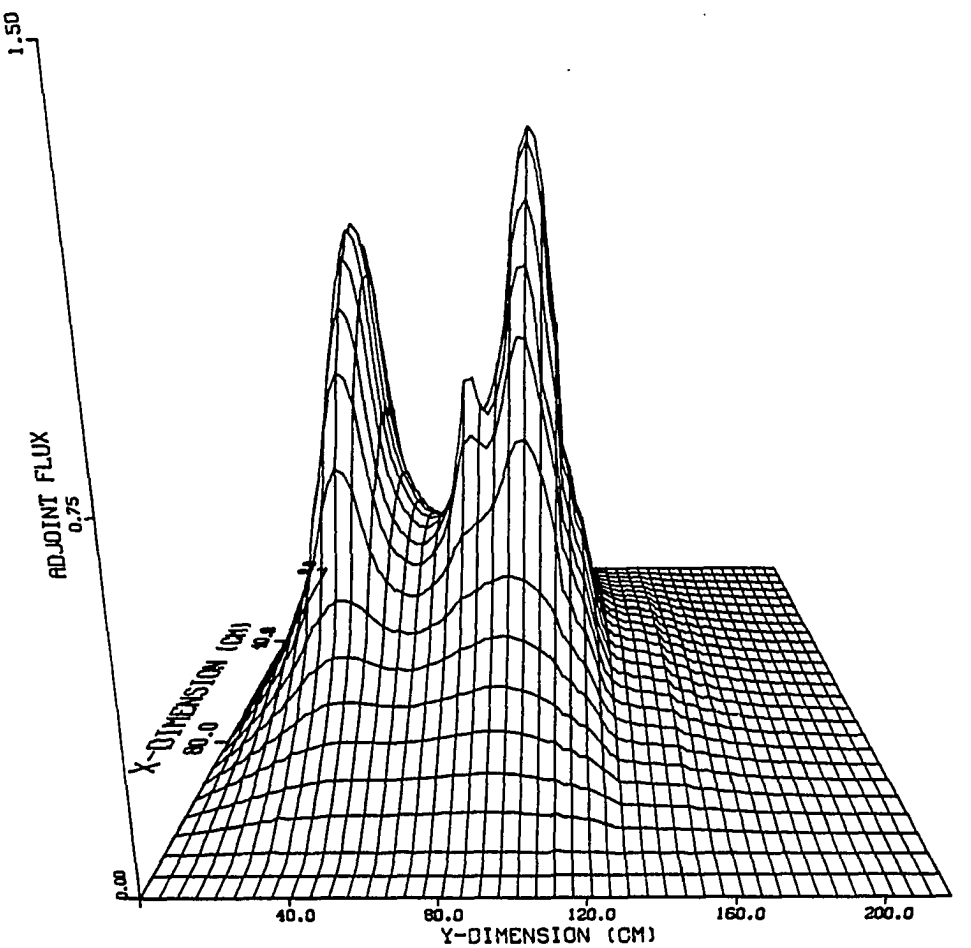

FIGURE 5.9. Thermal adjoint flux for the detector D4

equation (4.1). Note that in the one-group formalism the adjoint and forward systems are identical. Different mesh spacings were tried especially near the source region for the forward and the adjoint source for adjoint calculations. A mesh spacing of 0.5 cm was used near the source and was increased to 1 cm and 2 cm at distances larger than 5 cm from the source. This was found to give reasonably good results. The Exterminator calculations were within 1% of the analytical solutions up to a distance of 4 cm from the source. Note that in Exterminator-2 the source is of finite size and strength unlike the analytical model where the source is a delta function. The gradient of the function was determined by finding the difference in values at two mesh points, on either side of the point of interest, separated by a distance of 1 cm. It was observed that even with less than 1% error in the function values, the error in the gradients of the functions were about 10%. This error increased when the mesh separation distance was decreased for reasons previously described.

Once the flux and the adjoint functions are obtained their gradients at the vibration site along the x and y direction may be calculated. These values were used in equation (3.31a) and (3.31b) to obtain the unit response functions W_x and W_y along the x and y directions, respectively. The constant γ is lumped with other constants

or may be taken as unity.

The vibrator motion was assumed to be one-dimensional and periodic. The median value of the APSD of the detector response, R'_i, of the ith detector due to a vibrator at r_p may be obtained from equation (3.42) as

$$R'_i = W^2 xx/2, \tag{5.1}$$

where W is equal to W_x and xx = X1 for the EW motion of the vibrator, and W is equal to W_y and xx = X2 in the case of NS vibrator motion. The parameter xx represents the APSD of the square of the amplitude of motion. If the vibrator strength γ or other arbitrary constants involved in the calculation of W are not known, they may be lumped along with the parameter xx. Since four detectors were available, calculations were performed using five detector patterns, consisting of four detectors and four combinations of three detectors as shown in Figure 5.10. The actual vibrator location is 11 in Figure 5.1. Numerical investigations using the information matrix and the confidence region or maximum likelihood techniques will be discussed next.

C. Numerical Investigation of the Vibrator Problem in the UTR-10 Reactor

The vibration amplitude function xx is set equal to unity in equation (5.1) and it can be used in equation

Pattern P1	D1	D2	D3	D4
Pattern P2	D1	D2	D3	
Pattern P3	D1		D3	D4
Pattern P4		D2	D3	D4
Pattern P5	D1	D2		D4

FIGURE 5.10. Detector patterns used in analyzing data from UTR-10 reactor

(3.61) to obtain the likelihood function and the information matrix may be calculated using equation (3.62). The likelihood function is now a function of the two location parameters XP and YP. Since the actual location of the vibrator was known, the information matrix was evaluated at this point for the different detector patterns. From this 2 x 2 matrix the standard error involved in the estimation of the location parameters was determined. These values (in cm) for the different detector patterns for an assumed σ_f of 30% are shown in Table 5.1 for the cases of east-west (EW) and north-south (NS) modes of vibration. Note that the calculation of the information matrix requires the derivatives of the W_x and W_y functions with respect to both XP and YP. This was done numerically in the same manner the derivatives of the flux and the adjoint functions were

determined as described previously.

TABLE 5.1. Expected standard error in the estimation of the location parameters, XP and YP, for the different detector patterns used in the UTR-10 reactor

Detector Pattern	EW		NS	
	XP	YP	XP	YP
P1	1.06	1.27	1.50	7.15
P2	1.09	1.28	1.85	9.01
P3	1.15	1.29	1.73	8.11
P4	7.22	9.68	1.92	8.9
P5	1.08	1.28	1.85	9.05

The following conclusions were drawn from these results. The detector pattern P4 with D1 missing, is the poorest pattern, as far as the estimation of the vibrator location parameters are concerned. In the case of EW vibrations (see Table 5.1) pattern P1 with four detectors does not show an improvement over other patterns with only three detectors. None of the patterns are suitable for estimating the location for the NS vibration with 30% noise because of the large error in YP. In this case, pattern P4 may not be any worse than the other patterns. It should be pointed out that, with lower values of σ_f for the data, it may be possible to estimate location of the vibrator moving

in the NS direction with these patterns.

It is possible to do a maximum likelihood or confidence region calculation with simulated detector signals. This type of analysis may also be used to obtain information regarding detector patterns before the actual experiment is carried out.

In analyzing the experiment it was assumed that there were twelve potential vibrator sites, one in each fuel assembly, in the reactor. The eleventh location (Figure 5.1) was the actual location. Since the actual location of the vibrator was known, equation (5.1) along with a multiplicative type error model was used to generate detector signals as explained in Chapter IV. The natural logarithm of the four detector signals, for a vibrating absorber situated at the eleventh location, using an assumed fractional standard deviation of 0.3 is shown in Table 5.2. Both the EW and NS cases are shown under the column 'THEOR' (Theoretical). The experimental (EXPTL) cases will be described in a later section.

A search for the parameter xx, that minimized the function Q (equation 3.57), was carried out for each of the five detector patterns over the twelve potential vibrator locations. As pointed out earlier, Q has a chi-squared distribution. These minimum values are shown in Tables 5.3 through 5.7 for the various detector patterns, under the

TABLE 5.2. The natural logarithm of the APSD of the simulated detector signals for $\sigma_f = 0.3$ and the normalized and corrected experimental values

Detector	EW			NS		
	THEOR	EXPTL		THEOR	EXPTL	
	0.3	UNFLO	FLO	0.3	UNFLO	FLO
D1	-12.67	-12.59	-12.40	-13.16	-13.96	-12.90
D2	-15.50	-15.52	-15.94	-15.60	-15.28	-15.67
D3	-14.78	-14.71	-14.73	-14.61	-14.28	-14.89
D4	-14.73	-14.87	-14.63	-14.51	-14.35	-14.44

column 'THEOR'. With four detectors, for a 90% confidence value, the χ^2 is 7.78 and with three detectors it is 6.25. The values in the Tables 5.3 through 5.7 may be compared to the respective values given above. The grand minimum represents the maximum likelihood estimate for the vibrator location. All the locations with values of Q less than the above 90% confidence values must be taken as potential candidates. The external noise is neglected in all these calculations.

In all the cases studied, with up to 30% noise on the data, the minimization returned values for the amplitude parameters that were within 1% of the true value.

For the case of the EW vibrations, detector patterns P1, P3 or P5 may be used for the localization even with 30% noise on the data. Detector pattern P2 cannot differentiate

TABLE 5.3. The minimum for Q (equation 3.57) at the 12 potential vibrator sites for simulated and experimental data for detector pattern P1

	EW				NS			
	THEOR		EXPTL		THEOR		EXPTL	
LOC	0.1	0.3	UNFLO	FLO	0.1	0.3	UNFLO	FLO
1	4049.37	411.12	15.20	946.59	1132.91	109.46	14.88	21.94
2	4114.72	418.02	15.45	954.59	1237.82	120.14	15.10	23.05
3	4212.17	428.12	15.87	962.52	1337.79	130.21	15.27	24.04
4	4050.78	411.84	15.07	958.17	1344.63	130.30	15.14	23.84
5	4118.45	418.45	15.45	956.14	1261.92	120.94	14.80	22.52
6	4108.04	417.15	15.46	950.06	1180.76	111.82	14.56	21.15
7	1295.35	124.74	5.59	619.31	124.79	12.17	23.13	7.39
8	1073.90	101.86	4.80	558.39	104.94	10.70	24.36	6.78
9	156.36	11.48	1.39	217.59	62.91	6.62	26.27	5.81
10	16389.30	1751.03	62.27	4070.85	20.91	3.47	30.26	4.37
11	2.20	2.20	0.21	159.50	2.20	2.20	34.49	2.98
12	635.23	56.92	3.09	417.18	7.30	0.38	29.98	3.72

(based on the 90% confidence value for x^2) between locations 9 and 11 when the noise level was raised to 30% (see EW vibrations in Table 5.4). The detector pattern P4, with D1 removed, predicted five locations in the south core with 30% noise. This was also predicted by the information matrix analysis. Detector D1 has a strong capability for resolving a vibration source in location 10 as compared to location 11 as indicated by the large difference in Q for these two locations. This is mainly due to the large difference in the gradient terms of the unit response function W_x at these

TABLE 5.4. The minimum for Q (equation 3.57) at the 12 potential vibrator sites for simulated and experimental data for detector pattern P2

	EW				NS			
	THEOR		EXPTL		THEOR		EXPTL	
LOC	0.1	0.3	UNFLO	FLO	0.1	0.3	UNFLO	FLO
1	3498.30	359.19	11.35	924.65	1130.37	109.45	15.46	15.48
2	3539.81	363.65	11.48	929.92	1232.01	120.11	15.90	16.32
3	3551.42	364.93	11.51	927.30	1324.80	129.87	16.37	17.07
4	3614.18	371.57	11.74	949.79	1314.91	128.87	16.55	16.97
5	3552.64	365.02	11.52	932.61	1203.11	117.19	16.46	16.02
6	3496.95	359.07	11.34	920.83	1082.37	104.60	16.36	14.99
7	1186.84	116.60	4.32	631.45	108.98	8.38	22.90	4.63
8	963.36	93.54	3.56	569.23	89.38	6.96	24.29	4.21
9	48.66	3.41	0.33	221.61	52.44	3.73	26.73	3.59
10	15053.29	1617.29	52.85	4004.78	12.89	1.02	31.38	2.61
11	1.34	1.34	0.09	143.66	1.34	1.34	36.80	1.81
12	546.52	50.56	2.06	425.59	5.69	0.34	32.38	2.49

two locations.

In the case of NS vibrations, detector patterns P1 and P5 are the only ones that can uniquely predict the actual location with 10% noise. All the other patterns predict more than one location. The situation worsened as the noise level was increased. Note that in this case P4 appeared to be better than in the case of the EW vibration.

These results showed the effect of the detector pattern on the localization technique. The positioning of the detectors was found to be important. A larger number of

TABLE 5.5. The minimum for Q (equation 3.57) at the 12 potential vibrator sites for simulated and experimental data for detector pattern P3

	EW				NS			
	THEOR		EXPTL		THEOR		EXPTL	
LOC	0.1	0.3	UNFLO	FLO	0.1	0.3	UNFLO	FLO
1	3867.50	392.46	14.00	1265.03	1081.14	104.52	6.88	16.02
2	3919.09	397.89	14.19	1280.04	1166.68	113.20	6.30	16.79
3	3986.64	404.79	14.51	1298.56	1243.85	120.88	5.62	17.44
4	3891.18	395.56	13.94	1274.39	1235.33	119.35	4.94	17.25
5	3924.34	398.49	14.20	1281.79	1149.25	109.63	4.47	16.27
6	3906.04	396.34	14.19	1275.38	1067.67	100.47	4.22	15.27
7	1147.05	106.80	4.64	432.74	68.62	5.01	22.26	4.54
8	946.64	86.37	3.98	366.73	46.55	3.29	23.58	4.08
9	154.71	11.11	1.29	74.10	26.87	1.88	25.06	3.59
10	14301.82	1513.69	51.47	4232.13	6.03	1.33	28.46	2.78
11	2.13	2.13	0.18	8.73	2.13	2.13	31.34	2.04
12	578.70	49.72	2.64	244.80	5.87	0.05	27.08	2.52

detectors may not always mean better results. The detector D1 seemed to have the most significant effect on the results, for the EW mode of vibration.

The results obtained through numerical investigations were verified by the experiment described in the next section.

TABLE 5.6. The minimum for Q (equation 3.57) at the 12 potential vibrator sites for simulated and experimental data for detector pattern P4

	EW				NS			
	THEOR		EXPTL		THEOR		EXPTL	
LOC	0.1	0.3	UNFLO	FLO	0.1	0.3	UNFLO	FLO
1	1236.37	127.92	4.82	54.40	555.07	58.17	6.56	11.34
2	1274.30	131.92	5.00	55.59	619.06	64.78	7.55	12.01
3	1330.61	137.67	5.33	53.55	674.72	70.41	8.49	12.49
4	1244.86	129.39	4.69	66.96	661.04	68.45	8.63	11.97
5	1275.95	132.14	4.99	56.57	587.23	59.98	8.06	10.59
6	1271.47	131.46	5.04	52.21	517.99	52.06	7.57	9.22
7	3.27	0.84	0.15	113.36	54.22	8.37	0.14	3.63
8	0.22	0.43	0.24	112.65	51.86	8.21	0.22	3.40
9	60.81	5.68	1.02	93.22	32.90	5.67	0.19	2.98
10	41.43	6.40	0.09	151.20	16.89	3.43	0.26	2.50
11	0.57	0.57	0.25	115.71	0.57	0.57	0.57	1.82
12	1.38	0.04	0.30	100.26	0.63	0.38	0.76	1.59

D. The Measurement Procedures

The vibrating absorber was operated at a single frequency (2.5 Hz) with the absorber motion either in the EW or NS directions. Measurements were taken with both the vibrator thimble unflooded (UNFLO) and flooded (FLO). The reactor power throughout the measurements was kept steady (within 3%) of the nominal value of 200W.

The LVDT signal was used to normalize (see section E) all the detector signals. This removed any amplitude

TABLE 5.7. The minimum for Q (equation 3.57) at the 12 potential vibrator sites for simulated and experimental data for detector pattern P5

	EW				NS			
	THEOR		EXPTL		THEOR		EXPTL	
LOC	0.1	0.3	UNFLO	FLO	0.1	0.3	UNFLO	FLO
1	2196.16	216.74	9.00	508.95	254.52	19.75	9.99	9.75
2	2239.39	221.25	9.16	512.20	283.10	22.30	9.97	10.08
3	2363.79	234.26	9.61	522.00	324.08	26.06	9.95	10.60
4	2051.87	201.72	8.47	498.24	374.41	30.80	9.96	11.27
5	2229.61	220.23	9.12	511.57	425.53	35.70	10.01	11.97
6	2280.31	225.52	9.31	515.10	480.66	41.06	10.08	12.75
7	1117.11	108.40	4.80	468.67	100.95	10.68	13.92	7.56
8	953.52	91.30	4.19	427.08	92.06	10.08	14.41	7.21
9	152.79	10.40	1.06	164.22	55.57	6.37	15.49	5.81
10	14308.26	1532.04	50.41	2908.75	19.95	3.46	17.74	3.95
11	1.83	1.83	0.06	121.00	1.83	1.83	20.15	2.03
12	567.35	51.45	2.74	321.82	7.29	0.24	17.24	3.12

dependence of the detector signals due to small inconsistent amplitude values of the vibrations. The LVDT signal and signal from one of the four detector channels were input into the spectrum analyzer (see Figure 5.4). The signals were assumed to be time stationary to make up for the fact that they were not taken simultaneously. Eight root-mean-square averages of these signals were taken and using a Fast Fourier Transform (FFT) based digital algorithm the square root of the APSD of the two signals, the transfer function phase and magnitude, and the coherence between the signals

were calculated. These data, for a region of interest around a frequency of 2.5 Hz, were transferred to the HP-85 computer and stored on disk (see Appendix C program TRANS). The flat top passband was used while taking measurements with the analyzer, since this is the most accurate passband for measuring amplitudes of periodic signals. It should be pointed out that the amplitude (peak height) of the APSD spectrum is the quantity of interest in these measurements. The APSD of the LVDT and the four detector signals, for a typical measurement, for the EW absorber motion and with the vibrator thimble flooded are shown in Figure 5.11. In these measurements the coherence function was greater than 0.9 indicating a strong correlation between the LVDT signal and any of the four detector signals.

E. Analysis of Experimental Data

The APSD data (peak value at the frequency of interest) for both the LVDT and the detector signal shown in Figure 5.11 for example, consist of the signal plus a background. At frequencies away from the peak region, in each case, the spectrum is due to the background only. An average value of the background, was determined using 4 bins of data, in the background region, on either side of the peak. The following background correction was then applied to the data. Let R'_{Mi}, R_{Mi}, and R_{Bi} represent the measured APSD,

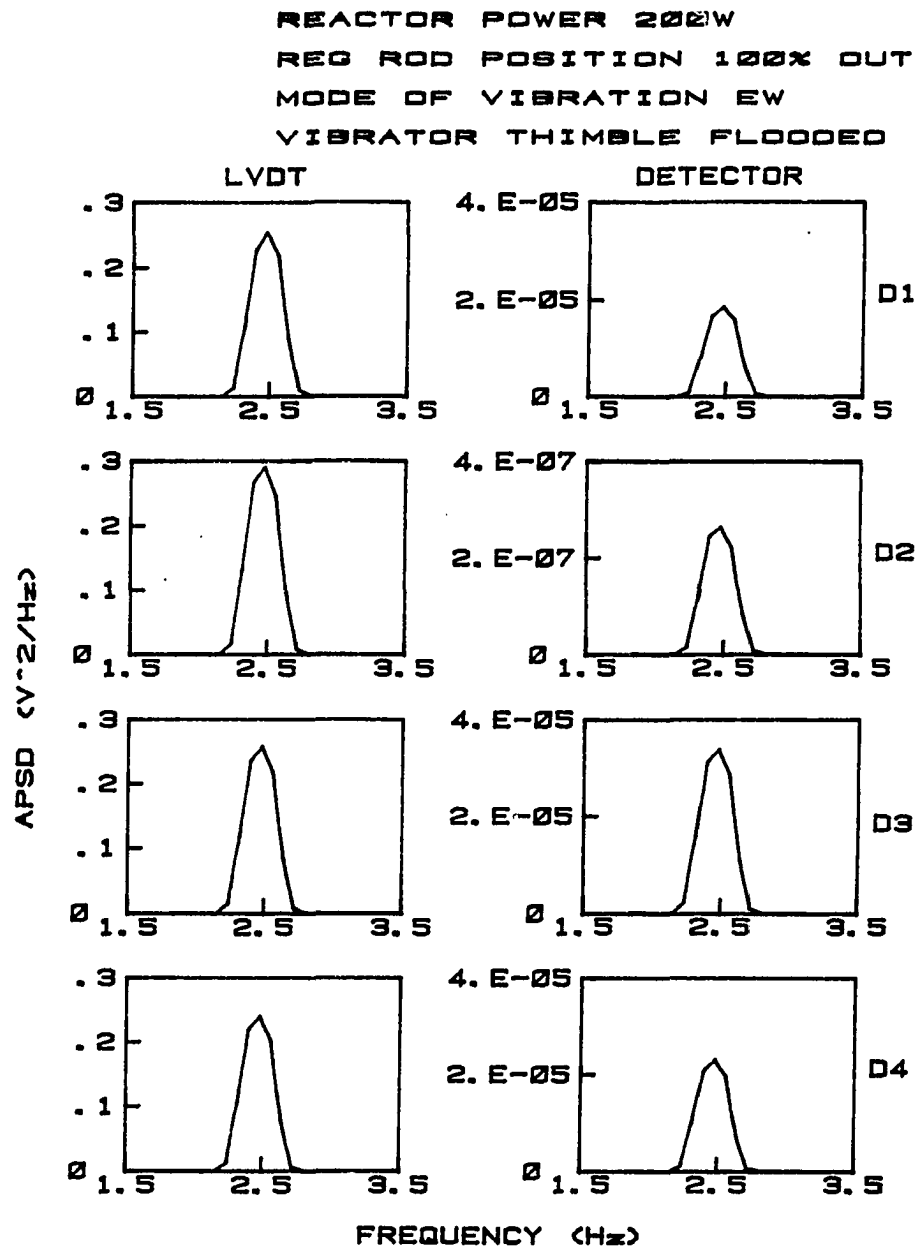

FIGURE 5.11. The APSD of the detector signals and the LVDT signals for a typical measurement

the corrected APSD and the average of the background for the detector D_i, respectively. Similarly, R'_L, R_L, and R_{LB} represent the measured, corrected and average background APSDs for the LVDT. Then the normalized APSD, R_{Ni}, of the signal for detector D_i is given by

$$R_{Mi}/R_L = (R'_{Mi}-R_{Bi})/(R_L-R_{LB}). \tag{5.2}$$

Now, R_{Mi} may be written as

$$R_{Mi} = R'_i G_i C \tag{5.3}$$

where R'_i is given by equation (5.1) for one-dimensional motion, G_i is the ith channel gain factor and the proportionality constant, C, relates the measured value to that modeled by equation (5.1). This constant involves the absorber strength, γ, steady state flux, ϕ_o, and the normalization involved in the calculation of the adjoint function.

The corrected APSD of the LVDT signal, R_L, is proportional to the APSD of the amplitude of motion xx. Therefore,

$$R_L = C_L xx \tag{5.4}$$

where C_L is a proportionality constant. In terms of the ratio of equation (5.3) to equation (5.4), R_{Ni}, may be written as

$$R_{Ni} = W^2 G_i C/C_L \qquad (5.5)$$

where R'_i is replaced with equation (5.1). The natural logarithm of equation (5.5) yields

$$\ln R_{Ni} = \ln W^2 + \ln G_i + \ln(C/C_L). \qquad (5.6)$$

The measurements were repeated n (at least 3) times. The average value of these n measurements is shown in Table 5.8. These measurements were used to obtain an unbiased estimate of the standard deviation. This is also shown in Table 5.8 for the different detectors and for the various situations considered.

TABLE 5.8. The average natural logarithm of the measured detector APSDs and the estimates of σ_f

Detector	EW				NS			
	UNFLO		FLO		UNFLO		FLO	
	APSD	σ_f	APSD	σ_f	APSD	σ_f	APSD	σ_f
D1	-13.19	.39	-9.56	.04	-15.59	.23	-15.10	.25
D2	-12.40	.28	-9.39	.06	-13.19	.18	-14.10	.10
D3	-12.35	.25	-8.95	.03	-12.95	.07	-14.07	.38
D4	-12.97	.28	-9.30	.04	-13.48	.19	-14.09	.09

The inter-channel calibration factor or $\ln G_i$, was determined as follows. The four detectors were placed in the thermal column and a set of measurements were taken with

the vibrator moving in one direction (for example EW). One of the channels, say D3, was assumed to have a gain of 1 and the others were normalized with respect to this detector. In the thermal column, since the terms $\ln(C/C_L)$ and $\ln W$ are the same for all the detectors,

$$\ln G_i = \ln R_{Ni} - \ln R_3. \qquad (5.7)$$

The logarithm of the gain factors, $\ln G_i$, assuming channels D3 or D4 to have a gain factor of 1 ($\ln G_i = 0$), is shown in table 5.9. In order to normalize the ith detector signal to the channel D3 signal, for example, $\ln G_i$ given by equation (5.7) is subtracted from the logarithm of the normalized detector signal. Therefore,

$$\ln R_{Ni} - \ln G_i = \ln W^2 + \ln(C/C_L). \qquad (5.8)$$

TABLE 5.9. The natural logarithm of the inter-channel calibration factors assuming unit gain for channels 3 or 4

Detector	Normalizer	
	Channel 3	Channel 4
D1	-2.96	-2.50
D2	-0.76	1.22
D3	0.0	0.46
D4	-0.46	0.0

In order to perform the localization of the vibrator, it is not necessary to evaluate the constant $\ln(C/C_L)$. The minimization will return a value of the amplitude parameter that is modified by this constant. Thus, the localization is not altered by the presence of this constant. But, to get the absolute value of the amplitude parameter this constant must be evaluated. Since the vibrator location is known, the model response may be evaluated for each detector location. This, when substituted in equation (5.8) along with a measured value for each detector gives a value for $\ln(C/C_L)$. This factor is a measure of how well the model predicts the actual detector response since for an exact fit, it would be a constant independent of position. The calculated $\ln(C/C_L)$ terms were found to be reasonably constant for the four detectors, and an average value was used in equation (5.8) to correct the measured detector signals. Table 5.2 shows the measured detector signals after all the corrections have been applied. They can be compared with the theoretical values also shown there. Because of the normalizations used the inferred vibration amplitude must be unity.

F. Discussion of Results

The normalized and corrected detector data were used in the minimization programs. A minimization of the exponent of the likelihood function (3.51), with respect to the vibration amplitude parameter, was performed over the twelve locations for the different detector patterns. The value of σ_f obtained from the measurements was used in the calculations. Tables 5.3 through 5.7 summarize the results. Each of the columns in these tables represent a different case.

Since σ_f was estimated from the data, as shown in chapter III, the quantity, Q, that is being minimized at each location, has an F distribution. Using tabulated values for the F distribution, one can try to see how many locations fall within, for example, a 90% confidence region. But, this was not done since Q does not seem to have an F distribution. This anomaly could be due to a model bias which is not accounted for in these calculations. Also, it should be noted that the normalizations performed on the basic measured data may alter the statistics. It is possible that the log-normal distribution assumed for the data is not correct either.

Because of these reasons, rather than trying to do goodness-of-fit analysis, the localization was performed by determining the location, among the twelve potential

locations, for which the grand minimum occurred. This is the maximum likelihood point estimate. Measurements were made with the vibrator thimble both flooded and unflooded, since it was not known which of the two situations was modeled best by the Exterminator code. The presence of air in the vibrator thimble was not included in the model.

In the case of EW vibration, location 11, the actual location was obtained as the maximum likelihood estimate for both the flooded and unflooded situations. Detector patterns P1, P2, P3 and P5, yielded the above result. Pattern P4, as predicted by the numerical investigation, was found to be the poorest one. The overall pattern of localization followed the results from the theoretical analysis.

In the case of the NS vibration, the unflooded situation did not yield good results. This can be explained on the basis that the model overpredicts the response of the detector D1 as seen from Table 5.2. The difference between the modeled and corrected experimental values for D1 is larger by a factor of 2 when compared to that for the other detectors. The calculated value of $\ln(C/C_L)$ was approximately constant for the detectors D2, D3 and D4, while for D1 it was smaller by a factor of three. All the patterns except P4 identified the whole north core as potential site. The pattern P4 which did not use Detector

D1 predicted a location in the South core. The situation changed when the vibrator tube was flooded. All the patterns, including pattern P4, predicted location 11 as the vibrator site. This was also predicted in the numerical investigation when σ_f was reduced from .3 to .1 as shown in the columns under 'THEOR' of Tables 5.3 through 5.7.

The experimental and analytical (from numerical investigation) results compared very well. The fact that the numbers are not F distributed needs further investigation. Nevertheless this investigation provided experimental proof as to the feasibility of the localization techniques developed in this work.

VI. SUMMARY OF RESULTS AND CONCLUSIONS

The purpose of this work was to develop reliable techniques to estimate, using noise analysis techniques, parameters associated with the vibration of reactor components. The following goals were achieved:

1. Theoretical background for the vibration problem was developed, and the calculation (with some simplifying assumptions) of the detector responses for the UTR-10 was performed.
2. Techniques, based on the maximum-likelihood and confidence region methods, were developed to estimate the vibration parameters. The use of the Fisher information matrix in determining an optimum pattern of detectors was demonstrated.
3. The techniques were tested numerically, on a simple reactor model using computer simulated detector signals. Analysis based on the Fisher information matrix showed that some detector patterns are better than others for vibration identification. The variances of the parameters were found to decrease as the detectors moved close to the vibrator and also as the number of detectors increased. The same number of detectors rearranged in a different pattern may provide a better analysis. The maximum-

likelihood estimates, obtained by analyzing computer simulated data, for locations were within 2 cm and the amplitudes were within 5% of the actual value. These results were obtained with 50% noise on the detector signals, 20% external noise (or a model bias), and for different detector patterns. It was observed that external noise, at least in the way it was modeled, did not affect the localization significantly. It was found that to estimate all the parameters simultaneously, one needs at least the same number of detectors as the number of parameters. If the locations are restricted to grid points, one needs at least one detector more than the number of amplitude parameters. In practice, it may be necessary to use more than the above numbers since some detectors may not be optimally located. The size and shape of confidence regions for the parameters increased with larger fractional standard deviation and external noise and smaller number of detectors.

4. The validity of the estimation techniques was experimentally verified by performing an experiment on the UTR-10 reactor. Analysis using the information matrix and computer simulated

data showed that detector D1 may have a significant effect on the estimation process, at least for the EW mode of vibration. The measured data were analyzed using the techniques developed and it was found that the localization was possible using 'good' detector patterns determined earlier by numerical investigation. The amplitude of motion of the vibrator was determined within 3% of the true value. It was observed that the localization was not affected by an arbitrary constant resulting from unknown normalization; however, the amplitude factor can be determined only relative to this arbitrary constant. This arbitrary constant calculated for different locations is a measure of how well the model describes the measured detector response. It should be the same everywhere in the core if the measured and modeled values agree. It was observed that the flooded case of the vibrator thimble was modeled more accurately by the exterminator code for the NS mode of vibration. Detector pattern P4, with the detector next to the vibrator missing, was the poorest pattern for the EW mode of vibration.

The techniques developed proved to be promising to localize and estimate the amplitude of vibrations in a reactor core using in-core detector signals. The following general scheme may be used to analyze the vibration problem.

1. For the reactor of interest, develop a detailed neutronic noise model and calculate the response of detectors for potential vibrators (the location of both are known). The sophistication of the computer code is determined by the accuracy of estimation required and limited by the cost involved.
2. Perform numerical investigations to determine an optimal detector pattern, if an approximate location and amplitude of vibration are known.
3. Obtain data (usually in the frequency domain) using the optimal detector pattern.
4. Analyze the data using maximum likelihood or confidence region techniques to estimate the vibration parameters. Note that one needs to take into account external noise and model bias to obtain correct estimates. It may also be possible to show by numerical investigation that the effects of these factors are negligible up to some limits.

VII. SUGGESTIONS FOR FUTURE WORK

Some suggestions for possible improvements on the present work and further work are included in the following:

1. A better experimental apparatus, which is capable of moving in predictable trajectories, could be designed. This could be used to obtain calibrations for the responses. Measurements were not taken simultaneously for all the channels. Storage and analysis of data needs to be considered. Better methods to calculate gradients and efficient methods to do the minimization searches need to be developed.
2. It was found that the distribution of the data was not the same as the one assumed. The statistical modeling must be considered in detail and any variation from the assumed distribution (for example due to data manipulation) must be taken into account.
3. In this study, the detector responses were assumed to be real. The response without this assumption could be calculated and the improvements thus produced could be studied. It was observed that when a larger detector was used in the core, the measured detector responses were quite different from the calculated values. This

shows the need for the development of a computer model which can take into account the perturbation produced by the detectors.

4. The case of only a single vibrator was considered in this work. Numerical investigations could be performed for the case of multiple sources to reveal any limitations. Experimental verification may require the use of a large number of detectors.
5. The use of the cross-power spectral density should be investigated. This will provide additional information which may reduce the number of detectors required.
6. In this study it was assumed that the detector signals came from data with the same variance, which may not always be true. Modifications involved in the statistical theory should be developed.
7. The case of stochastic vibrations should be studied. A method was suggested, in Chapter III, to determine a bound for the parameter estimates, and the effect of this restriction on the estimates needs to be investigated.
8. The experiment could be carried out in reactors where the detector patterns can be changed

easily, for studying the effect of detector patterns. Data from a power reactor, with vibrations that can be determined using other methods, could be analyzed to verify the validity of the techniques developed. Application to liquid metal fast breeder reactors would be of interest.

VIII. REFERENCES

1. A. M. Weinberg and H. C. Schweinler, Theory of oscillating absorber in a chain reactor, Phys. Rev. 74 851 (1948).

2. W. J. Bailey, K. H. Rising and M. Tokar, Fuel performance annual report for 1980, NUREG/CR-2410 (PNL-3953) (1981).

3. S. E. Stephenson, D. P. Roux and D. N. Fry, Neutron fluctuation spectra in the Oak Ridge research reactor, Report ORNL-TM-1401 (1966).

4. A. Lucia, E. Ohlmer and D. Schwalm, Correlation between neutron noise and fuel element oscillations in the ECO-reactor, Atomkernenergie, 22, 1 (1973).

5. D. N. Fry, Experience in reactor malfunction diagnosis using on-line noise analysis, Nucl. Technol. 10, 273 (1971).

6. C. W. Mayo, Detailed neutron noise analysis of pressured water reactor internal vibrations, Atomkernenergie 29, 9 (1977).

7. J. A. Thie, Core motion monitoring, Nucl. Technol. 45, 5 (1979).

8. G. Kosály, Noise investigations in Boiling-water reactors, Prog. Nucl. Energy 5, 145-149 (1980).

9. M. M. R. Williams and R. Sher, Reactor Noise-SMORN-II, Prog. Nucl. Energy 1, Pergamon Press (1977).

10. M. M. R. Williams, N. J. McCormick Reactor Noise-SMORN-III, prog. Nucl. Energy 9, Pergamon Press (1982).

11. M. M. R. Williams, N. J. McCormick, Reactor Noise-SMORN-IV, Prog. Nucl. Energy 15, Pergamon Press (1984).

12. J. A. Thie, Power Reactor Noise (American Nuclear Society, La Grange Park, Illinois, 1981).

13. P. Bernard, J. Cloue, C. Messainguiral, R. Balyens, P. Mathot, J. Satinet and C. Puyal, PWR Core Monitoring by in-core noise analysis, Prog. Nucl. Energy 9, 541 (1982).

14. D. N. Fry, J. March-Leuba, F. J. Sweeney, Use of Neutron Noise for diagnosis of in-vessel anomalies in light water reactors, NUREG/CR-3303, ORNL/TM-8774 (1984).

15. F. J. Sweeney, J. P. A. Renier, Sensitivity of detecting in-core vibrations and boiling in pressurized water reactors using ex-core neutron detectors, NUREG/CR-2996 (ORNL/TM-8549) (1984).

16. M. M. R. Williams, Reactivity changes due to random vibrations of central rods and fuel elements, Nucl. Sci. Engr. 40, 144 (1970).

17. M. Antonopoulos-Domis, Reactivity and neutron noise density excited by random rod vibrations Annals of Nuclear Energy 3, 451 (1976).

18. I. Pázsit, Investigation of space dependent noise induced by a vibrating absorber, Atomkernenergie 30 No. 1, 29 (1977).

19. I. Pázsit, Two-group theory of noise in reflected reactors with application to vibrating absorbers, Annals of Nuclear Energy 5, 185 (1978).

20. H. Van Dam, Neutron noise in boiling water reactors, Atomkernenergie 27, 8 (1976).

21. I. Pázsit and G. Th. Analytis, Theoretical investigation of neutron noise diagnostics of two-dimensional control rod vibrations in a PWR, Annals of Nuclear Energy 5, 171 (1980).

22. S. J. Lee and R. W. Albrecht, The use of neutronic fluctuations to locate a vibrating control rod in a PWR model, Nucl. Sci. and Engr. 83, 427 (1983).

23. I. Pázsit and O. Glöckler, On the neutron noise diagnostics of pressurized water reactor control rod vibrations. I. Periodic vibrations, Nucl. Sci. and Engr., 85, 167-177 (1983).

24. I. Pâzsit and O. Glöckler, On the neutron noise diagnostics of pressurized Water Reactor control rod vibrations. II. Stochastic vibrations, Nucl. Sci. and Engr., 88, 77-87 (1984).

25. R. A. Danofsky and R. A. Hendrickson, Response of in-core Neutron detectors of a Nuclear reactor to Moving Core Components, Iowa State University Engineering Research Institute 84216, 1984.

26. M. Al-Ammar, Use of local-global ratio in detecting component vibration in reactors, Ph.D. dissertation, Iowa State University, 1981 (unpublished).

27. M. Salih, Response of in-core neutron detectors to a vibrating absorber based on the detector adjoint function, M.S. thesis, Iowa State University, 1981 (unpublished).

28. R. J. Borland, Effects of neutron flux gradient and detector vibrator geometry on the local-global responses of the UTR-10 reactor, M.S. thesis, Iowa State University, 1982 (unpublished).

29. J. T. Sankoorikal, Neutron detector response to a vibrating absorber located in a fuel assembly, M.S. thesis, Iowa State University 1983 (unpublished).

30. W. J. Hennessy, An investigation of the two-dimensional Neutron Noise field generated by a moving neutron absorber using UTR-10 reactor. M.S. thesis, Iowa State University, 1983 (unpublished).

31. R. A. Hendrickson, J. T. Sankoorikal, W. J. Hennessy and R. A. Danofsky, Spatial characteristics of the response of a Neutron detector to a moving absorber, Trans. of Am. Nucl. Soc. 45, 707 (1983).

32. M. Kamal Kalbasi, The effect of the direction of motion of a vibrating absorber on the response of an in-core detector, M.S. thesis, Iowa State University 1985 (unpublished)

33. J. T. Sankoorikal, R. A. Danofsky, H. T. David, R. A. Hendrickson and Margot Tollefson, Statistical estimation of vibration parameters of nuclear reactor core components, Trans. of the Am. Nucl. Soc. 49, 429 (1985).

34. A. M. Mood, F. A. Graybill, D. C. Boes, Introduction to the Theory of Statistics (3rd. Ed., McGraw-Hill, New York, 1974).

35. R. V. Hogg and Allen. T. Craig, Introduction to Mathematical Statistics, (4th Ed., MacMillan, New York 1978).

36. S. D. Silvey, Optimal Design: An Introduction to the Theory for Parameter Estimation (Chapman and Hall, London, 1980).

37. T. B. Fowler, M. L. Tobias, D. R. Vondy, EXTERMINATOR-2. A Fortran Code for Solving Neutron Diffusion Equations in one and two dimensions, ORNL-4078 (1967).

38. G. I. Bell and S. Glasstone, Nuclear Reactor Theory(Van Nostrand Reinhold, New York, 1970).

39. M. Ash, Nuclear Reactor Kinetics (McGraw-Hill, New York, 1979).

40. M. M. R. Williams, Random Process in Nuclear Reactors (Pergamon Press, Oxford, England, 1974).

41. D. L. Hetrick, Dynamics of Nuclear Reactors (The University of Chicago press, Chicago, 1971).

42. F. B. Hildebrandt, Methods of Applied Mathematics (Prentice Hall, Inc., Englewood Cliffs, NJ, 1965).

43. P. M. Morse and H. Feshbach, Methods in Theoretical Physics (McGraw-Hill, New York, 1953).

44. J. S. Bendat and A. G. Piersol, Random Data Analysis and Measurement Procedures (Wiley-Interscience, New York 1971).

45. R. A. Danofsky, Department of Nuclear Engineering, Iowa State University, private communications, 1986.

46. R. V. Churchill, Complex Variables and Applications, 2nd Ed. McGraw-Hill Book Co Inc. New York (1960).

47. M. C. Kendall and Alan Stuart, The Advanced Theory of Statistics (Vol. 1, 3rd Ed. Hafner Publishing Co., 1969).

48. M. C. Kendall and Alan Stuart, The Advanced Theory of Statistics (Vol. 2, 3rd Ed. Hafner Publishing Co., 1969).

49. H. T. David, Department of Statistics, Iowa State University, private communication, 1986.

50. S. D. Silvey, Statistical Inference (Chapman and Hall, London, 1975).

51. R. A. Hendrickson, R. A. Danofsky, A. F. Rohach and D. M. Roberts, Safety Analysis Report for the Training Reactor UTR-10, Iowa State University Engineering Research Institute 82418, 1981.

52. R. F. Barry, LEOPARD-A spectrum dependent non-spatial depletion code for IBM-7094, WCAP-3269-26 (1963).

53. M. L. Tobias, and T. B. Fowler, Equipoise Method - a simple procedure for few group diffusion calculation in two and three dimensions, Nucl. Sci. Engr. 12, 513 (1962).

IX. ACKNOWLEDGEMENTS

I consider myself fortunate to have Dr. R. A. Danofsky as my major professor and I thank him for the valuable guidance, encouragement and patient assistance that I received from him in completing this work. I gratefully acknowledge the valuable suggestions, and critical comments received from Drs. B. I. Spinrad, R. A. Hendrickson, A. F. Rohach, H. T. David, R. G. Brown and D. M. Roberts. I express my sincere thanks to Drs. Danofsky and Spinrad for all the special help they have given to my family. The numerous services and help received from Margot Tollefson, Masoud Feiz, Jordi Roglans-Ribas, Byron Reeder, Tom Zimmerman, Jim Hraback, Mike Winter, Scott State, Dr. R. E. Williams and Dorothy Blair are appreciated. The financial support received from National Science Foundation, Dr. Spinrad and the Nuclear Engineering department is acknowledged. I express my fondest thanks to my parents for their love and support and my wife Mercy who, without any reservation, gave up all that she rightfully deserved to help me complete this work.

X. APPENDIX A

A. Development of the Two-group Diffusion Noise Model

The time-dependent two-group diffusion equations, using standard notations (39), are given by

$$D_1\nabla^2\phi_1-(\Sigma_{a1}+\Sigma_{R1})\phi_1+\Sigma_j \lambda_j C_j+(1-\beta)(\nu\Sigma_{f1}\phi_1+\nu\Sigma_{f2}\phi_2) = v_1^{-1}\,\partial\phi_1/\partial t \qquad (A.1)$$

and

$$D_2\nabla^2\phi_2-\Sigma_{a2}\phi_2+\Sigma_{R1}\phi_1 = v_2^{-1}\,\partial\phi_2/\partial t \qquad (A.2)$$

where c_j is given by

$$\beta_j(\nu\Sigma_{f1}\phi_1+\nu\Sigma_{f2}\phi_2)-\lambda_j C_j = \partial C_j/\partial t. \qquad (A.3)$$

In a nonmultiplying medium the $\nu\Sigma_f$ terms are zero. It is assumed that the vibration of the absorber rod produces fluctuations only in the thermal absorption cross-section. The procedure described in Chapter III is followed to obtain an equation similar to equation (3.9) for the Fourier transform of the fluxes. This can be written as

$$\begin{bmatrix} l_{11} & l_{12} \\ l_{21} & l_{22} \end{bmatrix}\begin{bmatrix} \Delta\phi_1 \\ \Delta\phi_2 \end{bmatrix} = \begin{bmatrix} 0 \\ \Delta_{a2}\phi_{20} \end{bmatrix} \qquad (A.4)$$

where

$$l_{11} = D_1\nabla^2-(\Sigma_{a1}+\Sigma_{R1})-j\omega/v_1+\nu\Sigma_{f1}((1-\beta)+Z) \tag{A.5}$$

$$l_{12} = \nu\Sigma_{f2}((1-\beta)+Z) \tag{A.6}$$

$$l_{21} = \Sigma_{R1} \tag{A.7}$$

$$l_{22} = D_2\nabla^2-\Sigma_{a20}-j\omega/v_2 \tag{A.8}$$

and

$$Z = \sum_i \lambda_i\beta_i/(j\omega+\lambda_i) \tag{A.9}$$

Note that when all the reactor constants are assumed to be fluctuating, the right hand side of equation (A.4), the source term, will involve many components (22).

In the plateau region of the reactor response $\omega/v_1 << (\Sigma_{a1}+\Sigma_{R1})$ and $\omega/v_2 << \Sigma_{a20}$ and so they are neglected in equations (A.5) and (A.8). Also, $\lambda << \omega$ and therefore, the magnitude of Z is small compared to $(1-\beta)$, and it is neglected. In this case $\Delta\phi_1$ and $\Delta\phi_2$ are real. Therefore, equations (A.5), (A.6), and (A.8) reduce to

$$l_{11} = D_1\nabla^2-(\Sigma_{a1}+\Sigma_{R1})+\nu\Sigma_{f1}(1-\beta) \tag{A.10}$$

$$l_{12} = \nu\Sigma_{f2}(1-\beta) \tag{A.11}$$

$$l_{22} = D_2\nabla^2-\Sigma_{a20} \tag{A.12}$$

The equation adjoint to (A.4) may now be written as

$$\begin{bmatrix} l_{11} & l_{21} \\ l_{12} & l_{22} \end{bmatrix} \begin{bmatrix} \psi_1 \\ \psi_2 \end{bmatrix} = \begin{bmatrix} 0 \\ -\Sigma_{d2} \end{bmatrix} \qquad \text{(A.13)}$$

where the detector cross section for a thermal neutron detector is considered, since only the fluctuations in the thermal flux is of interest. In multiregion calculations, for the region with no source (vibrator) the right hand side of both equations (A.3) and (A.13) are set equal to zero.

The solutions of the steady state counterparts of equations (A.1), (A.2) and (A.3) give the flux in the critical reactor. The steady state system of equations may be obtained, if $(1-\beta)$ in equations (A.10) and (A.11) is set to one, and the right hand side of (A.4) is set to zero and if (A.12) is used for l_{22}. In this study, the static code Exterminator-2 (37) was used to do an eigenvalue calculation. The transverse buckling was adjusted to obtain an eigenvalue of unity. The critical flux obtained was used for the calculations in Chapter V.

As mentioned in Chapter III a static code, that can solve a source problem, may be used to obtain solutions for the forward system (A.4) or the adjoint system (A.13). In this project, the code Exterminator-2 was used. To solve the forward system, for the solution which is equivalent to

the Green's function solution, a source of unit strength is specified in a small region around the source point. Note that when the cross sections are entered, the value of $\nu\Sigma_f$ is multiplied by $(1-\beta)$.

An adjoint calculation was found to be preferable to a forward calculation for the analysis of the problem in Chapter V. The adjoint system of equations may be now written as (from A.13)

$$D_1\nabla^2\psi_1-\Sigma'_{a1}\psi_1-\Sigma'_{R1}\psi_1+\nu\Sigma'_{f2}\psi_2 = 0 \qquad (A.14)$$

$$D_2\nabla^2\psi_2-\Sigma_{a2}\psi_2-\Sigma'_{R1}\psi_1 = 1 \qquad (A.15)$$

where it can be shown that

$$\Sigma'_{a1} = \Sigma_{a1}+\Sigma_{R1}-(1-\beta)(\nu\Sigma_{f1}+\Sigma_{f2}) \qquad (A.16)$$

$$\Sigma'_{R1} = (1-\beta)\nu\Sigma_{f2} \qquad (A.17)$$

$$\nu\Sigma'_{f1} = 0 \qquad (A.18)$$

$$\nu\Sigma'_{f2} = \Sigma_{R1} \qquad (A.19)$$

$$\Sigma_{d2} = 1 \text{ (arbitrary)} \qquad (A.20)$$

The constant Σ'_{a1} may be negative for some cases. These 'artificial' cross sections are substituted into the code and an adjoint source, Σ_{d2}, is specified as a source at the detector location. The resulting solutions will be the adjoint functions that were used in Chapter V.

XI. APPENDIX B

A. Tables of Constants

TABLE B.1. Atom densities and volume fractions used in LEOPARD

Region type	Pellet			CL[a]	MOD[b]	EX[c]		NLF[d]
	Al[e]	U235[f]	U238[f]	Al[e]	H_2O[e]	AL[e]	H_2O[e]	
1 Graphite	All graphite region							
2 N2 N3 N4 N5 S3 S4 S5 (262 gm)	1	1.3497E-3	8.7956E-5	1	1	.7061	.2939	.1764
3 N1 N6 (240 gm)	1	1.2364E-3	8.0573E-5	1	1	.7770	.2230	.2202
4 N6 (196 gm)	1	1.0097E-3	6.5801E-5	1	1	.7770	.2230	.2202
5 S1 (229 gm)	1	1.1797E-3	7.6880E-5	1	1	.7770	.2230	.2202
6 S2 (240 gm)	1	1.3488E-3	8.7898E-5	1	1	.7061	.2936	.1764
7 Water gap	All water region							

[a] CLAD.

[b] MODERATOR.

[c] EXTRA REGION.

[d] Non Lattice Fraction.

[e] Aluminum, H_2O volume fractions.

[f] Atom densities * 1.E24.

TABLE B.2. Macroscopic cross sections calculated using LEOPARD

TYPE	GROUP	D	Σ_R	Σ_a	$\nu\Sigma_f$
1	1	1.1652	2.5296E-3	0.0	0.0
	2	9.9154E-1	0.0	3.0145E-4	0.0
2	1	1.3972	3.5204E-2	2.0866E-3	2.0694E-3
	2	2.1709E-1	0.0	5.6717E-2	8.4723E-2
3	1	1.4138	3.3499E-2	1.9147E-3	1.8059E-3
	2	2.2799E-1	0.0	5.1478E-2	7.4262E-2
4	1	1.4141	3.3656E-2	1.7093E-3	1.4785E-3
	2	2.2632E-1	0.0	4.5842E-2	6.2233E-2
5	1	1.4139	3.3538E-2	1.8635E-3	1.7236E-3
	2	2.2759E-1	0.0	5.0092E-2	7.1305E-2
6	1	1.3972	3.5208E-2	2.0814E-3	2.0700E-3
	2	2.1709E-1	0.0	5.6693E-2	8.4674E-2
7	1	1.3421	4.3514E-2	7.8383E-4	0.0
	2	1.7124E-1	0.0	1.8200E-2	0.0
8	(detector or vibrator region) use 7 if in fuel use 1 if in graphite				
	Source = 1.0				

TABLE B.3. The mesh pattern used for UTR-10 reactor

X-Mesh size (cm)	Mesh point	Y-Mesh size (cm)	Mesh point
5.0	7	5.4	7
3.95	8	1.35	12
0.5	10	0.85	13
3.95	11	0.5	15
2.3	12	0.85	16
0.5	14	1.35	21
0.45	15	2.41	24
0.5	17	2.0	26
3.75	19	0.5	28
0.5	21	2.0	32
3.25	22	1.87	33
0.5	24	0.5	35
3.25	25	1.87	36
0.5	27	2.0	40
3.75	28	0.5	42
1.85	29	2.0	44
0.5	31	2.41	47
0.85	32	1.35	52
0.5	41	0.85	53
0.3	42	0.5	55
0.2	43	0.85	56
3.55	44	0.42	57
0.5	46	0.5	67
4.15	47	1.33	68
5.0	53	5.0	71
		2.0	73
		0.5	76
		2.0	78
		7.64	88

TABLE B.4. Cross sections used in Exterminator-2 for the calculation of the adjoint function

TYPE	GROUP	D	Σ'_R	Σ'_a	$\nu\Sigma'_f$
1	1	1.1652	0.0	2.5296E-3	0.0
	2	9.9154E-1	0.0	3.0145E-4	2.5296E-3
2	1	1.3972	8.4130E-2	-4.8894E-2	0.0
	2	2.1709E-1	0.0	5.6717E-2	3.5204E-2
3	1	1.4138	7.3743E-2	-4.0123E-2	0.0
	2	2.2799E-1	0.0	5.1478E-2	3.3499E-2
4	1	1.4141	6.1797E-2	-2.7900E-2	0.0
	2	2.2632E-1	0.0	4.5842E-2	3.3656E-2
5	1	1.4139	7.0806E-2	-3.7116E-2	0.0
	2	2.2759E-1	0.0	5.0092E-2	3.3538E-2
6	1	1.3972	8.4081E-2	-4.8847E-2	0.0
	2	2.1709E-1	0.0	5.6693E-2	3.5208E-2
7	1	1.3421	0.0	4.4298E-2	0.0
	2	1.7124E-1	0.0	1.8200E-2	4.3514E-2
8	(detector or vibrator region)			use 7 if in fuel use 1 if in graphite	
	Adjoint source = 1.0				

XII. APPENDIX C

A. Listing of Computer Programs

This section contains a listing of some of the programs used in this work. The subroutine 'RESPON' calculates the unit response functions for the square reactor, given the detector and vibrator locations. It also calculates the derivatives of the unit response functions with respect to the vibrator location. The subroutine 'SIMDET' calculates the simulated detector signals using the unit responses calculated by 'RESPON' and random numbers obtained from a subroutine 'GGNML'. The subroutine 'MINXAM' finds the minimum of the likelihood function in the X1, X2, and X3 space. Subroutine 'FLIK' calculates the likelihood function at various values of the amplitude parameters. A similar subroutine was used to do the minimization of the location parameters and in this case the unit response functions need to be calculated at each new location. It was observed that in the case of minimizing all the five parameters, it was more efficient to keep the location and amplitude parameters in two different minimization routines than minimize all five parameters simultaneously. Looping between the two subroutines was continued until a specified convergence criteria was met.

The confidence region for the XP and YP parameters were determined using the subroutine 'CONFID'. The response functions are calculated using a subroutine 'RESP' which calls the subroutine 'RESPON'. Using the gradient of the chi-squared function at a starting point a projection is made to the parameter value that gives the required chi-squared value. Calculations are repeated until the required point is found within a specified accuracy. It is necessary to use 'good' guesses, initially, for these subroutines to work efficiently. The program 'TRANS' transfers the data from the Frequency Spectrun Analyser to the computer for a selected region of the frequency span and stores it on disk.

1. RESPON

```
      SUBROUTINE RESPON(VIBX,VIBY,DETX,DETY,WX,WY,WXX0,WXY0,WYX0,WYY0)
      IMPLICIT REAL*8 (A-H,O-Z)
      REAL*8 KINF,MSQD,KM2,KM
      A=270.D0
      EMAX=35.D0
      NMAX=900
      BETA=.007D0
      BZ2=0.0D0
      KINF=1.0152D0
      MSQD=56.D0
      B=A
      B02=-BZ2+(KINF-1.D0)/MSQD
      B2=B02-KINF*BETA/MSQD
      PI=31415927.D-7
      X0=VIBX
      Y0=VIBY
      B1=PI/A
      P1=B1*B1
      P2=DSIN(B1*X0)
      P3=DSIN(B1*Y0)
      P4=DCOS(B1*X0)
      P5=DCOS(B1*Y0)
      PHI=P2*P3
      DPX=B1*P4*P3
      DPY=B1*P2*P5
      DPX2=-P1*PHI
      DPY2=DPX2
      DPXY=P1*P4*P5
      XD=DETX
      YD=DETY
      SG=0.D0
      SDGX=0.D0
      SDGY=0.D0
      SDGX2=0.0D0
      SDGY2=0.0D0
      SDGXY=0.0D0
      M=1
30    BM=M*PI/A
      BM2=BM*BM
      KM2=BM2-B2
      KM=DSQRT(DABS(KM2))
      T1=DSIN(BM*XD)
      T2=DSIN(BM*X0)
      T3=DCOS(BM*X0)
      T4=T2/T3
      IF(KM2.LT.0.0)THEN
      T5=DSIN(KM*Y0)
      T6=DCOS(KM*Y0)
      T7=T5/T6
      T8=DSIN(KM*YD)
      T9=DTAN(KM*B)
      IF(YD.LT.Y0)THEN
      GT=2.D0/A*T1*T2*T5*T8/KM*(1.D0/T7-1.D0/T9)
      DGXT=BM*GT/T4
      DGYT=-2.D0/A*T1*T2*T8*(T5+T6/T9)
      DGX2T=-BM2*GT
      DGY2T=-KM*KM*GT
      DGXYT=BM*DGYT/T4
      ELSE
      T10=DCOS(KM*YD)
```

```
      GT=2.D0/A*T1*T2*T5/KM*(T10-T8/T9)
      DGXT=BM*GT/T4
      DGYT=KM*GT/T7
      DGX2T=-BM2*GT
      DGY2T=-KM*KM*GT
      DGXYT=BM*KM*GT/T4/T7
      ENDIF
      ELSE
      S1=0.D0
      S2=0.D0
      S3=0.D0
      S4=0.D0
      S5=0.D0
      ICOU=0
      Z3=KM*(2.D0*B-Y0-YD)
      Z4=KM*(YD+Y0)
      Z5=KM*2.D0*B
      IF(YD.LT.Y0)THEN
      Z1=KM*(Y0-YD)
      Z2=KM*(2.D0*B+YD-Y0)
      ELSE
      Z1=KM*(YD-Y0)
      Z2=KM*(2.D0*B+Y0-YD)
      ENDIF
      IF(Z1.GT.EMAX)GO TO 100
      ICOU=ICOU+1
      S1=DEXP(-Z1)
100   IF(Z2.GT.EMAX)GO TO 110
      ICOU=ICOU+1
      S2=DEXP(-Z2)
110   IF(Z3.GT.EMAX)GO TO 120
      ICOU=ICOU+1
      S3=DEXP(-Z3)
120   IF(Z4.GT.EMAX)GO TO 130
      ICOU=ICOU+1
      S4=DEXP(-Z4)
130   IF(Z5.GT.EMAX)GO TO 140
      ICOU=ICOU+1
      S5=DEXP(-Z5)
140   IF(ICOU.EQ.0)GO TO 40
      GT=T1*T2/A/KM*(S1+S2-S3-S4)/(1.D0-S5)
      DGXT=BM*GT/T4
      DGX2T=-BM2*GT
      DGY2T=KM*KM*GT
      IF(YD.LT.Y0)THEN
      DGYT=T1*T2/A*(-S1+S2-S3+S4)/(1.D0-S5)
      ELSE
      DGYT=T1*T2/A*(S1-S2-S3+S4)/(1.D0-S5)
      ENDIF
      DGXYT=BM*DGYT/T4
      ENDIF
      IF(M.LT.NMAX) THEN
      M=M+1
      SG=SG+GT
      SDGX=SDGX+DGXT
      SDGY=SDGY+DGYT
      SDGX2=SDGX2+DGX2T
      SDGY2=SDGY2+DGY2T
      SDGXY=SDGXY+DGXYT
      GO TO 30
```

```
      ELSE
      WRITE(6,*)DETX,DETY,'NO CON FOR THIS'
      ENDIF
40     WX=SG*DPX+PHI*SDGX
       WY=SG*DPY+PHI*SDGY
       WXXO=SG*DPX2+2.DO*DPX*SDGX+PHI*SDGX2
       WXYO=SG*DPXY+SDGY*DPX+DPY*SDGX+PHI*SDGXY
       WYXO=SG*DPXY+SDGX*DPY+DPX*SDGY+PHI*SDGXY
       WYYO=SG*DPY2+2.DO*DPY*SDGY+PHI*SDGY2
      RETURN
      END
```

2. SIMDET

```
      SUBROUTINE SIMDET
      DIMENSION RNAVE(10),ZRAN(30)
      REAL*8 DSEED
      DSEED=10.D7
      NR=30
      CALL GGNML(DSEED,NR,ZRAN)
      CALL GGNML(DSEED,NR,ZRAN)
      X1=.01
      X2=.01
      X3=.0071
      XP=125.0
      YP=125.0
      ND=5
      DO 10 IDET=1,ND
      READ(5,*)DETX,DETY
      CALL RESPON(XP,YP,DETX,DETY,WX,WY,WXXO,WXYO,WYXO,WYYO)
      RM=WX*WX*X1+WY*WY*X2+WX*WY*X3
      CALL GGNML(DSEED,NR,ZRAN)
      SUM=0.0DO
      DO 60 I=1,NR
60    SUM=SUM+ZRAN(I)
      RNAV(IDET)=DLOG(RM)+SIGMA*SUM/NR
10    CONTINUE
      WRITE(6,*)'@@@@@@@@@@@@@@@@'
      WRITE(6,*)'RNAVE',(RNAV(I),I=1,ND)
      WRITE(6,*)'@@@@@@@@@@@@@@@@'
      RETURN
      END
```

3. MINXAM

```
      SUBROUTINE MINXAM (X1,Y1,Z1,XX,YY,ZZ)
C***
C***     THIS SUBROUTINE FINDS THE MINIMUM POINT OF
C***     THE LIKELIHOOD FUNCTION IN X Y Z SPACE
C***
C***     COMMON BLOCK /STEPS/ FOR INITIAL STEP SIZES
C***
         COMMON /STEPS/ VXSTEP,VYSTEP,XSTEP,YSTEP,ZSTEP
      DIMENSION X(7),Y(7),Z(7),F(7)
      X(1)=X1
      Y(1)=Y1
      Z(1)=Z1
      HX=XSTEP
      HY=YSTEP
      HZ=ZSTEP
      ICOUNT=1
      IHALVE=1
      NF001=0
   10   DO 20 I=2,7
        X(I)=X(1)
        Y(I)=Y(1)
        Z(I)=Z(1)
   20   CONTINUE
   30   X(2)=X(1)+HX
        X(3)=X(1)-HX
        Y(4)=Y(1)+HY
        Y(5)=Y(1)-HY
        Z(6)=Z(1)+HZ
        Z(7)=Z(1)-HZ
        DO 40 I=1,7
        IER=0
        CALL FLIK(X(I),Y(I),Z(I),F(I),IER)
        IF (IER.EQ.1) THEN
        NF001=NF001+1
        ENDIF
   40   CONTINUE
        FSMALL=F(1)
        LSMALL=1
        DO 50 I=2,7
        IF (F(I).LT.FSMALL) THEN
        LSMALL=I
        FSMALL=F(I)
        ENDIF
   50   CONTINUE
C***       PRINT*,X(LSMALL),Y(LSMALL),Z(LSMALL)
C*** PRINT*,FSMALL,LSMALL,ICOUNT,IHALVE
      IF (LSMALL.EQ.1) THEN
      HX=HX/2.
      HY=HY/2.
      HZ=HZ/2.
      ICOUNT=ICOUNT+1
      IHALVE=IHALVE+1
      IF (IHALVE.GT.5) GO TO 60
      IF (ICOUNT.GT.1000) GO TO 60
      GO TO 30
      ENDIF
      X(1)=X(LSMALL)
      Y(1)=Y(LSMALL)
      Z(1)=Z(LSMALL)
      ICOUNT=ICOUNT+1
```

```
      IF (ICOUNT.LT.1000) GO TO 10
   60   XX=X(1)
      YY=Y(1)
      ZZ=Z(1)
      CALL FLIK(XX,YY,ZZ,FF,IER)
      IF (NF001.GT.0) THEN
      WRITE(15,*)'--------------'
      WRITE(15,*)'DIAGNOSTIC FLIK001 - WARNING; ARGUMENT OF LN'
      WRITE(15,*)'TERM WAS NEGATIVE. CROSS TERM WAS DELETED AND'
      WRITE(15,*)'THE CALCULATION CONTINUED. DELETION MAY AFFECT'
      WRITE(15,*)'ANSWERS. NUMBER OF DELETIONS MADE =',NF001
      WRITE(15,*)'--------------'
      ENDIF
      WRITE(15,*)'X,Y,Z OPTIMIZATION ROUTINE'
      WRITE(15,*)'ICOUNT=',ICOUNT,'  IHALVE=',  IHALVE,'  FMIN=',FF
      WRITE(15,*)'CALCULATED OPTIMUM VALUES OF X, Y, Z ARE'
      WRITE(15,*)XX,YY,ZZ
      WRITE(15,*)'############################'
      PRINT*,'X,Y,Z OPTIMIZATION ROUTINE'
      PRINT*,'ICOUNT=',ICOUNT,'  IHALVE=',  IHALVE,'  FMIN=',FF
      PRINT*,'CALCULATED OPTIMUM VALUES OF X, Y, Z ARE'
      PRINT*,XX,YY,ZZ
      PRINT*,'############################'
   70   RETURN
      END
      SUBROUTINE FLIK (XX,YY,ZZ,FF,IER)
C***
C***     THIS SUBROUTINE CALCULATES THE LIKELIHOOD FUNCTION
C***     BASED ON THE  X, Y, Z VIBRATION PARAMETERS AND THE
C***     VIBRATOR POSITION BEING ANALYZED
C***
      DIMENSION RNAVE(8),SIGMA(8),WX(8),WY(8),DETX(8),DETY(8)
      COMMON /ARRS/ RNAVE,SIGMA
      COMMON /VARS/ IFLAG1,NTTA,ND,CONST
      COMMON /RESP/ WX,WY,DETX,DETY
      FF=0.0
      DO 10 I=1,ND
      IF(IFLAG1.EQ.1)THEN
      SGMA=SIGMA(1)
      ELSE
      SGMA=SIGMA(I)
      ENDIF
      XTERM=WX(I)*WX(I)*XX/2.
      YTERM=WY(I)*WY(I)*YY/2.
      CRSTRM=WX(I)*WY(I)*ZZ
         RM=XTERM+YTERM+CRSTRM
      IF (RM.LT.0.0) THEN
      IER=1
      RM=XTERM+YTERM
      ENDIF
      IF (RM.EQ.0.0) THEN
      FF=1.0E+3
      GO TO 20
      ENDIF
      RML=ALOG(RM*CONST)
      F=(RNAVE(I)-RML)**2
         FF=FF+F/(SGMA**2)
   10   CONTINUE
         FF=FF*NTTA
   20   RETURN
```

4. CONFID

```
      SUBROUTINE CONFID
      REAL X1(50)
      REAL Y1(50),Y2(50)
      COMMON /CLOC/ XSTART,YSTART,CHISQR
    1 NP1=0
      NP2=0
      IER=0
      PRINT*,'ENTER MAXIMUM VALUE OF J TO BE USED'
      READ*,JMAX
      PRINT*,'ENTER TOLERANCE (TYPICAL .1) ON BOUNDARY'
      READ*,TOL1
C***
C***  OUTSIDE LOOP FOR X VARIABLE
C***
      DO 400 I=1,NSTEPS
      NCOUN=0
C***
C***  BEGIN STEPPING ON X-VARIABLE
C***
      XA1=XSTART+(I-1)*XSTEP
      J=1
       IF(NP1.EQ.0)THEN
       XA2=YSTART
       ELSE
       XA2=Y1(NP1)
       ENDIF
     CALL RESP (XA1,XA2)
        CALL FLIK (XX,YY,ZZ,F11,IER)
    5   XA22=XA2+Y1STEP
     CALL RESP (XA1,XA22)
        CALL FLIK (XX,YY,ZZ,F12,IER)
        XCHI=XA2-(F11-CHISQR)/(F11-F12)*(XA2-XA22)
        XA2=XCHI
        CALL RESP(XA1,XCHI)
        CALL FLIK(XX,YY,ZZ,F11,IER)
        PER=ABS(F11-CHISQR)/CHISQR
        PRINT*,'J & X & Y & F',J,XA1,XA2,F11
        IF(PER.GT.TOL1)THEN
        J=J+1
        IF(J.LT.JMAX)GO TO 5
        ELSEIF(PER.LT.TOL1)THEN
        NP1=NP1+1
        X1(NP1)=XA1
        Y1(NP1)=XA2
        ENDIF
        J=1
         IF(NP2.EQ.0)THEN
         XA2=YSTART+Y1STEP*NSTEPS
         ELSE
         XA2=Y2(NP2)
         ENDIF
     CALL RESP (XA1,XA2)
        CALL FLIK (XX,YY,ZZ,F11,IER)
    7   XA22=XA2+Y1STEP
     CALL RESP (XA1,XA22)
        CALL FLIK (XX,YY,ZZ,F12,IER)
        XCHI=XA2-(F11-CHISQR)/(F11-F12)*(XA2-XA22)
        XA2=XCHI
        CALL RESP(XA1,XCHI)
        CALL FLIK(XX,YY,ZZ,F11,IER)
```

```
      PER=ABS(F11-CHISQR)/CHISQR
      PRINT*,'J & X & Y & F',J,XA1,XA2,F11
      IF(PER.GT.TOL1)THEN
      J=J+1
      IF(J.LT.JMAX)GO TO 7
      PRINT*,'WISH TO RESTART (1) OR CONTINUE (2) ON X VARIABLE'
      PRINT*,'OR SAVE (3) THIS DATA'
      READ*,LL1
      IF(LL1.EQ.1)THEN
      PRINT*,'ENTER NEW XSTART'
      READ*,XSTART
      GO TO 1
      ENDIF
      ELSEIF(PER.LT.TOL1)THEN
      NP2=NP2+1
      Y2(NP2)=XA2
      ENDIF
      IF(LL1.EQ.3)GO TO 500
400   CONTINUE
500   OPEN (UNIT=21,TYPE='NEW',NAME='XCON.DAT')
      OPEN (UNIT=22,TYPE='NEW',NAME='YBCN.DAT')
      OPEN (UNIT=23,TYPE='NEW',NAME='YTCN.DAT')
      WRITE(21,*) (X1(I),I=1,NP1)
      WRITE(22,*) (Y1(I),I=1,NP1)
      WRITE(23,*) (Y2(I),I=1,NP2)
      RETURN
      END
```

5. TRANS

```
10 ! DATA TRANSFER FROM ANALYZER TO DISK.
ONLY BINS 23 TO 40 OF A,B,XM.XP,C"
20 CLEAR @ BEEP 50,200 @ BEEP 40,200
30 OPTION BASE 1
40 DIM A(18),B(18),A9(102)
50 DISP "ENTER LABEL "
60 INPUT L$
70 REMOTE 711
80 OUTPUT 711 ;"AA1MN1AM1SC1"
90 L1=1
100 GOSUB 410
110 OUTPUT 711 ;"AA0AB1"
120 L1=3
130 GOSUB 410
140 OUTPUT 711 ;"AB0AX1"
150 J=1
160 Z$="AM"&VAL$(J)
170 OUTPUT 711 ;Z$;"MP30LMK"
180 ENTER 711 ; C1,C2
190 OUTPUT 711 ;"LXS"
200 ENTER 711 ; C3
210 IF C1>.001*C3 THEN 220 ELSE 240 ! IF R
EADABLE BY MARKER
220 J=J+1
230 GOTO 160
240 L1=4
250 GOSUB 410
260 OUTPUT 711 ;"AX0PX1"
270 L1=5
280 GOSUB 410
290 OUTPUT 711 ;"PX0CH1"
300 L1=6
310 GOSUB 410
320 LOCAL 711
330 CREATE L$,1,1020
340 ASSIGN# 1 TO L$
350 FOR K=1 TO 102
360 PRINT# 1 ; A9(K)
370 NEXT K
380 ASSIGN# 1 TO *
390 BEEP 200,200 @ BEEP 100,200
400 STOP
```

```
410 FOR I=23 TO 39
420 I1=I-22
430 Q$="MP"&VAL$(I)
440 OUTPUT 711 ;Q$;"HLTLMKRUN"
450 ENTER 711 ; A(I1),B(I1)
460 NEXT I
470 IF L1=1 THEN 480 ELSE 520
480 FOR K1=1 TO 17
490 A9(K1)=B(K1)
500 NEXT K1
510 L1=2
520 FOR K2=1 TO 17
530 I2=K2+(L1-1)*17
540 A9(I2)=A(K2)
550 NEXT K2
560 RETURN
570 END
```